2871

SANDIA REPORT SAND84—0996 • Unlimited Release • UC-70
Printed June 1985

SAI
T&MSS
LIBRARY

Nevada Nuclear Waste Storage Investigations Project

Benchmarking NNWSI Flow and Transport Codes: Cove 1 Results

Nancy K. Hayden

Prepared by
Sandia National Laboratories
Albuquerque, New Mexico 87185 and Livermore, California 94550
for the United States Department of Energy
under Contract DE-AC04-76DP00789

Issued by Sandia National Laboratories, operated for the United States Department of Energy by Sandia Corporation.
NOTICE: This report was prepared as an account of work sponsored by an agency of the United States Government. Neither the United States Government nor any agency thereof, nor any of their employees, nor any of their contractors, subcontractors, or their employees, makes any warranty, express or implied, or assumes any legal liability or responsibility for the accuracy, completeness, or usefulness of any information, apparatus, product, or process disclosed, or represents that its use would not infringe privately owned rights. Reference herein to any specific commercial product, process, or service by trade name, trademark, manufacturer, or otherwise, does not necessarily constitute or imply its endorsement, recommendation, or favoring by the United States Government, any agency thereof or any of their contractors or subcontractors. The views and opinions expressed herein do not necessarily state or reflect those of the United States Government, any agency thereof or any of their contractors or subcontractors.

Printed in the United States of America
Available from
National Technical Information Service
U.S. Department of Commerce
5285 Port Royal Road
Springfield, VA 22161

NTIS price codes
Printed copy: A06
Microfiche copy: A01

SAND84-0996
Unlimited Release
Printed June 1985

DISTRIBUTION
UC-70

BENCHMARKING NNWSI FLOW AND TRANSPORT CODES: COVE 1 RESULTS

Nancy K. Hayden
Sandia National Laboratories
Albuquerque, NM 87185

SAI
T&MSS
LIBRARY

ABSTRACT

The code verification (COVE) activity of the Nevada Nuclear Waste Storage Investigations (NNWSI) Project is the first step in certification of flow and transport codes used for NNWSI performance assessments of a geologic repository for disposing of high-level radioactive wastes. The goals of the COVE activity are (1) to demonstrate and compare the numerical accuracy and sensitivity of certain codes, (2) to identify and resolve problems in running typical NNWSI performance assessment calculations, and (3) to evaluate computer requirements for running the codes. This report describes the work done for COVE 1, the first step in benchmarking some of the codes. Isothermal calculations for the COVE 1 benchmarking have been completed using the hydrologic flow codes SAGUARO, TRUST, and GWVIP; the radionuclide transport codes FEMTRAN and TRUMP; and the coupled flow and transport code TRACR3D. This report presents the results of three cases of the benchmarking problem solved for COVE 1, a comparison of the results, questions raised regarding sensitivities to modeling techniques, and conclusions drawn regarding the status and numerical sensitivities of the codes.

NOMENCLATURE

Symbols

C = relative solute concentration

D = hydrodynamic dispersion coefficient (cm^2/s)

D_d = molecular diffusion coefficient (cm^2/s)

K = hydraulic conductivity (cm/s)

K_d = distribution coefficient (mL/g)

K_r = relative hydraulic conductivity (K/K_{sat})

n = outward normal direction vector of unit length

q = volumetric water flux ($cm^3/s\text{-}cm^2$)

s = volumetric percent water saturation

x = horizontal axis (cm)

z = vertical axis (cm)

η = porosity or empirical constant

Ψ = pressure head (cm)

Φ = total hydraulic head (cm), $\Phi = \Psi + z$

Θ = volumetric moisture content

ρ = density (gm/cm^3)

Subscripts

i = initial quantity or mesh index in x direction

j = mesh index in z direction

n = vector component in direction of outward normal, n

sat = saturated value

ACKNOWLEDGEMENTS

I express my appreciation to the team of modelers in this project for their dedication and insights: Bryan Travis, Roger Eaton, T. N. Narasimhan, Suresh Pahwa, Mulsen Alavi, and Mario Martinez. In addition, I thank Jeffrey Foster for his help in analyzing and plotting the results. Debra Medina and Betsy Barnett gave enthusiastic and untiring help in preparation of the final document. The support of Lynn Tyler, Felton Bingham, and C. Keller was crucial for keeping the momentum going for this project.

CONTENTS

Section		Page
Nomenclature		ii
Acknowledgements		iii
1.0	Introduction	1-1
2.0	Description of the Problem Addressed in COVE 1	2-1
2.1	COVE 1 Geometry	2-1
2.2	Material Properties for COVE 1N	2-3
2.3	Material Properties for COVE 1YMa and COVE 1YMb	2-8
2.3.1	Boundary and Initial Conditions for COVE 1YMa	2-12
2.3.2	Boundary and Initial Conditions for COVE 1YMb	2-12
2.4	Accuracy and Convergence Criteria	2-14
2.5	Output Variables	2-14
3.0	Description of Codes Used in COVE 1	3-1
3.1	Characteristics of Codes	3-1
3.1.1	TRACR3D	3-2
3.1.2	SAGUARO	3-2
3.1.3	FEMTRAN	3-5
3.1.4	TRUST	3-5
3.1.5	TRUMP	3-5
3.1.6	GWVIP	3-6
3.2	Numerical Formulations	3-6
4.0	Results and Discussion of COVE 1	4-1
4.1	Code Capabilities and Computer Requirements	4-1
4.2	Results of Calculations	4-3
4.2.1	Basis for Comparisons	4-3
4.2.2	Results of COVE 1N	4-3
4.2.3	Results of COVE 1YMa	4-24
4.2.4	Results of COVE 1YMb	4-29

CONTENTS (Continued)

Section		Page
5.0	Summary	5-1
	5.1 Results for COVE 1N	5-3
	5.2 Results for COVE 1YMa	5-5
	5.3 Results for COVE 1YMb	5-5
6.0	Conclusions	6-1
7.0	References	7-1
Appendix A	Computer Meshes and Run Statistics	A-1
Appendix B	COVE 1YMa Results	B-1
Appendix C	COVE 1YMa Results	C-1

TABLES

Table		Page
2-1	Properties for COVE 1YMa and COVE 1YMb	2-8
2-2	Summary of Boundary Conditions for COVE 1	2-13
3-1	COVE 1 Problems Solved	3-2
3-2	Characteristics of Hydrologic Codes Used in COVE 1	3-3
3-3	Characteristics of Radionuclide Transport Codes Used in COVE 1	3-4
4-1	Output Variables for COVE 1 Problems	4-4
4-2	Mass Balances and Convergence Criteria	4-5
4-3	COVE 1 Results Received for Final Evaluation	4-6
A-1	Category A Parameters - Computer Run Statistics	A-1

FIGURES

Figure		Page
1-1	Development and Certification of NNWSI Performance Assessment Codes	1-3
2-1	Geometry for COVE 1N	2-2
2-2	Boundary and Initial Conditions for COVE 1N	2-4
2-3	Characteristic Curves for COVE 1N	2-5
2-4	Boundary and Initial Conditions for COVE 1YMa and COVE 1YMb	2-9
2-5	Characteristic Curves for COVE 1YMa and COVE 1YMb	2-11
4-1	Water-Table Decline in COVE 1N	4-7
4-2	Moisture Content in COVE 1N	4-8
4-3	Hydraulic Head in COVE 1N	4-9
4-4	Relative Concentration Contours in COVE 1N	4-10
4-5	Concentration Contours in COVE 1N	4-11
4-6	Relative Concentrations in COVE 1N	4-12
4-7	Relative Concentrations at the Exit in COVE 1N	4-18
4-8	Concentration Contours in COVE 1N	4-19
4-9	Effect of Mesh Refinement on FEMTRAN Relative Concentrations in COVE 1N	4-22
4-10	Hydraulic-Head and Moisture-Content Profiles in COVE 1	4-23
A-1	SAGUARO Finite-Element Mesh	A-2
A-2	TRUST Finite-Difference Mesh	A-3
A-3	GWVIP Finite-Difference Mesh	A-4
A-4	TRACR3D Finite-Difference Mesh	A-5
A-5	FEMTRAN Finite-Element Mesh	A-6
B-1	Pressure-Head (a and b) and Hydraulic-Head (c) Contours for COVE 1YMa	B-2
B-2	Pressure Head Contours for COVE 1YMa	B-3
B-3	Moisture Content for COVE 1YMa at t = 100, 1,000, and 2,500 yr	B-4
B-4	Moisture Content for COVE 1YMa at t = 7,500 and 20,000 yr	B-5
B-5	Concentration Contours for COVE 1YMa at t = 100 and 1,000 yr	B-6
B-6	Concentration Contours for COVE 1YMa at t = 7,500 and 20,000 yr	B-7

FIGURES (Continued)

Figure		Page
B-7	Comparison of FEMTRAN to Analytic Approximation of COVE 1YMa	B-8
B-8	Hydraulic-Head and Relative-Concentration Profiles Along Right-Side Boundary for COVE 1YMa at t = 100 yr	B-9
B-9	Hydraulic-Head and Relative-Concentration Profiles Along Right-Side Boundary for COVE 1YMa at t = 1,000 yr	B-10
B-10	Hydraulic-Head and Relative-Concentrations Along Right-Side Boundary for COVE 1YMa at t = 7,500 yr	B-11
B-11	Relative-Concentration Histories at Two Interior Nodes for COVE 1YMa	B-12
B-12	Hydraulic-Head Profiles at Two Interior Nodes for COVE 1YMa at t = 100 yr	B-13
B-13	Pressure-Head Profiles at Two Interior Nodes for COVE 1YMa at t = 1,000 yr	B-14
B-14	Pressure-Head Profiles at Two Interior Nodes for COVE 1YMa at t = 7,500 yr	B-15
C-1	Hydraulic-Head Profiles at Two Interior Nodes for COVE 1YMb at t = 100 yr	C-2
C-2	Hydraulic-Head Profiles at Two Interior Nodes for COVE 1YMb at t = 1,000 yr	C-3
C-3	Hydraulic-Head Profiles at Two Interior Nodes for COVE 1YMb at t = 7,500 yr	C-4
C-4	Relative-Concentration History at an Interior Node for COVE 1YMb	C-5
C-5	Hydraulic-Head and Relative-Concentration Profiles Along Right-Side Boundary of COVE 1YMb at t = 100 yr	C-6
C-6	Hydraulic-Head and Relative-Concentration Profiles Along Right-Side Boundary of COVE 1YMb at t = 1,000 yr	C-7
C-7	Hydraulic-Head and Relative-Concentration Profiles Along Right-Side Boundary of COVE 1YMb at t = 7,500 yr	C-8

1.0 INTRODUCTION

The Nevada Nuclear Waste Storage Investigations (NNWSI) Project, managed by the Nevada Operations Office of the U.S. Department of Energy (DOE), is examining the feasibility of constructing a repository in tuff for the disposal of high-level radioactive wastes at Yucca Mountain, Nevada. Before the DOE can obtain construction, operating, and decommissioning licenses for the repository from the Nuclear Regulatory Commission (NRC), the long-term performance of the repository must be assessed.

A major concern in the assessment of long-term performance is the possible release of radionuclides to the environment after the repository has been closed. In order to predict possible releases, it is necessary to define the existing and future hydrologic and geochemical systems of the tuff hundreds of meters below the land surface. Because these systems are heterogeneous, and because the changes to the subsurface environment may not occur for tens to hundreds of thousands of years, it is necessary to develop tools with which to make long-term projections accurately. Among these tools are the codes used to model (1) amounts and distributions of groundwater, rates of groundwater flow, and hydrologic pathways through the tuff, and (2) radionuclide transport along the hydrologic pathways to predict rates and concentrations of radionuclide fluxes at specified boundaries.

The performance assessment codes used for analyses in license application proceedings must be certified to be numerically correct and physically valid as required by the NRC in 10 CFR 60 (NRC, 1983). This certification is particularly important for the NNWSI Project because applications of the hydrologic codes being used in this project represent new fields of endeavor. Historically, these types of

codes have not been used for predicting hydrologic flow and radionuclide transport in hard rock such as that found at Yucca Mountain. In order to certify these codes, Sandia National Laboratories (SNL) is conducting verification and validation activities funded by the NNWSI Project. The first of these activities, code verification (COVE), is the subject of this report.

In NUREG-0856 (Silling, 1983), the NRC specifies criteria for the documentation of computer codes used for the management of high-level radioactive waste and describes the verification and validation activities that must be performed. The NRC has defined "verification" and "validation," as well as other terms frequently used in this report, as follows:

Model--A representation of a process or system.

Mathematical model--A mathematical representation of a process or system.

Component model--A logically distinct subset of a model.

Numerical method--A procedure for solving a problem primarily by a sequence of arithmetic operations.

Numerical model--A representation of a process or system using numerical methods.

Computer code--A set of computer instructions for performing the operations specified in a numerical model.

Verification--Assurance that a computer code correctly performs the operations specified in a numerical model.

Validation--Assurance that a model as embodied in a computer code is a correct representation of the process or system for which it is intended.

Figure 1-1 graphically depicts the process followed for developing, applying, and certifying the NNWSI performance assessment codes. In the first step, a computer code is developed or an existing code is selected for a particular application, and a user's manual is

STEP 1. DEVELOP COMPUTER CODE AND WRITE USER'S MANUAL

STEP 2. EVALUATE COMPUTER REQUIREMENTS USING REPRESENTATIVE SAMPLE PROBLEMS

STEP 3. CERTIFY COMPUTER CODE FOR PERFORMANCE ASSESSMENT OF HIGH-LEVEL RADIOACTIVE WASTE REPOSITORY SYSTEM.

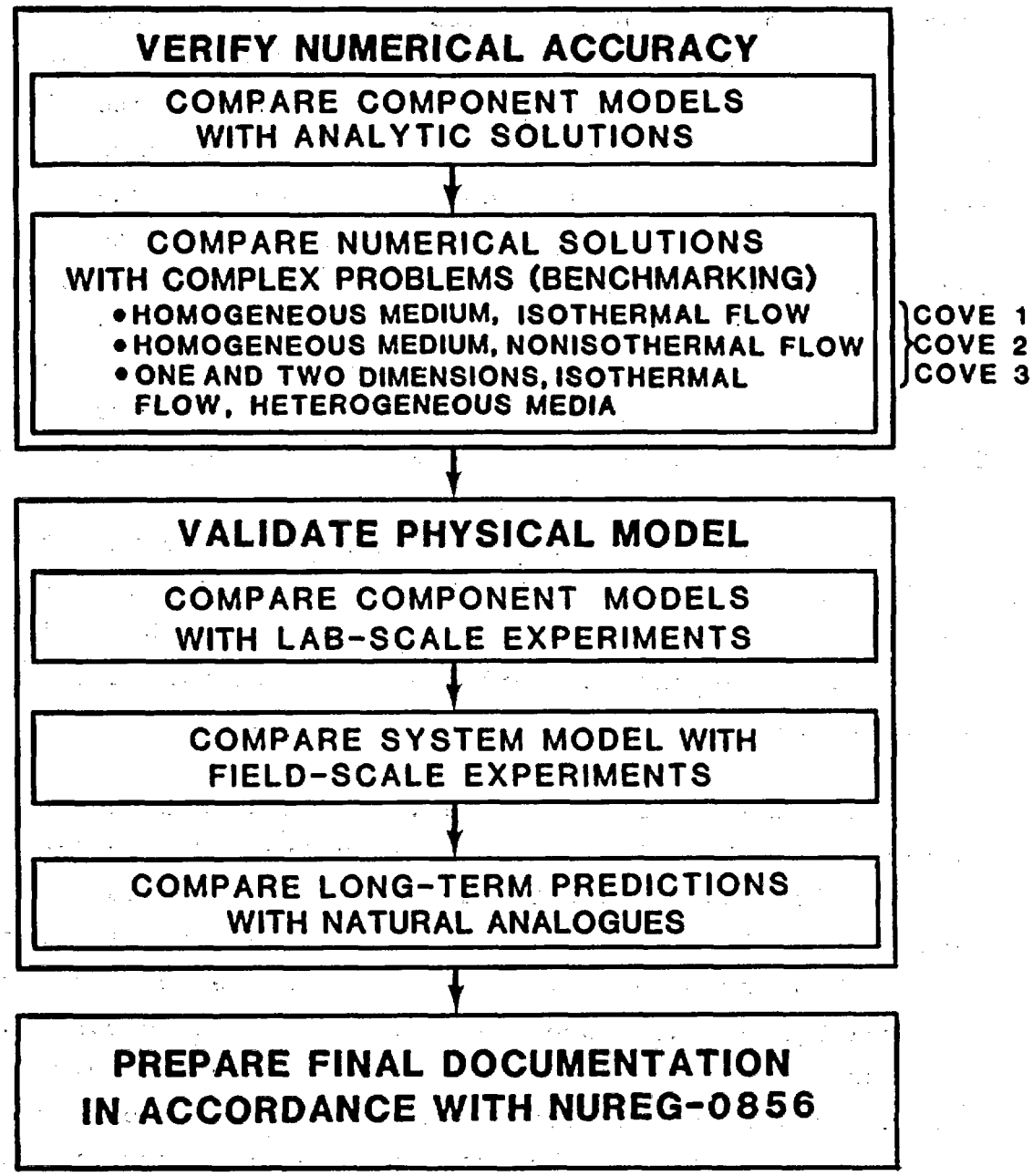

Figure 1-1. Development and Certification of NNWSI Performance Assessment Codes

prepared. In the second step, several practical tasks are undertaken concurrently with the initiation of the third step, certification. These tasks include evaluation of computer requirements and identification of any problems involved in running the code for applications specific to the Yucca Mountain site.

Figure 1-1 includes an expanded description of the certification process (Step 3). During verification, the numerical correctness of a code and its sensitivity to various modeling parameters, such as mesh size and the size of time-step increments, are determined. The numerical correctness of the code can be partially demonstrated by comparing the results produced by component models in the code to analytic solutions. However, when problems are addressed that are so complex that they have no analytic solution, the code used to solve the problem is benchmarked. Benchmarking involves the comparison of numerical solutions generated by a complex code to the results of different but equivalent computer codes used to solve the same problem. In verifying the numerical accuracy of a code by benchmarking or other methods, not only must the code's numerical correctness be demonstrated, but the sensitivity of the numerical method to variations in modeling parameters must also be examined. These tasks are accomplished by varying the modeling parameters, such as time step, mesh size, and convergence criteria, and by observing the extent to which the variations affect a predicted outcome.

After the numerical accuracy of a code has been verified for a particular application, the code is validated. During validation, the code is first compared with laboratory experiments in which the relevancy of physical assumptions is tested on a small, controlled scale in a laboratory. Second, the models for the geohydrological and geochemical systems developed using the code are compared with field-scale experiments to validate the predictions of bulk behavior. This step usually requires formulating special functions to describe laboratory measurements of physical behavior in terms of macroscopic, averaged properties. Each of these special functions is validated as an integral part of the model developed using the computer code.

Finally, to validate the physical assumptions regarding processes that occur very slowly over long periods of time, the code is used to simulate natural analogues. The results of these simulations are compared with observed behavior.

Because of the large-scale heterogeneities in geologic media and the long time-scale of the processes simulated by performance assessment codes, validation of the codes can never be complete. However, a high degree of confidence in the predictions made using computer codes can be obtained by careful and judicious application of the certification process described above.

The three COVE activities that currently compose the verification step in the certification procedure are shown in Figure 1-1. Currently, these problems include: (1) isothermal flow in a homogeneous medium (COVE 1), (2) nonisothermal flow in a homogeneous medium (COVE 2), and (3) one- and two-dimensional isothermal flow in heterogeneous media (COVE 3).

In COVE 1, steady-state flow and concentration fields were calculated for an initial value problem in which water and a contaminant were allowed to drain out of a porous medium (a simulation of a sand plot) in which the contaminant is initially distributed in the upper 0.1 m of the plot. Three cases of this problem were run using different material properties, initial conditions, and boundary conditions.

Six codes were used in COVE 1. Three of these codes, SAGUARO (Eaton et al., 1983), TRUST (Narasimhan and Witherspoon, 1976, 1977; Narasimhan et al., 1978), and GWVIP (Metcalfe, 1984; Pahwa, 1983) are hydrologic flow codes. FEMTRAN (Martinez, 1985) and TRUMP (Edwards, 1972) are radionuclide transport codes and were coupled with the flow fields generated by SAGUARO and TRUST, respectively, to predict radionuclide movement in the flow fields. TRACR3D (Travis, 1984) is a stand-alone code that calculates both fluid flow and radionuclide transport. Before the COVE 1 study was begun, these codes had been benchmarked to a limited extent, but they had not been benchmarked for

a coupled flow and transport problem or against each other. In particular, the codes had not been compared using problems representative of the hydrologic conditions at Yucca Mountain.

In COVE 2 and COVE 3, benchmarking activities will continue. COVE 3 benchmarking will compare the results produced by codes that model transport of heat, liquid water, and vapor using NORIA (Bixler, in preparation), WAFE (Travis, in preparation), TOUGH (Pruess, in preparation, and possibly PETROS (Hadley, 1985). COVE 2 will investigate the behavior of the isothermal flow and transport codes on one- and two-dimensional problems in which the layered units at Yucca Mountain are simulated on a field scale. Eventually, the results of COVE 2 and COVE 3 benchmarking activities will be compared with results of laboratory and field tests performed by NNWSI.

Section 2 of this report contains a description of the problem solved in COVE 1 and the material properties, initial conditions, and boundary conditions used in the three cases studied. In Section 3, the codes used in COVE 1 are described in detail. Section 4 presents the results of COVE 1, Section 5 summarizes the study, and Section 6 presents the conclusions.

This report contains three appendices. Appendix A provides descriptions of the mesh, time steps, and other computer statistics used in generating the numerical solutions for each code. Appendix B contains graphics showing the results of COVE 1YMa, and Appendix C contains graphics showing the results of COVE 1YMb.

2.0 DESCRIPTION OF THE PROBLEM ADDRESSED IN COVE 1

2.1 COVE 1 Geometry

The hydrogeologic setting at Yucca Mountain consists of partially saturated to saturated, fractured and unfractured, layered volcanic rock units. The most likely conceptual model of water flow and radionuclide transport through the unsaturated units of Yucca Mountain depicts infiltration of water through the rock matrix of the layered units (Montazer and Wilson, 1984). The problem chosen for COVE 1, isothermal water drainage and contaminant transport in a variably saturated porous medium, includes the physics of this conceptual flow model for Yucca Mountain. A small-scale problem in a homogeneous porous medium was selected for COVE 1 so that code capabilities and numerical sensitivities could be investigated using small mesh sizes and run times before proceeding to site-scale problems.

Figure 2-1 shows the geometry of the hypothetical problem and the region modeled in COVE 1. The hypothetical, three-dimensional plot of a porous medium being drained is depicted in Figure 2-1(a). Taking into account symmetry planes, the region to be modeled is reduced to the 5-m x 1.5-m vertical plane shown in the cross-hatched area in Figure 2-1(b). A base case and two variations of the problem were run using the geometry in Figure 2-1(b). The plot, initially at a saturation of S_o, is drained through an exit "hole" located 0.75 m below the surface at the right boundary. The base case (COVE 1N) was originally posed and solved numerically by Pickens et al. (1979).

The same geometry was used in all three cases, but the material properties, and initial and boundary conditions were varied. In the second and third cases (COVE 1YMa and COVE 1YMb), material properties

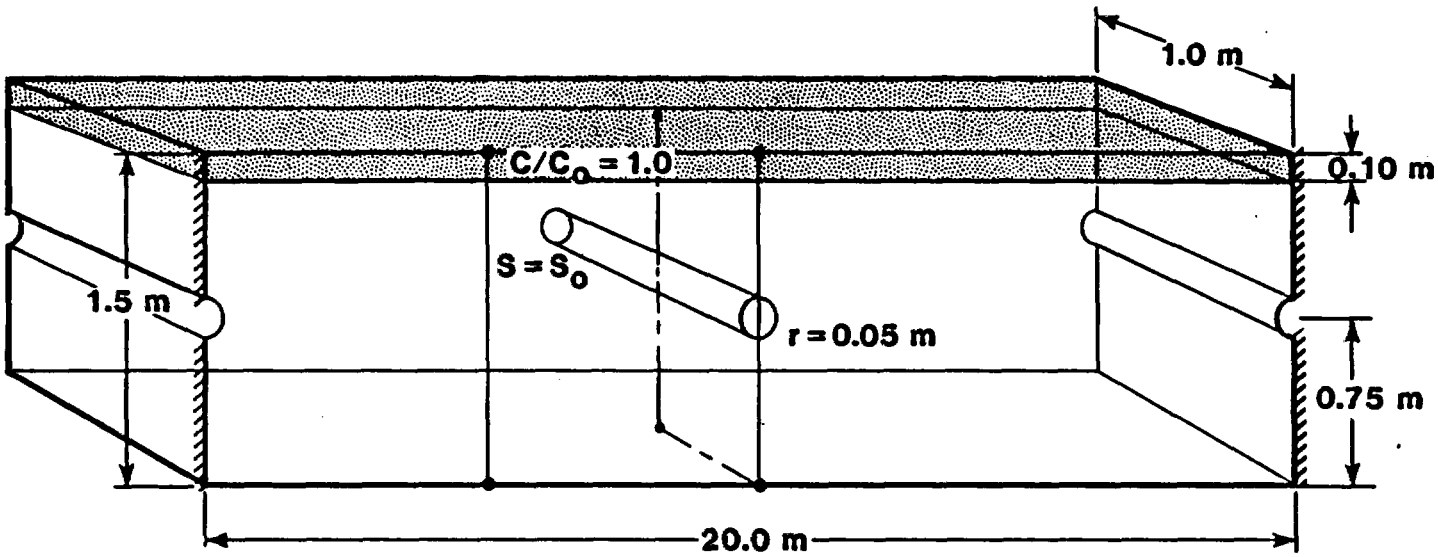

a. Three-Dimensional Geometry of Hypothetical Plot Simulated in COVE 1

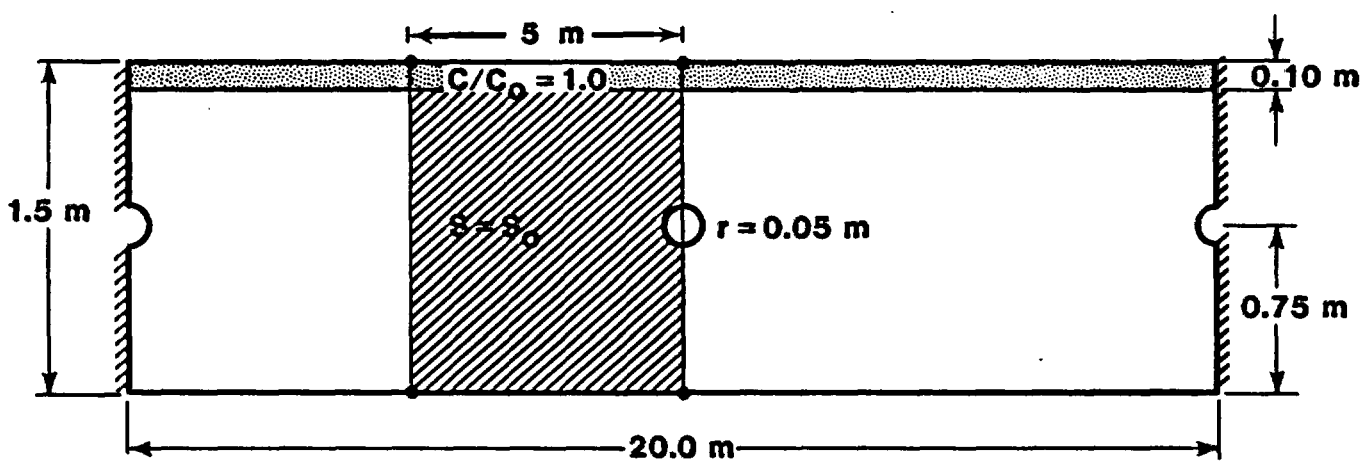

b. Two-Dimensional Cross-Hatched Area Modeled in COVE 1

Figure 2-1. Geometry for COVE 1N

and initial conditions representative of Yucca Mountain were used, but the boundary conditions were varied. In this report, "representative" refers to properties and conditions based on data derived from testing of core samples taken from Yucca Mountain. These data are those that were available when the COVE 1 problems were defined in August, 1983.

2.2 Material Properties for COVE 1N

In COVE 1N, sand that is initially saturated is allowed to drain to an equilibrium, variably saturated condition in a 24-hr period (Figure 2-2a). The contaminant is a stable, nonreacting solute initially present in the upper 0.10 m of the sand (Figure 2-2b). Characteristic curves for pressure head and hydraulic conductivity as functions of water content and hydrologic parameters are for medium-grain sand (Figure 2-3). The analytic equation corresponding to the characteristic curve in Figure 2-3a for moisture content is

$$\theta(\Psi) = \theta_o \frac{\cosh\{(\Psi/\Psi_m)^k + \varepsilon\} - \sigma}{\cosh\{(\Psi/\Psi_m)^k + \varepsilon\} - \sigma} \tag{1}$$

where

$$\sigma = \frac{\theta_o - \theta_r}{\theta_o + \theta_r} \cosh \varepsilon,$$

$$\theta_o = 0.3, \ \Psi_m = 38.71 \text{ cm},$$

$$\varepsilon = 0.0, \ \theta_r = 0.09,$$

$$k = -2.85.$$

In Equation 1, θ_o is saturated moisture content, k and ε are empirical constants, Ψ_m is the negative pressure at θ_r, and θ_r is the residual moisture content.

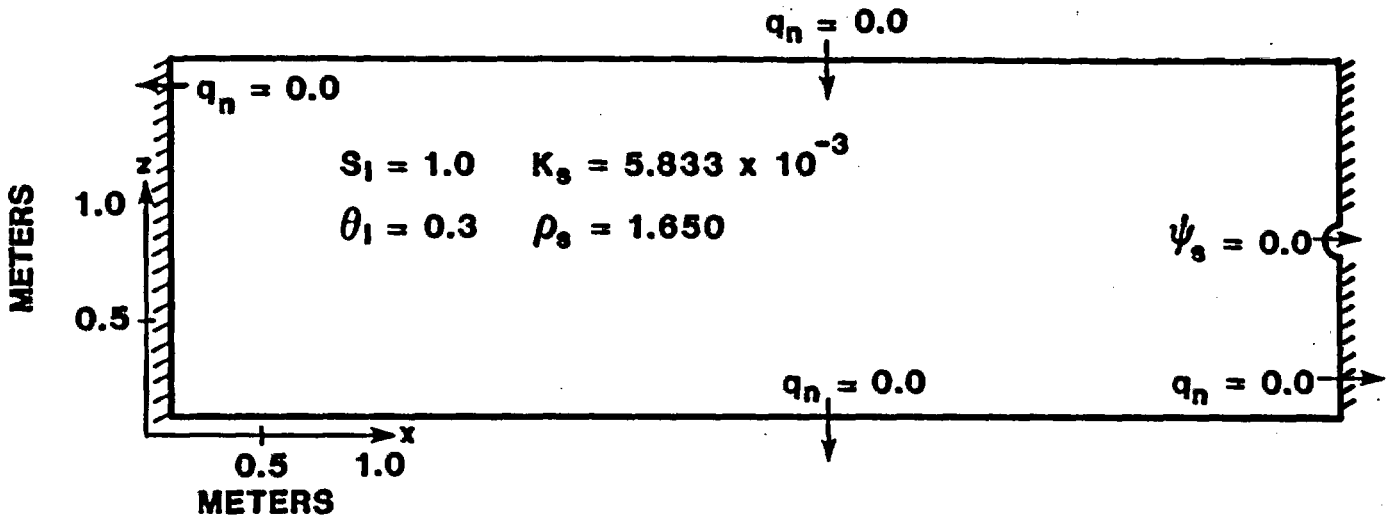

a. Hydrologic Boundary and Initial Conditions

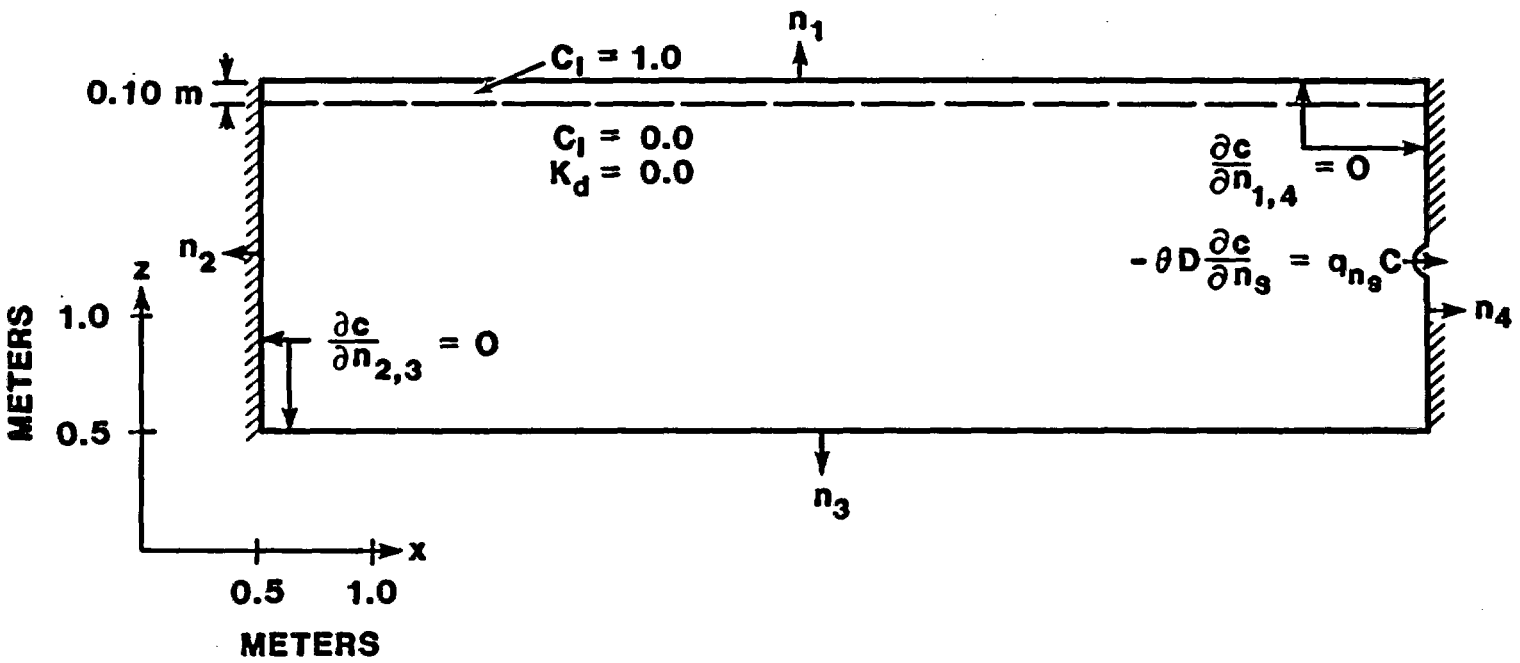

b. Solute Boundary and Initial Conditions

Figure 2-2. Boundary and Initial Conditions for COVE 1N

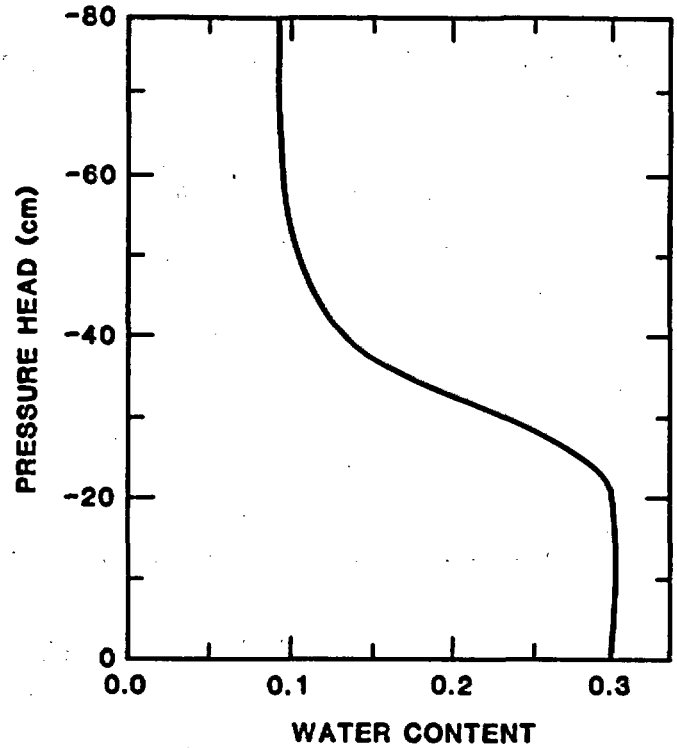

a. Pressure Head

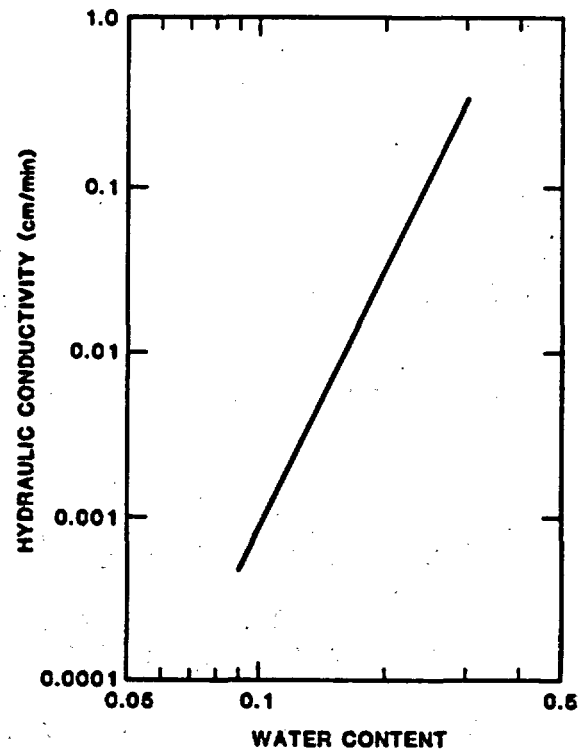

b. Hydraulic Conductivity

Figure 2-3. Characteristic Curves for COVE 1N

The analytic equation for the hydraulic conductivity shown in Figure 2-3b is

$$K(\theta) = \mu\theta^{\eta} \tag{2}$$

where

μ = 4.703 cm/s

η = 5.561.

In Equation 2, μ and η are empirical constants.

The molecular diffusion coefficient was given as:

$$D_d = D_o a \exp(b\theta) \tag{3}$$

where

a = 0.003

b = 10.0

$D_o = 2.0 \times 10^{-5}$ cm^2/s (free water diffusivity).

In Equation 3, a and b are empirical constants.

Finally, the components of the hydrodynamic dispersion tensor were given as:

$$\begin{aligned} D_{XX} &= \alpha_L V_X^2/V + \alpha_T V_Z^2/V + D_d \\ D_{ZZ} &= \alpha_T V_X^2/V + \alpha_L V_Z^2/V + D_d \\ D_{XZ} &= D_{ZX} = (\alpha_L - \alpha_T)\, V_X V_Z/V \end{aligned} \tag{4}$$

where

α_T = 0.4 cm (transverse dispersivity)

α_L = 2.0 cm (longitudinal dispersivity)

V = resultant velocity vector

V_X, V_Z = horizontal, vertical components of velocity vector.

Some of the modelers departed from the geometry and boundary conditions given above for COVE 1N. Bryan Travis at Los Alamos National Laboratory (LANL) used an exit hole 5 cm in diameter instead of 5 cm in radius in the TRACR3D calculations. T. Narasimhan and Mulsen Alavi at Lawrence Berkeley Laboratories (LBL) initially used a seepage-face boundary condition at the exit in TRUST and subsequently reran the TRUST calculations using the constant pressure-head specification shown in Figure 2-2.

In Pickens et al. (1979), the transient results for the spatial distributions of the water table position, hydraulic heads, and water contents were presented graphically. These results were generated using a finite-element code developed by Pickens. The contaminant transport was calculated using constant dispersivity, and the resulting relative concentrations were presented as functions of time and space.

In COVE 1N, the published solutions of this relatively simple unsaturated flow and transport problem were compared to solutions generated using current performance assessment codes: SAGUARO and FEMTRAN; TRACR3D; and TRUST and TRUMP. In order to isolate the effects of numerical techniques using a simple problem, the area and time extent in COVE 1N were limited and did not include radioactive decay, material layering, or dependence of retardation parameters on moisture content. Neither did COVE 1N test the ability of the codes to model the highly nonlinear material properties of the tuff units at Yucca Mountain.

2.3 Material Properties for COVE 1YMa and COVE 1YMb

To test the codes on a simple problem using material properties and hydrologic conditions representative of Yucca Mountain, COVE 1YMa and COVE 1YMb were defined to investigate any changes in code capabilities and numerical sensitivities. The geometry used in COVE 1N was retained, but the problem was redefined to cover longer time periods using material properties and boundary and initial conditions representative of an unsaturated tuff unit at Yucca Mountain. The same set of material properties and initial conditions were used in COVE 1YMa and COVE 1YMb, but the boundary conditions varied.

The density, porosity, saturated hydraulic conductivity, and saturation state are those of a nonwelded, zeolitized tuff sample taken at from a depth of 474 m in Drillhole USW GU3 at Yucca Mountain (Peters et al., 1982; Gee, 1983). These constant material properties are given in Table 2-1 and are shown in Figure 2-4.

TABLE 2-1

PROPERTIES FOR COVE 1YMa AND COVE 1YMb

ρ (dry bulk)	1.55 gm/cm^3
η (average)	0.324
K_{sat}	1.5×10^{-10} cm/s
s (estimated)*	0.85

*This estimated value of saturation state was based on preliminary data. Since the completion of COVE 1 calculations, this estimate is being revised by the USGS (Montazer and Wilson, 1984).

A nonwelded unit instead of a densely welded unit was modeled because the conceptual model of flow in the nonwelded units is relatively simple. Matrix flow is always expected to dominate in the nonwelded, zeolitized units (Montazer and Wilson, 1984); therefore, the

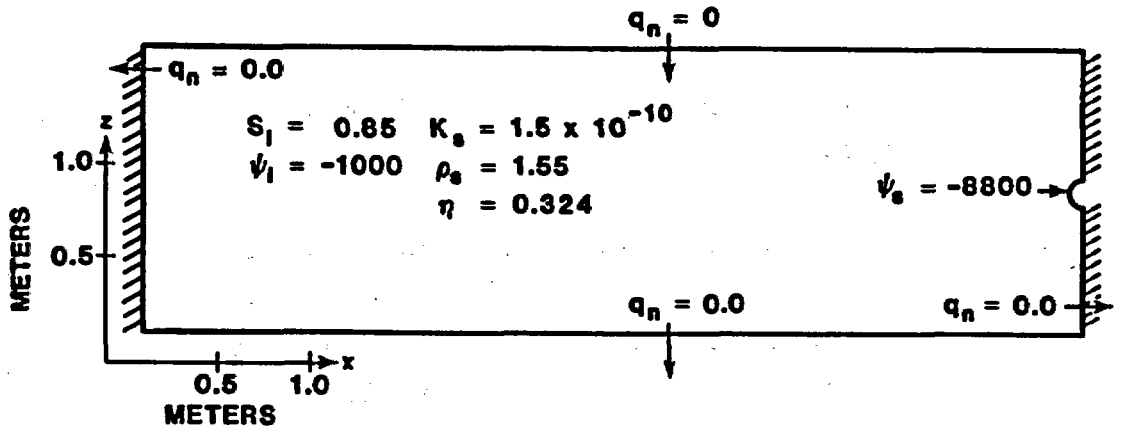

a. Hydrologic Conditions--COVE 1YMa

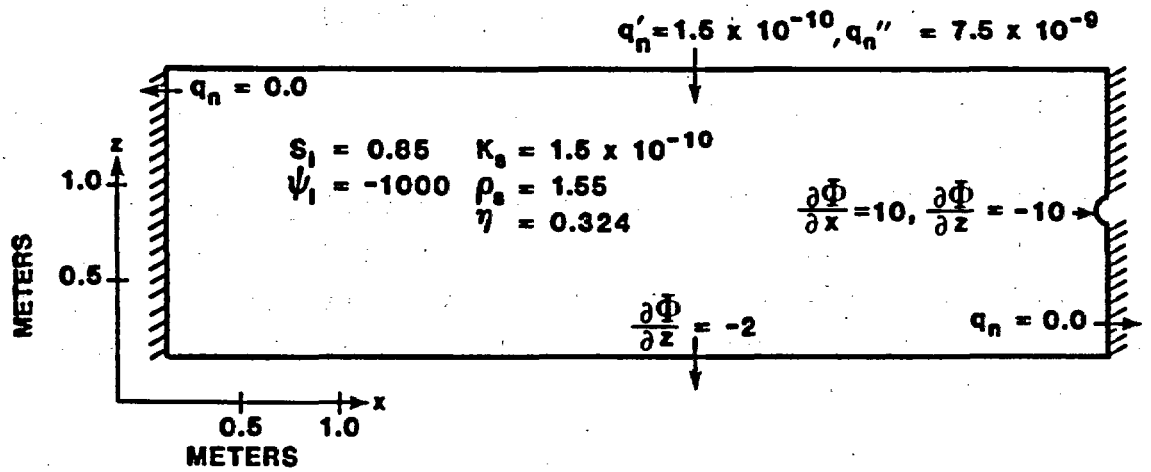

b. Hydrologic Conditions--COVE 1YMb

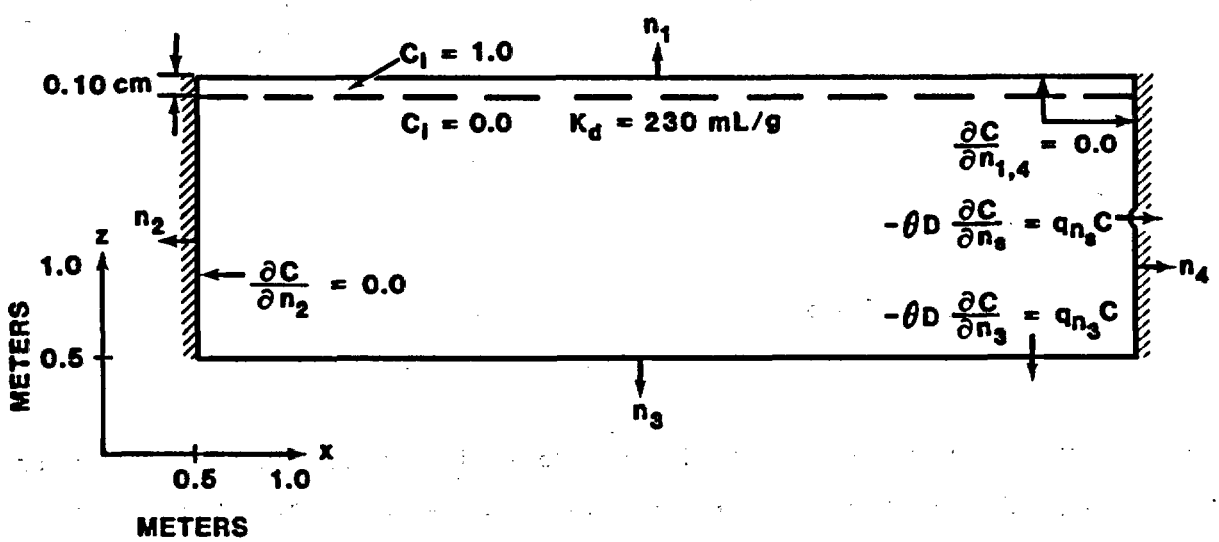

c. Solute Conditions--COVE 1YMa and COVE 1YMb

Figure 2-4. Boundary and Initial Conditions for COVE 1YMa and COVE 1YMb

single-porosity, homogeneous porous medium model used in the COVE 1 problems is appropriate.

The relations used in COVE 1YMa and COVE 1YMb are for

$\Theta(\Psi)$ = moisture content as a function of pressure head, Ψ (Peters et al., 1982; Gee, 1983)

$K_r(\Theta)$ = relative hydraulic conductivity as a function of Θ (Gee, 1983; Peters et al., 1982).

The moisture-content curve was derived by fitting the empirical data to the theoretical model of Haverkamp, et al. (1977) using statistical methods. The relative-conductivity curve was calculated according to a model developed by Mualem (1976) These curves are shown in Figure 2-5. The curves for hydraulic conductivity in Figure 2-5 were generated by numerical evaluation of the following equation from Mualem's work:

$$K/K_{sat} = \Phi^{1/2}\left[1 - \left\{1 - \Phi^{1/m}\right\}^{m}\right]^{2} \qquad (5)$$

where

$$\Phi = \frac{\Theta - \Theta_r}{\Theta_s - \Theta_r}$$

Θ_s = saturated moisture content = η
Θ_r = residual moisture content = 0.085.

The value of m is 1.0 for the nonwelded samples used. To guarantee consistency between codes, the modelers were requested to use tables in the COVE 1YM calculations instead of the analytic expression. Linear interpolation was to be used between data points for the material properties, and saturation for $\Psi > -15$ cm was to be assumed.

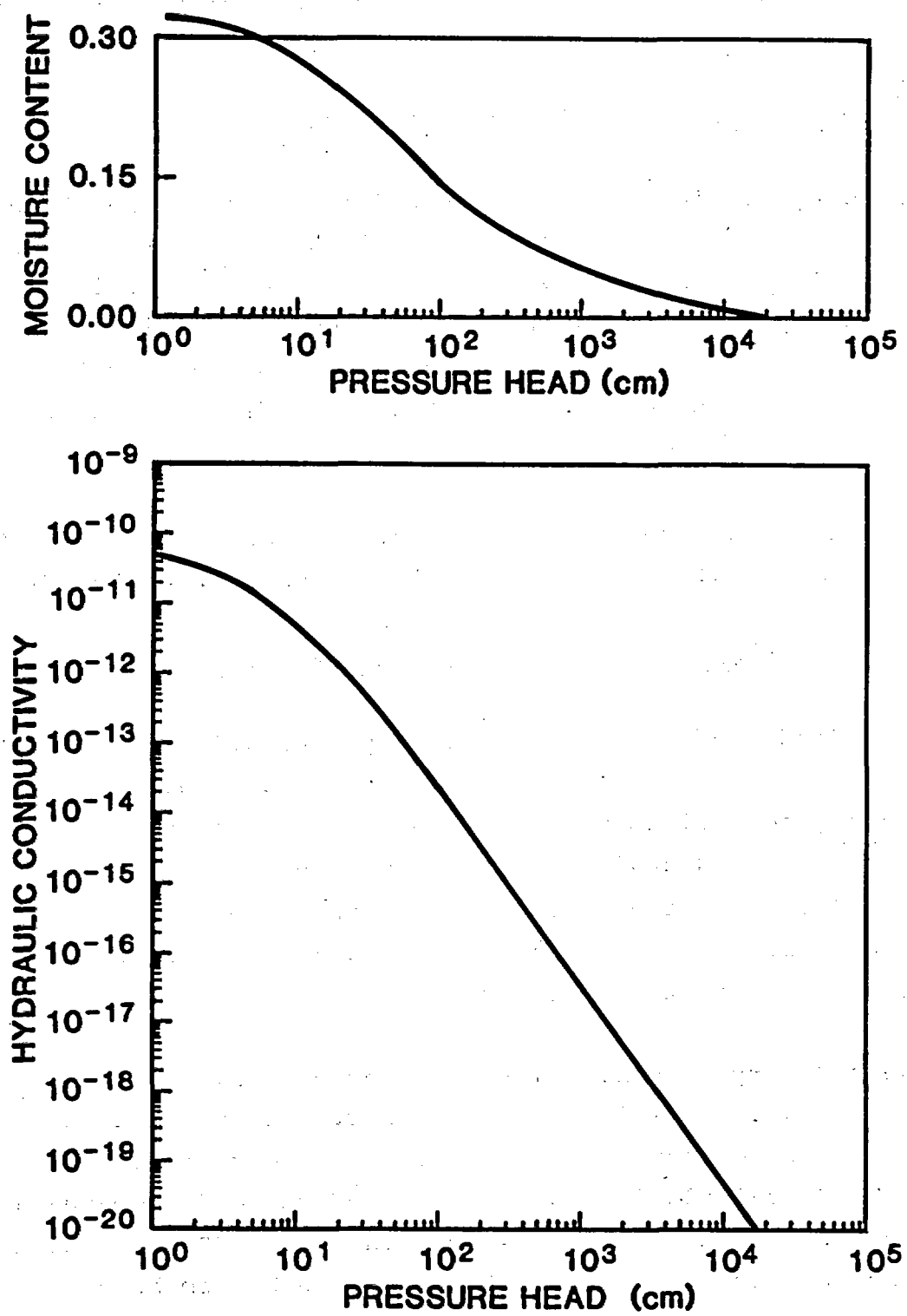

Figure 2-5. Characteristic Curves for COVE 1YMa and COVE 1YMb

The contaminant was retarded using an equilibrium, linear isotherm to describe sorption. An equilibrium distribution coefficient of K_d = 230 mL/g was given.

2.3.1 Boundary and Initial Conditions for COVE 1YMa

Boundary and initial conditions for COVE 1YMa are shown in Figure 2-4a. There was no flux into or out of the tuff material except at the exit. A pressure head of Ψ = -8,800 cm was prescribed at the exit to provide a potential sink for water flow. The initial saturation was 85%. Hydrodynamic dispersion occurred as the result of molecular diffusion alone; the molecular diffusion coefficient was $D_d = 8.33 \times 10^{-6}$ cm^2/s.

Calculations were to model the system for at least 7,500 yr; however, some modelers performed calculations for up to 20,000 yr.

2.3.2 Boundary and Initial Conditions for COVE 1YMb

The third case, COVE 1YMb, was a perturbation of COVE 1YMa. The same material properties and initial conditions were used, but different boundary conditions were imposed. A flux was prescribed at the upper boundary, and drainage was allowed out of the bottom boundary (Figure 2-4b). The flux prescribed at the upper boundary was varied in time by imposing a pulse of water midway through the time period of the calculations at t = 5,000 yr.

The boundary and initial conditions prescribed for all three COVE 1 cases are summarized in Table 2-2. In two instances, the modelers departed from these prescribed boundary conditions: the initial TRUST calculations were performed using a seepage-face boundary condition at the exit hole, and, in the TRACR3D calculations for COVE 1YMb, a pressure of Ψ = +980 cm at the bottom boundary was inadvertently imposed.

TABLE 2-2

SUMMARY OF BOUNDARY CONDITIONS FOR COVE 1

Boundary*	COVE 1N	COVE 1YMa	COVE 1YMb
Left			
(0, Z)	$\frac{\partial \Psi}{\partial X} = 0$	$\frac{\partial \Psi}{\partial X} = 0$	$\frac{\partial \Psi}{\partial X} = 0$
Right			
$(5, Z > Z_t')$	$\frac{\partial \Psi}{\partial X} = 0$	$\frac{\partial \Psi}{\partial X} = 0$	$\frac{\partial \Psi}{\partial X} = 0$
$(5, Z < Z_t'')$	$\frac{\partial \Psi}{\partial X} = 0$	$\frac{\partial \Psi}{\partial X} = 0$	$\frac{\partial \Psi}{\partial X} = 0$
$(5, Z_t'' < Z < Z_t')$	$\Psi = 0$	$\Psi = -8{,}800$ cm	$\frac{\partial \Phi}{\partial Z} = -10.0$ $\frac{\partial \Phi}{\partial X} = 10.0$
Bottom			
(X, 0)	$\frac{\partial \Psi}{\partial Z} + 1 = 0$	$\frac{\partial \Psi}{\partial Z} + 1 = 0$	$\frac{\partial \Psi}{\partial Z} + 1 = 0$
Top			
(X, 1.5)	$\frac{\partial \Psi}{\partial Z} + 1 = 0$	$\frac{\partial \Psi}{\partial Z} + 1 = 0$	$q_n' = 1.5 \times 10^{-10}$ cm/s for $t < 5{,}000$ yr $q_n'' = 7.5 \times 10^{-9}$ cm/s for $5{,}000 < t < 5{,}000 + \Delta t$ where $\Delta t = 1.918 \times 10^{-2}$ yr (1 wk) $q_n'' = 1.5 \times 10^{-10}$ cm/s for $t > 5{,}000 + \Delta t$

*Z_t' = upper Z boundary of exit hole.

Z_t'' = lower Z boundary of exit hole (distances are in meters).

2.4 Accuracy and Convergence Criteria

A common criterion for accuracy was developed to aid in interpreting results. A reasonable common criterion for all the codes was selected based on the maximum allowable change in pressure within an iteration. The accuracy specification was

$$\frac{\Psi''_{i,j} - \Psi'_{i,j}}{\Psi'_{i,j}} < 0.1\% \qquad (6)$$

where

Ψ'' = pressure head at new iteration
Ψ' = pressure head at previous iteration.

In most instances, however, modelers varied this criterion, sometimes in response to specifications in the codes. The actual criteria used are shown in Table 4-2.

2.5 Output Variables

The hydraulic heads, pressure heads, moisture contents, constant-pressure contours, and concentration profiles were calculated as functions of time and space. The water velocities, as well as the pressure heads, were compared in COVE 1N, 1YMa, and 1YMb in order to interpret the concentration results because the concentration calculations use water velocity fields, not pressure fields, as input from the hydrologic calculations. These output variables are discussed in Section 4.

3.0 DESCRIPTION OF CODES USED IN COVE 1

Several codes have been developed or specifically modified to use for NNWSI performance assessment calculations. In COVE 1, five of these codes were benchmarked by generating four sets of solutions to the problem published by Pickens et al.: SAGUARO, TRUST, FEMTRAN, a modified version of FEMWASTE (Yeh and Ward, 1981), TRUMP, and TRACR3D. SAGUARO and TRUST are codes that solve the partial differential equation for fluid flow in unsaturated porous media based on Darcy's law, which results in Richard's equation (Freeze and Cherry, 1979). GWVIP, a reservoir engineering code, was also used to perform the hydrologic calculations. In addition to Richard's equation, GWVIP includes a second momentum equation that accounts for air resistance to water flow. No contaminant transport calculations were made for the flow fields generated with GWVIP. FEMTRAN and TRUMP are mass-transport codes and were used to predict contaminant movement for the flow fields generated by SAGURO and TRUST, respectively. TRACR3D is a stand-alone code that calculates both fluid flow, based on Richard's equation, and mass transport. The mass-transport codes, FEMTRAN, TRUMP, and TRACR3D, are based on the advection-diffusion equation and conservation equations, with the inclusion of sorption as an additional term in the conservation equation. Sorption was modeled as an equilibrium, linear-diffusion process in COVE 1YMa and COVE 1YMb.

3.1 Characteristics of Codes

The cases solved by each code for COVE 1 are shown in Table 3-1. The characteristics of the codes are given in Tables 3-2 and 3-3, which summarize information described in the rest of this section and in the cited references.

TABLE 3-1

COVE 1 PROBLEMS SOLVED

	COVE 1N		COVE 1YMa		COVE 1YMb	
	Water Flow	Solute Transport	Water Flow	Solute Transport	Water Flow	Solute Transport
TRACR3D	X	X	X	X	X	X
SAGUARO	X		X		X	
FEMTRAN		X		X		X
TRUST (LBL)	X		X		X	
TRUST (PNL)	X					
TRUMP				X		X
GWVIP	X		X			

3.1.1 TRACR3D

TRACR3D is a three-dimensional, finite-difference, isothermal water-flow and contaminant-transport code developed at LANL by Bryan Travis. TRACR3D has been used at LANL to interpret experiments for geochemical transport properties of tuff. The code has been modified extensively from its original form as an oil-shale analysis code to aid in the analysis of the geochemical experiments and to perform phenomenological studies for radioactive waste disposal.

3.1.2 SAGUARO

The finite-element code, SAGUARO, was developed at SNL by Roger Eaton for the NNWSI Project to model nonisothermal water flow in a variably saturated, porous medium and has been used for near- and far-field modeling. It is based on the saturated-flow code, MARIAH (Gartling and Hickox, 1980 and 1982), which has been used at SNL to model saturated flow systems in geologic media and in weapons studies. SAGUARO is being used at SNL for the NNWSI Project to perform phenomenological studies of water-flow mechanisms, to make two-dimensional

TABLE 3-2

CHARACTERISTICS OF HYDROLOGIC CODES USED IN COVE 1

Code	Dimension	Numerical Technique	Governing Equations	Solution Technique	Boundary Conditions
TRACR3D[a]	3-D	Finite difference combined with method of characteristics, orthogonal elements	Air- and water-mass conservation, Richard's equation	Implicit, iterative, successive over-relaxation techniques	Specified pressure, fluid saturation or flux, free flow, ponding
SAGUARO[b]	2-D	Galerkin finite-element with quadrilateral or triangular elements,	Liquid-water mass and energy conservation, Richard's equation, Soret effect, Boussinesq model	Gaussian elimination, Crank-Nicolson	Specified heads or fluid flux, ponding
TRUST[c]	3-D	Integrated finite difference, arbitrary element shape	Liquid-water mass conservation, Richard's equation	Mixed implicit/ explicit	Specified heads or fluid flux, seepage face
GWVIP[d]	3-D	Finite difference, orthogonal elements	Gas and water-mass conservation, Richard's equation	No information available	No information available

a. Travis, 1984.
b. Eaton, 1983.
c. Narasimhan and Witherspoon, 1976 and 1977; Narasimhan et al., 1978.
d. Pahwa, 1983.

TABLE 3-3

CHARACTERISTICS OF RADIONUCLIDE TRANSPORT CODES USED IN COVE 1

Code	Dimension	Numerical Technique	Governing Equation	Transport Processes	Physical Models	Solution Technique	Boundary Conditions
TRACR3D[a]	3-D	Finite difference combined with method of characteristics	Solute conservation	Advection, dispersion, diffusion	Radioactive decay chains, equilibrium adsorption nonequilibrium sorption	Explicit or Runge-Kutta	Specified concentration or flux, leaching, band release
FEMTRAN[b]	2-D	Galerkin finite element, quadrilateral elements with bilinear functions	Solute conservation, Darcy's Law	Advection, dispersion, diffusion	Radioactive decay chains, equilibrium adsorption	Gaussian elimination	Specified concentration or flux, leaching, band release
TRUMP[c]	3-D	Integrated finite difference	Solute conservation	Diffusion, advection	Radioactive decay equilibrium sorption	Mixed implicit/explicit	Specified concentration and flux

a. Travis, 1984.

b. Martinez, 1985.

c. Edwards, 1972.

models of flow systems at Yucca Mountain, and to identify preferential pathways of water-flow for performance assessment sensitivity studies.

3.1.3 FEMTRAN

FEMTRAN, developed at SNL by Mario Martinez as an expansion of FEMWASTE, is a two-dimensional, finite-element, isothermal radionuclide transport code that requires a hydrologic field as input. Several unique features were incorporated in the FEMTRAN code to facilitate coupling with SAGUARO and to enhance the accuracy of the transport calculations. One such feature is the ability to calculate velocity histories from a given pressure-field history instead of requiring that velocities be input directly.

3.1.4 TRUST

The TRUST code is a three-dimensional, isothermal water-flow code originally developed at LBL by T. Narasimhan. It has been used widely for general unsaturated-flow problems in compressible, porous media. Two versions were run for COVE 1N: one at LBL and one at PNL. The original author is using the code at LBL for the NNWSI Project to make phenomenological studies of water-flow mechanisms and to do site-scale modeling. The version at PNL is essentially the same and is used by modelers at PNL to support both DOE and NRC studies. Only the LBL version was used subsequently in COVE 1YMa and COVE 1YMb.

3.1.5 TRUMP

The TRUMP code was originally developed by Edwards as a general, three-dimensional, finite-difference solver for heat transfer. As such, it solves the advection-diffusion equation but does not include mechanical dispersion. Narasimhan has modified the TRUMP code to model advective-diffusive transport of decay chains of radionuclides. TRUMP was used to solve the nondispersive transport for COVE 1YMa and COVE 1YMb by entering the hydrologic field generated by TRUST. Contaminant transport in COVE 1N was not calculated because TRUMP does not include a dispersion model.

3.1.6 GWVIP

The GWVIP code is a two-phase reservoir engineering code developed by Intera (Pahwa, 1983). It may be used to model two- and three-dimensional nonisothermal flow of water, air, and vapor. The unique feature of GWVIP is a separate equation for the gas phase, which, in COVE 1, was the air phase. The governing equation for flow used in the other hydrologic codes is for water flow only. This representation of flow in unsaturated media is valid as long as there is no significant resistance to flow caused by the presence of air. The COVE 1 problems were run by GWVIP both with and without including air-phase resistance.

3.2 Numerical Formulations

In the process of solving the COVE 1 problems, some modifications were made in the codes. FEMTRAN was modified to calculate a velocity field from an input pressure field and to include subroutines that use curves typical of Yucca Mountain. Certain numerical techniques proved to be more accurate than others. For example, it was shown that an averaged, "lumped-mass" method of solution for velocities in the finite-element code, SAGUARO, did not work as well as the standard discontinuous method in FEMTRAN. These numerical sensitivities are discussed in Section 4.

The discretization of the domain was left up to each modeler. The meshes used by each code are shown in Appendix A (Figures A-1 through A-5). Each of the codes used mass balances to some degree as checks on the results. However, some of the codes did not have the capability to perform rigorous computation of mass balances for individual cells before being used in COVE 1. Subsequent work has established routines for calculating cell-mass balances in all the codes. The mass balances for the COVE 1 problems are compared in Section 4.

4.0 RESULTS AND DISCUSSION OF COVE 1

4.1 Code Capabilities and Computer Requirements

The capabilities of the codes used to model the unsaturated flow and transport problems were demonstrated by the qualitative agreement in most of the COVE 1 results. All codes except TRUMP, which had no dispersion model, generated similar flow and concentration fields for COVE 1N. However, the concentration results differed in the vicinity of the exit hole from those published by Pickens et al. The flow and concentration fields predicted by the codes for COVE 1YMa and COVE 1YMb were likewise in qualitative agreement. These results are significant because this is the first time that the pairs of codes--SAGUARO and FEMTRAN, and TRUST and TRUMP--have been used to solve the coupled problems of hydrologic flow and contaminant transport, and that the results have been compared. In this section, some of the problems that had to be resolved to obtain good solutions for the coupled problem are discussed. Some indications of the numerical accuracy and sensitivities of the codes are also shown by quantitative comparison of the results, where appropriate. The qualitative comparisons are shown in the contour plots and profiles in this section and in Appendices B and C.

Quantitative differences in the results were usually small (less than a few percent). For the hydraulic heads, the quantitative differences were within 20% for moisture contents but differed by as much as factors of 2 to 5 for the solute concentrations. Differences in solute concentrations were greatest very near the exit. Relative concentrations were seen to be sensitive to grid refinement through the velocity term, which depends on the gradients of the pressure across mesh cells. Differences in the modeling approaches, such as

interpretation of boundary conditions, grid refinement, time steps, and convergence criteria, account for some of the quantitative differences in the results. The mesh sizes and time steps are given in Table A-1.

The numbers of elements used for the codes were similar. Between 247 and 434 elements were used in the codes that calculate hydrology alone. A combined total of 1,287 to 1,728 elements was used for the hydrologic-flow and contaminant-transport results for COVE 1N. Because of the low fluxes in the problem, fewer elements were required for COVE 1YMa and COVE 1YMb, which allowed considerably coarser meshes to be used for transport calculations than were required in COVE 1N. The largest number of elements were used in the TRACR3D calculations where no attempt was made to optimize the mesh size.

The computer times varied from 120 s on an IBM 360 for the results of Pickens et al. in COVE 1N, to 1,920 s on a Cray for the TRACR3D results in COVE 1YMa. Although many more time steps were used, TRUST required much less computer time than the other codes. Typically, integrated finite-difference codes require less computer time. The times required for the TRUMP contaminant-transport calculations for COVE 1YMA and COVE 1YMb were reported by Narasimhan to be small compared to those required for TRACR3D and to be on the same scale as those shown in Table A-1 for FEMTRAN.

The computer-run statistics shown in Table A-1 indicate that these codes required similar but not equivalent mesh sizes and that the time might be significantly shorter using the integrated finite-difference method. However, because no optimization was done for the TRACR3D runs, and only limited sensitivity to mesh size and time-step size was investigated for the SAGUARO and FEMTRAN calculations, this conclusion is only tentative.

4.2 Results of Calculations

4.2.1 Basis for Comparisons

Two categories of results were compared, as shown in Table 4-1. In Category A, the statistics of running the codes were compared. The parameters in Category A--overall mass balances, run times, and accuracy and convergence criteria--are given in Table 4-2 and Table A-1 and are discussed below. The second set of results in Table 4-1, the results for Category B, are those variables analyzed to compare the solutions of the water-flow and contaminant-transport problem. All parameters were analyzed, but only significant results, representative of the comparisons of all of the parameters, are discussed in this report.

Not all participants were able to provide all Category B results, either because manpower was lacking or because a code did not have the capability to produce the results. The Category B output variables provided by each participant are summarized in Table 4-3 and are discussed in this section. These discussions reflect the consensus of the participants in the final COVE 1 workshop held in La Jolla, California, April 1984.

4.2.2 Results of COVE 1N

The Category B output variables published by Pickens et al. for the reference case, COVE 1N, were

- water-table position,
- water-table decline,
- hydraulic-head contours,
- moisture-content contours,
- relative-concentration contours, and
- relative-concentration history at the exit.

These Category B variables are compared in Figures 4-1 through 4-6.

TABLE 4-1

OUTPUT VARIABLES FOR COVE 1 PROBLEMS

Category A Results	Parameter
A1	Mesh
A2	Mass balances (and how formulated)
A3	Run times
A4	Accuracy and convergence criteria
A5	Input formulations, run listings, and estimated set-up time
	In the following list of variables, the water table location is that defined in COVE 1N. The corresponding variable in COVE 1YM is the uppermost contour for Ψ = -1,000 cm (COVE 1YMb) or fluid pressure (Ψ) at the exit (COVE 1YMa).

Category B Results	Variable
B1	Spatial position of water table (Ψ) at specified times: p,t*
B2	Water table decline or (Ψ) at left boundary (or at the exit for COVE 1 YMa) as a function of time: p,t
B3	Hydraulic head as a function of time, position: p,t
B4	Water content as a function of time, position: p,t
B5	Relative concentration as a function of time, position: p,t
B6	Volumetric concentration as a function of time, position: p,t
B7	Relative concentration at the exit as a function of time: p,t
B8	Velocity as a function of time at x = 5 m, z = mid-exit: p,t,h,v*
B9	Velocity as a function of time at x = 4.9 m, z = 0.85 m: p,t,h,v
B10	Velocity as a function of time at x = 5 m, z = 0.85 m: p,t,h,v
B11	Relative concentration as a function of height at x = 5 m, times as specified previously: p,t,
B12	Velocity as a function of height at x = 5 m; times are as specified previously: p,t,h,v

*p = plot
h = horizontal component
t = table
v = vertical component

TABLE 4-2

MASS BALANCES AND CONVERGENCE CRITERIA

Code	Mass Balance			Convergence Criteria[a] (cm)
	IN	IYMa	IYMb	
TRACR3D[b]	0.75%	<0.05%	4.2%	$\Delta P < 0.01$
SAGUARO[c]	<1%	<1%	<1%	$\Delta/P < 0.001$
TRUST[d]	<2%	2-8%	<1%	$\Delta P < 0.05$
GWVIP[c]	<0.01%	<0.03%	NA	$\Delta P < 0.1$ or $\Delta\theta < 0.05$
TRUMP	NA	e	d	
FEMTRAN	<1%	<1%	<1%	

a. ΔP is the maximum allowable change in pressure between successive iterations within a step.

b. Mass balance is calculated as one minus the current system mass normalized by the sum of the original system mass and the cumulative mass that flowed out the boundaries and source/sinks.

c. The mass balance is calculated as the difference between the sum of all mass that flowed out the boundaries and the rate of change of mass stored in the system within a time step, normalized by the current amount of mass in the system.

d. The mass balance is calculated as the current mass in the system minus the sum of the original system mass and all source/sinks and mass that flowed out the boundaries, normalized by the original mass in the system.

e. Information is unavailable or not calculated.

TABLE 4-3

COVE 1 RESULTS RECEIVED FOR FINAL EVALUATION

Code	A1	A2	A3	A4	A5	B1	B2	B3	B4	B5	B6	B7	B8	B9	B10	B11	B12
SAGUARO/FEMTRAN																	
COVE 1N	X	X	X	X	X	X	X	X	X	X	X	X	X	X	X	X	
COVE 1YMa	X	X	X	X	X	X	X	X	X	X	X	X	X	X	X	X	
COVE 1YMb	X	X	X	X	X	X		X	X	X	X	X	X	X	X	X	
TRACR3D																	
COVE 1N	X	X	X	X	X	X	X	X	X	X	X	X	X	X	X	X	X
COVE 1YMa	X	X	X	X	X		X	X	X	X	X	X	X	X	X	X	
COVE 1YMb	X	X	X	X	X			X	X	X	X	X	X	X	X	X	
TRUST/TRUMP																	
COVE 1N	X	X	X	X	X	X	X	X	X			X	X	X		X	
COVE 1YMa	X	X	X	X	X	X	X	X	X	X	X	X	X	X	X	X	
COVE 1YMb	X	X	X	X	X	X		X	X	X	X	X	X	X	X	X	X
GWVIP																	
COVE 1N	X	X	X	X		X	X	X	X			X	X				X
COVE 1YMa	X	X	X	X	X			X	X			X	X				X
COVE 1YMb																	

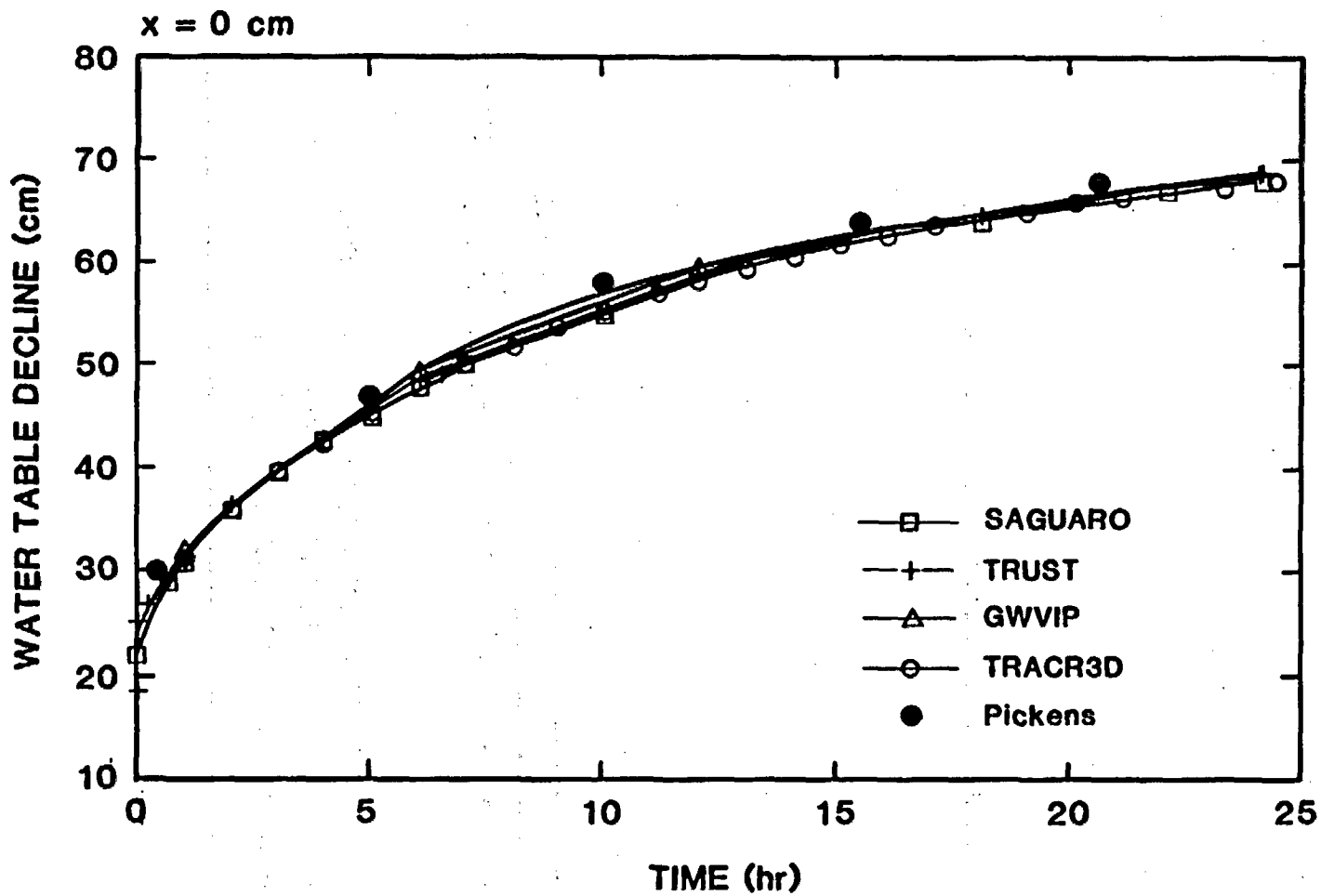

Figure 4-1. Water-Table Decline in COVE 1N

a) t = 1 hr

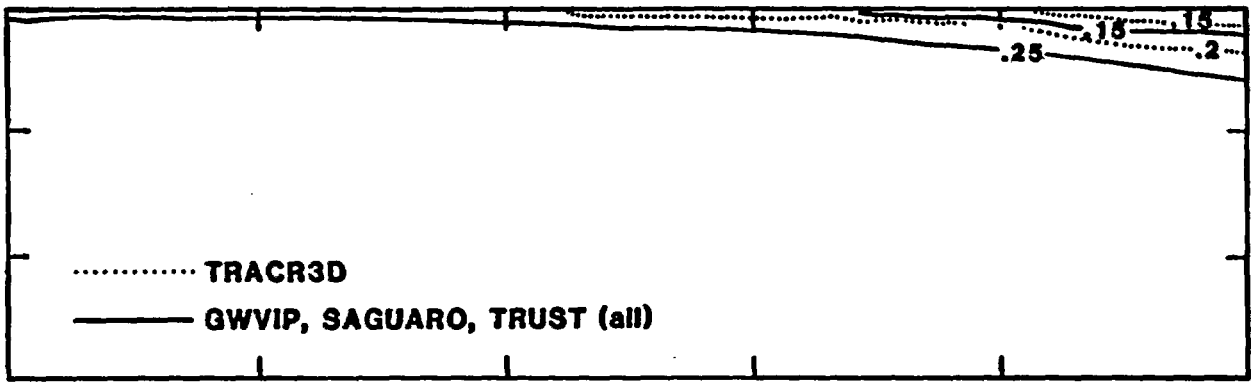

b) t = 12 hr

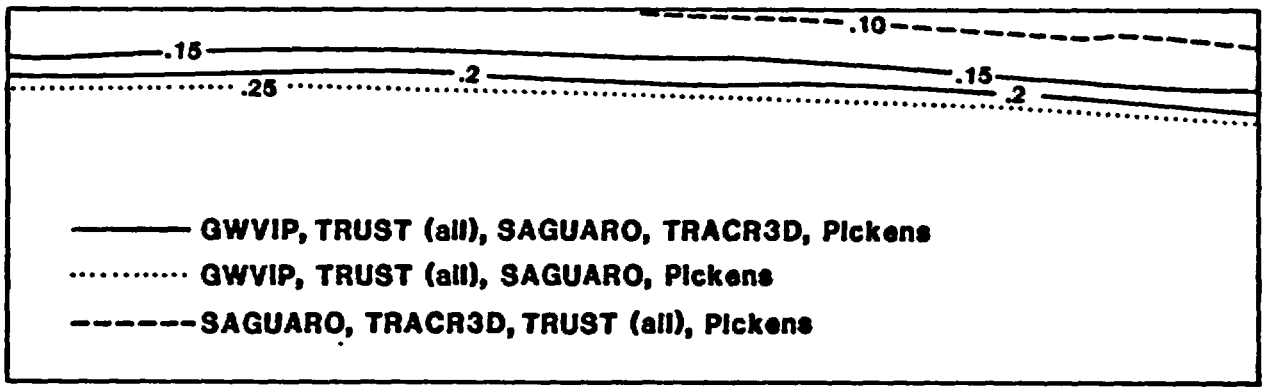

Figure 4-2. Moisture Content in COVE 1N

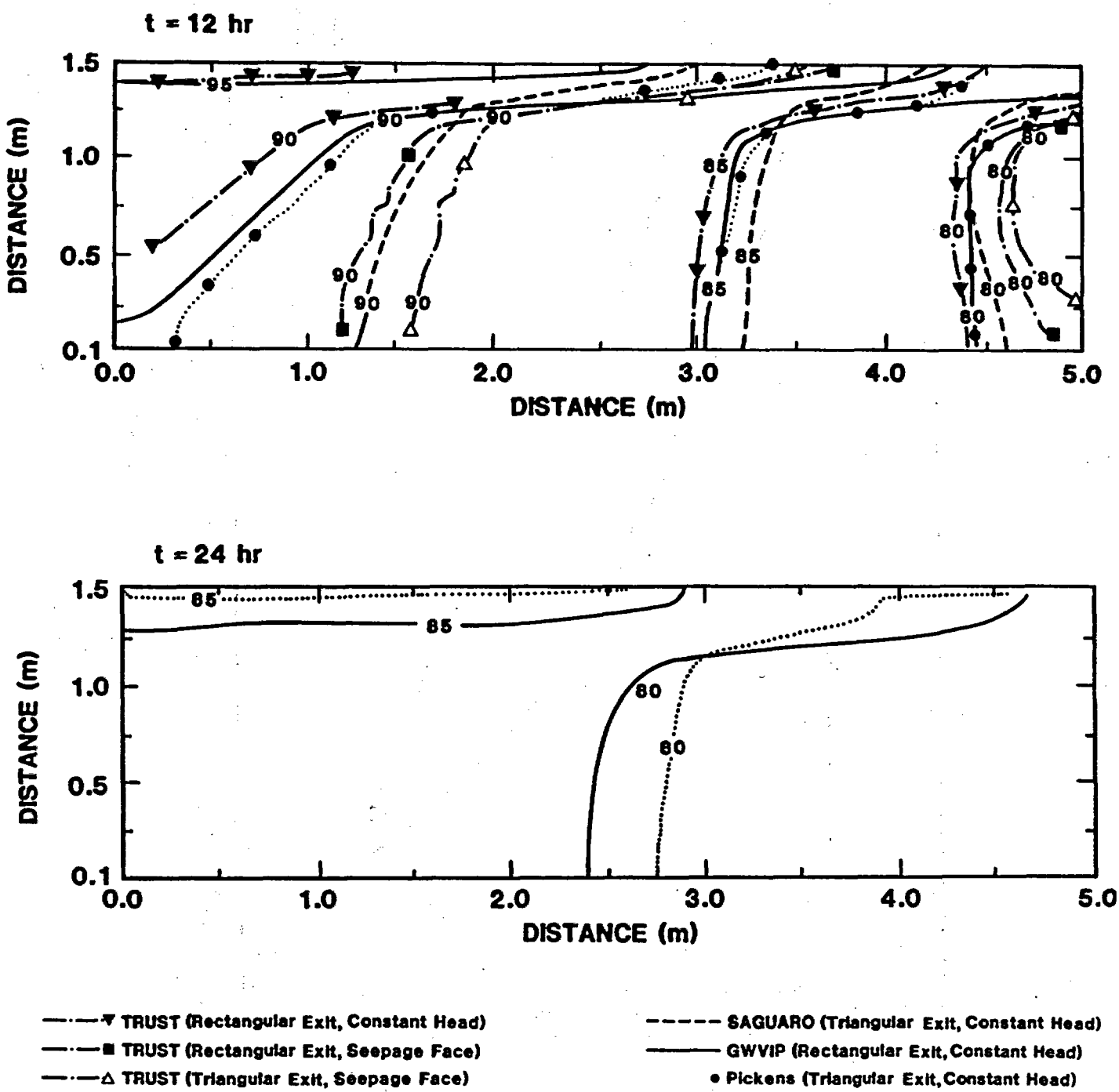

Figure 4-3. Hydraulic Head in COVE 1N

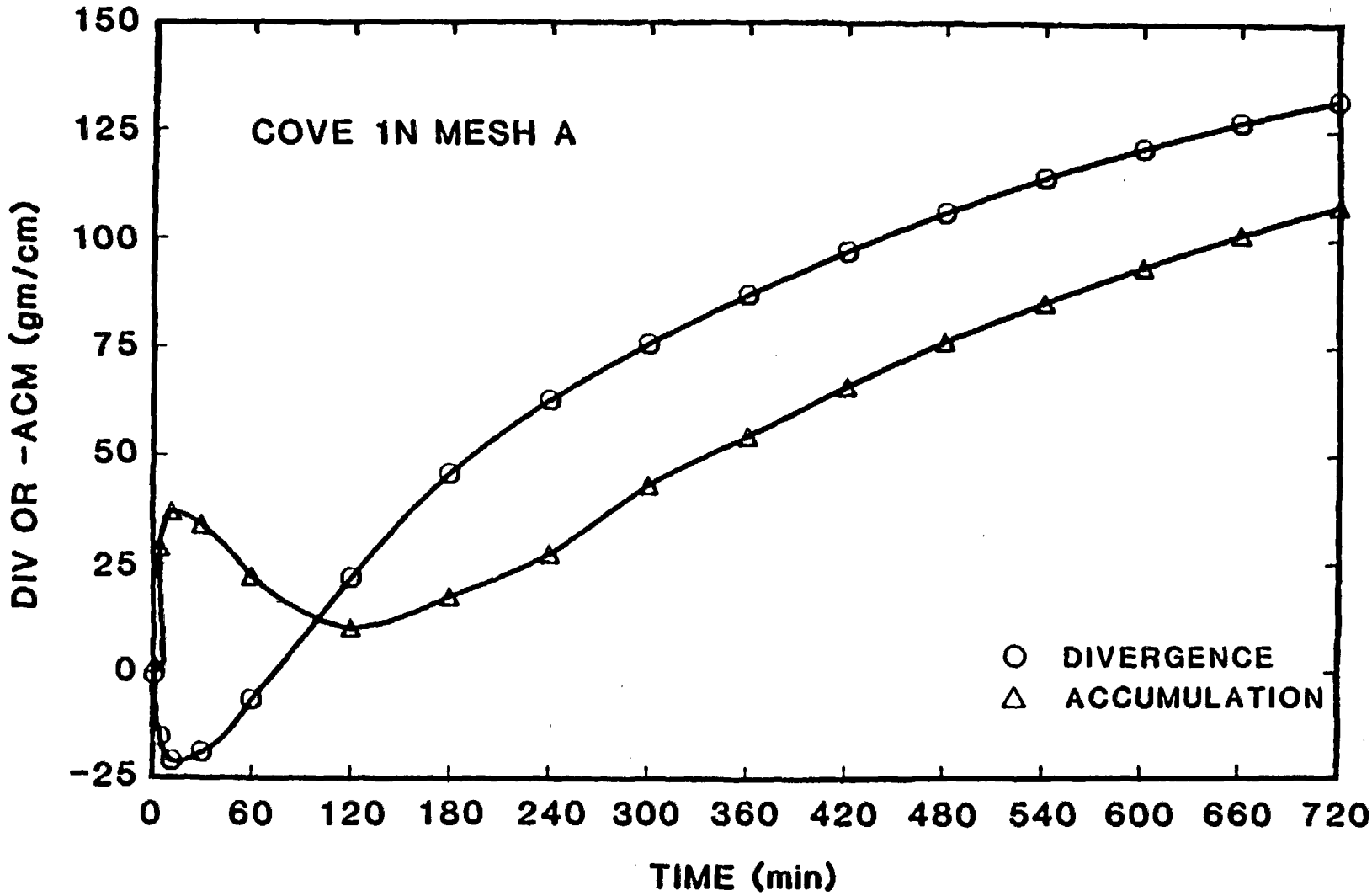

Figure 4-4. Mass Balance for FEMTRAN Calculations in COVE 1N

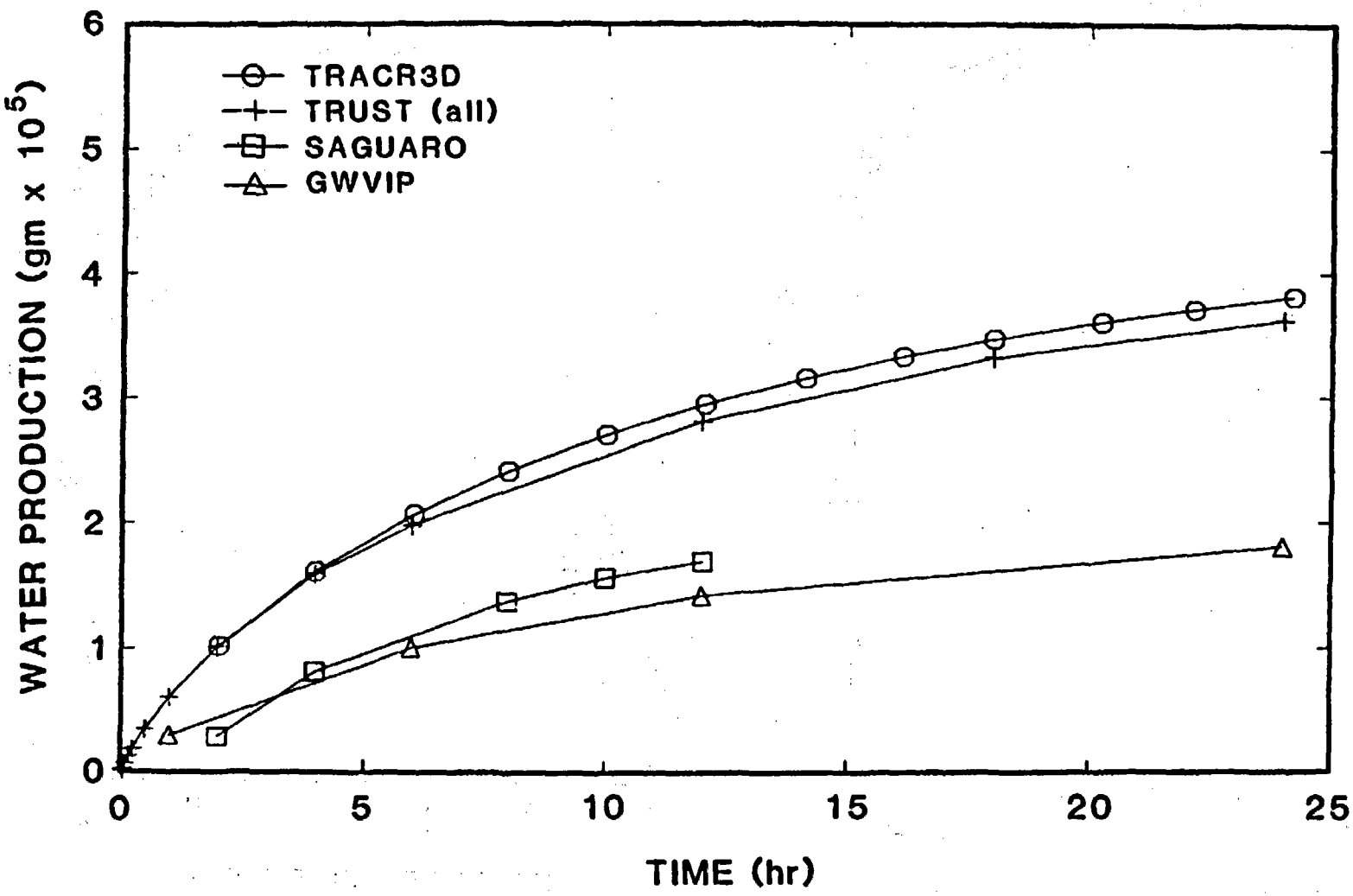

Figure 4-5. Water Production in COVE 1N

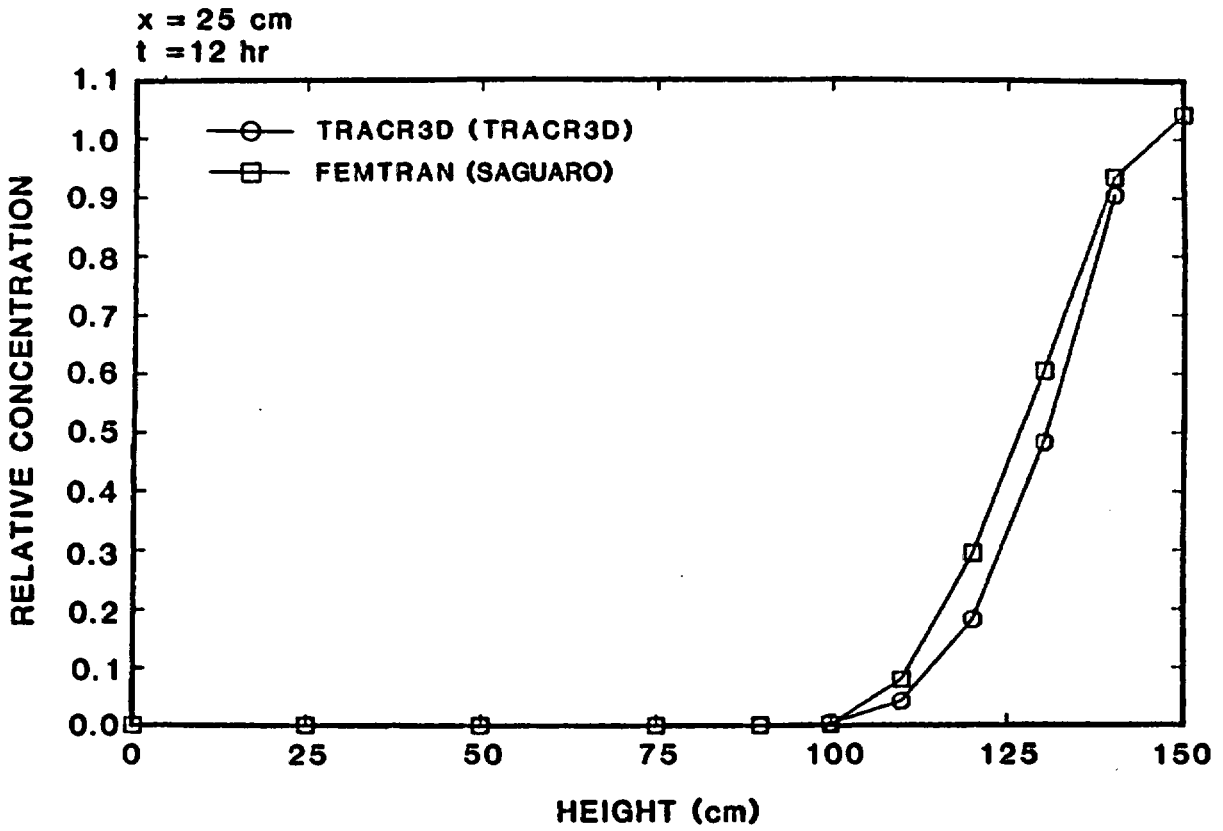

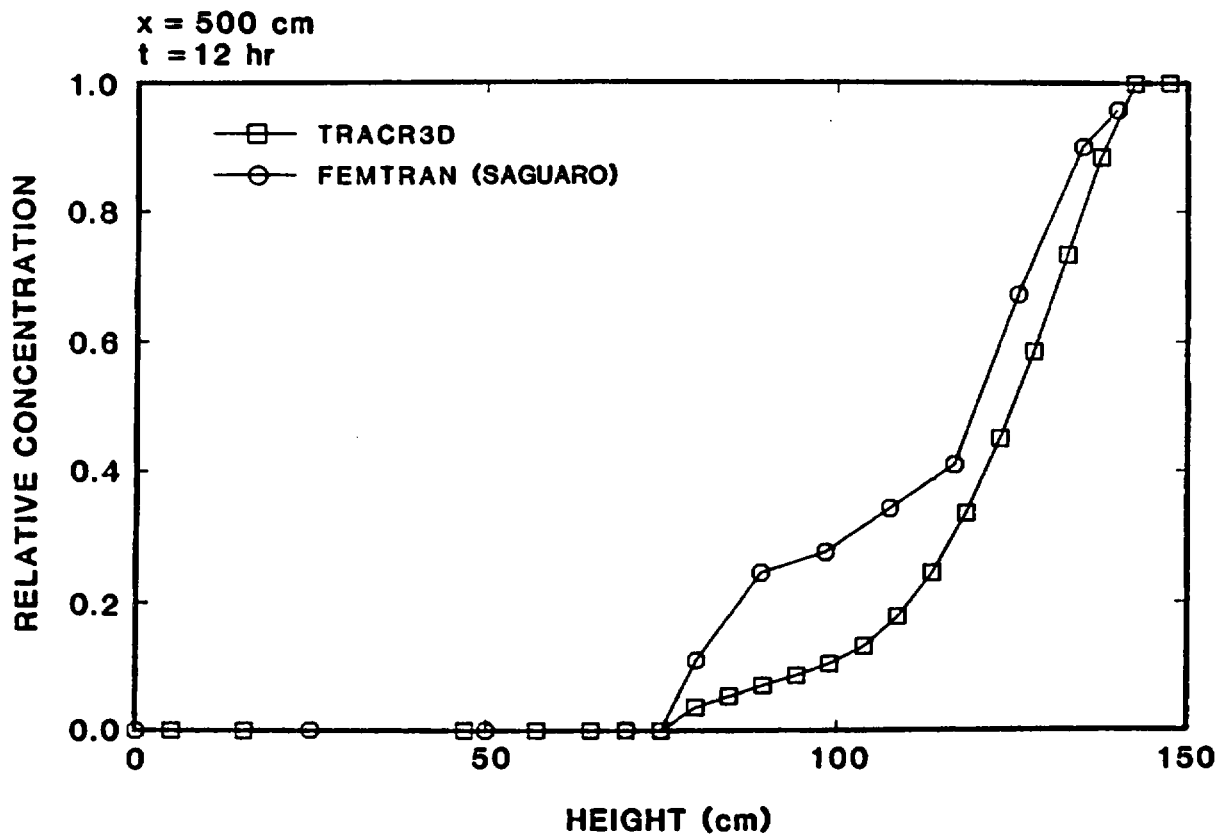

Figure 4-6. Relative Concentrations in COVE 1N

Water Table and Moisture Content

Figures 4-1 and 4-2 show that the water table decline and moisture-content contours, which reflect water table position, agree very well; there is less than 5% difference in the results.

Hydraulic Head

Hydraulic head contours (Figure 4-3) agree well on the right side of the system; however, on the left side, the results show two different behaviors. The 90-cm-head contours calculated using GWVIP, Pickens' model, and TRUST with a constant-pressure boundary condition, fell to the left of those calculated using SAGUARO. This discrepancy is not as great as it at first appears because the hydraulic head gradient is very small in this region. The actual values for the hydraulic heads at a point calculated by all the codes are in much closer agreement, within 7%.

In the TRUST calculations that used a seepage-face boundary condition at the exit, both rectangular and triangular exit geometries were used. A difference of about 50% in the exit area affected the hydraulic heads as shown in Figure 4-3. The triangular exit hole, which had the smaller area, resulted in a shift to the right in the head contours near the right boundary, indicating increased resistance to flow. The location of the head contours shifted to the left about 20%. However, the actual values for head differ only by 1% to 2% at any one location in the system.

Similar effects of exit area were reported in the SAGUARO calculations; that is, the location of the hydraulic-head contours differed by as much as 20% even though the actual values for the hydraulic head at a point varied by less than 1%. This apparently large difference in contours for small differences in head values is explained by the low gradients of hydraulic head (as low as 2.5%). This difference may also be seen for other variables, such as moisture content and relative concentration when the gradients are correspondingly

small. Thus, although contours can be instructive for qualitative comparisons in benchmarking activities, they can also be misleading if used for quantitative interpretations of relative accuracy and sensitivity.

Water Velocities, Mass Balances, and Cumulative Productions

The relative accuracies and sensitivities of the hydrologic calculations in COVE 1N were investigated to a limited extent by comparing water velocities, water-mass balances, and cumulative water productions at the exit. Water velocities were calculated by all the hydrologic codes from the gradients of the pressure within a cell. Darcy's law was used to derive these local velocities, which depend on the local mesh size. These velocities can be sensitive to the mesh size, especially in regions where gradients are large. The velocities in the regions surrounding the exit sometimes differed by as much as factors of 3. However, far away from the exit hole, the velocities were similar.

The mass balance in the hydrologic field used in FEMTRAN calculations for COVE 1N is indicated by comparing the divergence and accumulation of water mass in Figure 4-4. The global mass balance percentages of the other codes are listed in Table 4-2. The difference between the divergence and accumulation curves at 5 hr in Figure 4-4 indicates a net error of 20 gm/cm in the hydrologic field used by FEMTRAN. This error can be compared to an initial water mass in the system of 2.25×10^4 gm for a unit depth of 1 cm. Similarly, the mass balances shown in Table A-2 for the other codes used in COVE 1N are within 2%.

In comparing water production at the exit, the results from TRUST and TRACR3D showed more water exiting the flow domain than did SAGUARO and GWVIP (Figure 4-5). At 12 hr, TRUST and TRACR3D calculated a cumulative water flux out the exit hole of 2.85×10^3 gm/cm and 2.93×10^3 gm/cm, respectively; 1.68×10^3 gm/cm was predicted using SAGUARO and GWVIP. The maximum difference of almost a factor of 2 in

the water production, however, translates into the difference between 6% and 13% of the total amount of mass initially in the system.

Relative Concentrations

The profile shapes and absolute values in relative concentrations along the right boundary calculated by FEMTRAN differed from those calculated by TRACR3D. At the first COVE workshop, the modelers agreed that differences in the velocity fields and possible numerical losses could be reasons for this spread in the results. Thus, besides comparing the velocities at the exit for SAGUARO and TRACR3D, a more rigorous treatment of the impermeable boundaries was employed in FEMTRAN. Also, water productions at the exit were compared.

It was postulated that the treatment in the transport calculations of the impermeable boundary condition would have a potential effect on concentration results as the result of numerical losses in the finite-element codes. Finite-difference methods are able to impose a water-flux boundary condition of exactly zero at the right boundary. However, the finite-element water-flow calculations can generate both positive and negative velocities (on the order of 1.0×10^{-17} cm/s) along an impermeable boundary, which causes some contaminants to "leak" out. The small but nonzero negative velocities do not compensate for the loss of these contaminants from the system. The small negative fluxes that bring water back into the problem are a numerical artifact created by finite-element solution to the water-flow field to force a net integrated flux of zero over the entire impermeable boundary. However, these small negative velocities for water flowing back into the system do not convect contaminants in the transport-contaminant calculations. In the transport calculations, where the input velocity field is generated using an impermeable boundary condition for convective flux, the Neumann boundary condition given by Equation 7 should theoretically be sufficient to ensure an impermeable boundary for the solute:

$$\frac{\partial c}{\partial \vec{\eta}} = 0 \ . \qquad (7)$$

Equation 7 is the solute boundary condition specified in Figures 2-2(b) and 2-4(c) in which it is assumed that the water flux is everywhere zero at impermeable boundaries. This assumption is different from the assumption that a net water flux of zero is integrated over the entire impermeable boundary. Thus, when solving the convective-dispersive equation at impermeable boundaries, using Equation 7 as the boundary condition for solute transport, net convective water flux may be zero integrated over the entire impermeable boundary, but the corresponding net convective solute flux can be positive. To eliminate this problem, the convective flux summed with the diffusive gradient was specified to be zero by using the Cauchy boundary condition (Equation 8) in FEMTRAN at the impermeable boundaries to produce the final results reported here.

$$q_n C + \theta D \frac{\partial c}{\partial n} = 0 \ . \tag{8}$$

The degree of sensitivity to the boundary-condition specification will increase as the concentration fluxes of concern approach the order of numerical dispersion in a problem. When modeling the repository, this effect can be eliminated by judicious location of boundaries, choice of mesh size, and use of Equation 8 for impermeable boundaries in the transport calculations.

The comparisons at the exit hole illustrate the maximum differences between the codes because this region has the highest gradients and the most rapidly changing conditions, and is the most influenced by boundary conditions and the geometry of the numerical approximation. For instance, varying the number of nodes used at the exit hole in SAGUARO while keeping the same number of elements changed the spatial location of the head contours, near the exit hole only, by about 20%. (This result corresponded to a difference of only a few percent in the head at a single location, however.) Therefore, FEMTRAN and TRACR3D concentration profiles as functions of height were also compared at an interior node and at the right boundary (Figure 4-6). The agreement was better both qualitatively and quantitatively

at the interior node. The profiles at the interior node had the same shape and a maximum difference of 60%, compared to a difference of more than a factor of 2 near the exit.

TRACR3D results gave consistently lower concentrations than the FEMTRAN results. These concentration results were consistent with the comparison of the hydrologic results predicted by TRACR3D, SAGUARO, and Pickens et al. The concentrations at the exit (Figure 4-7), calculated by the Pickens model, FEMTRAN, and TRACR3D differed by up to a factor of 3. The greatest difference was between the Pickens' results and those of FEMTRAN and TRACR3D. At the La Jolla workshop, it was suggested that, because the differences persisted after treatment of velocities and numerical losses had been eliminated as problems, the manner in which the time steps were allowed to vary could be the cause for the discrepancies. Pickens et al. used 45 time steps for the problem, compared to 250 for TRACR3D and 92 for FEMTRAN, indicating the use of larger time steps. Stability analysis of the advection-diffusion equation shows that a "numerical-diffusion" term is introduced in the governing equation in numerical approximations that rely on differencing methods. This numerical-diffusion term is proportional to the product of the time step and the square of the velocity (Hirt, 1979). Using larger time steps results in increasingly greater effects of numerical diffusion, which can account for the higher concentration profiles at lower depths plotted by Pickens et al. and FEMTRAN. The use of larger time steps may also account for transport of contaminant below the exit in the Pickens calculations (Figure 4-8) not seen in any of the other calculations.

Effects of Boundary Conditions and Velocity Formulations on Results

The few qualitative differences in COVE 1 results were most evident at the boundaries of the system, where the finite-difference and finite-element solution techniques implement boundary conditions differently. In finite-difference codes, a no-flux condition can be specified exactly on a boundary; whereas, in the finite-element codes, small but nonzero local velocities are often calculated on a boundary.

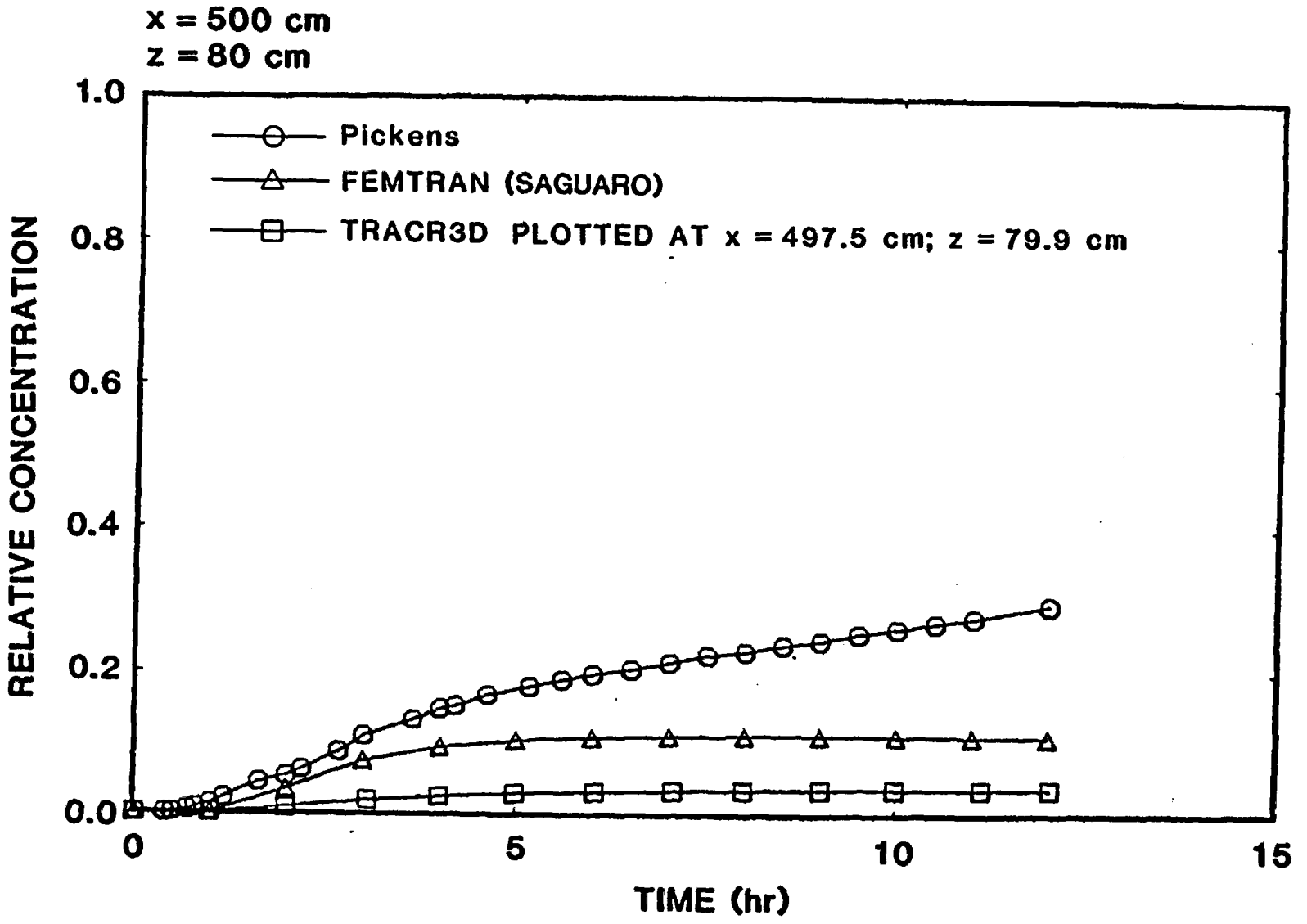

Figure 4-7. Relative Concentrations at the Exit in COVE 1N

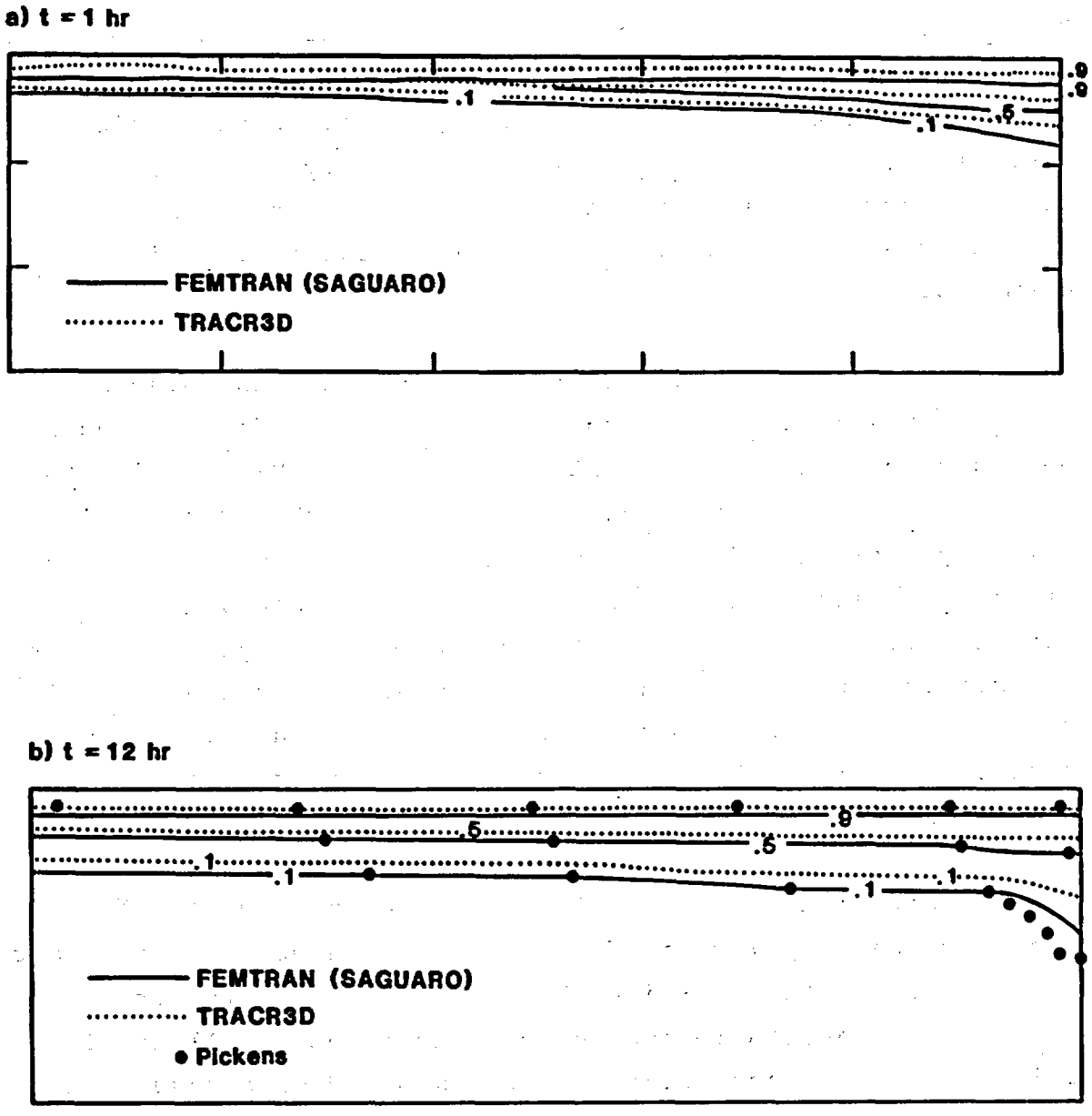

Figure 4-8. Concentration Contours in COVE 1N

Globally, the no-flux condition is strictly enforced in the finite-element codes because the local nonzero velocities on the boundary are both positive and negative and compensate for each other. In addition, the techniques of calculating velocities from the pressure fields in finite-element codes often result in discontinuous velocities at nodal points. Thus, the sensitivity of the solutions for pressure and relative concentration to the numerical technique used in the finite-element code, SAGUARO, to calculate velocities was examined.

Most finite-element water-flow codes use the discontinuous velocity formulation. The discontinuous velocity formulation is a direct method of calculating velocities by applying Darcy's law to the gradients of the continuous pressure field in each element. The resulting velocity field is discontinuous at the nodal points because there are discontinuities in the gradients at element boundaries. A lumped-mass matrix-solver option in SAGUARO can be used to generate continuous velocities, but use of this option smears out differences in pressure. Results using these two methods showed that the discontinuous method gave better mass balances and converged more quickly for the COVE 1N problem.

A third method was developed in the process of solving the COVE 1 problems that applies the finite-element method of weighted residuals to Darcy's law to determine the velocities from the pressure field. This method results in continuous velocities at all nodal points. This method was incorporated in FEMTRAN and gave results for concentration profiles and velocities near the exit that were almost identical to the results obtained using the discontinuous method in SAGUARO (Eaton and Martinez, in preparation). In contrast, the lumped-mass method smeared the velocities near the exit and the concentration profiles near the right boundary. Mass balances indicated that the lumped-mass method was nonconservative; whereas, the discontinuous and continuous methods resulted in essentially the same degree of accuracy indicated by mass balances of both water and contaminant.

The significant difference in the relative concentration histories calculated using FEMTRAN, TRACR3D, and Pickens' model occurred at the exit. This variance was attributed to several factors: difference in mesh sizes or geometries at the exit resulting in different velocity fields, the different formulation of velocity from pressure solutions, numerical losses at the right impermeable boundary, and numerical dispersion. The sensitivity of the individual transport results to some of these factors was examined by using the SAGUARO and FEMTRAN codes, the TRACR3D code, and a stability analysis of the advection-diffusion equation.

Three mesh sizes, which contained 247, 221, and 884 elements, were used for the hydrologic calculations in SAGUARO (Figures A-1a, A-1b, and A-1c). The coarsest mesh affected concentration results by about 20% (Figure 4-9). The pressure gradients, which became large only at the exit, were smeared over greater distances in the coarse mesh; thus, the velocities and concentrations were affected over a few exit diameters. The finest grid used in the calculations (884 elements) did not differ significantly from those that used the moderate 247-element grid, which indicates that the moderate grid was appropriate for the problem. It was surprising that the addition of 26 elements seemed to be as good as the addition of 663 elements, indicating that refinement beyond relatively coarse meshes may be unnecessary for NNWSI calculations.

The relative concentrations predicted by FEMTRAN in Figures 4-6 through 4-8 were calculated using the velocities produced by SAGUARO with the discontinuous method. As the mesh was refined (Figure 4-9), results from all three methods converged to yield the same profiles.

The hydraulic heads calculated using SAGUARO, TRACR3D, and TRUST, using a constant boundary condition (Figure 4-10a), were in close quantitative agreement (within a few percent) at the exit. The results of GWVIP differed from the results of other codes at the upper boundary; whereas, the results of TRUST using the seepage-face boundary condition differed from the others near the exit. There was

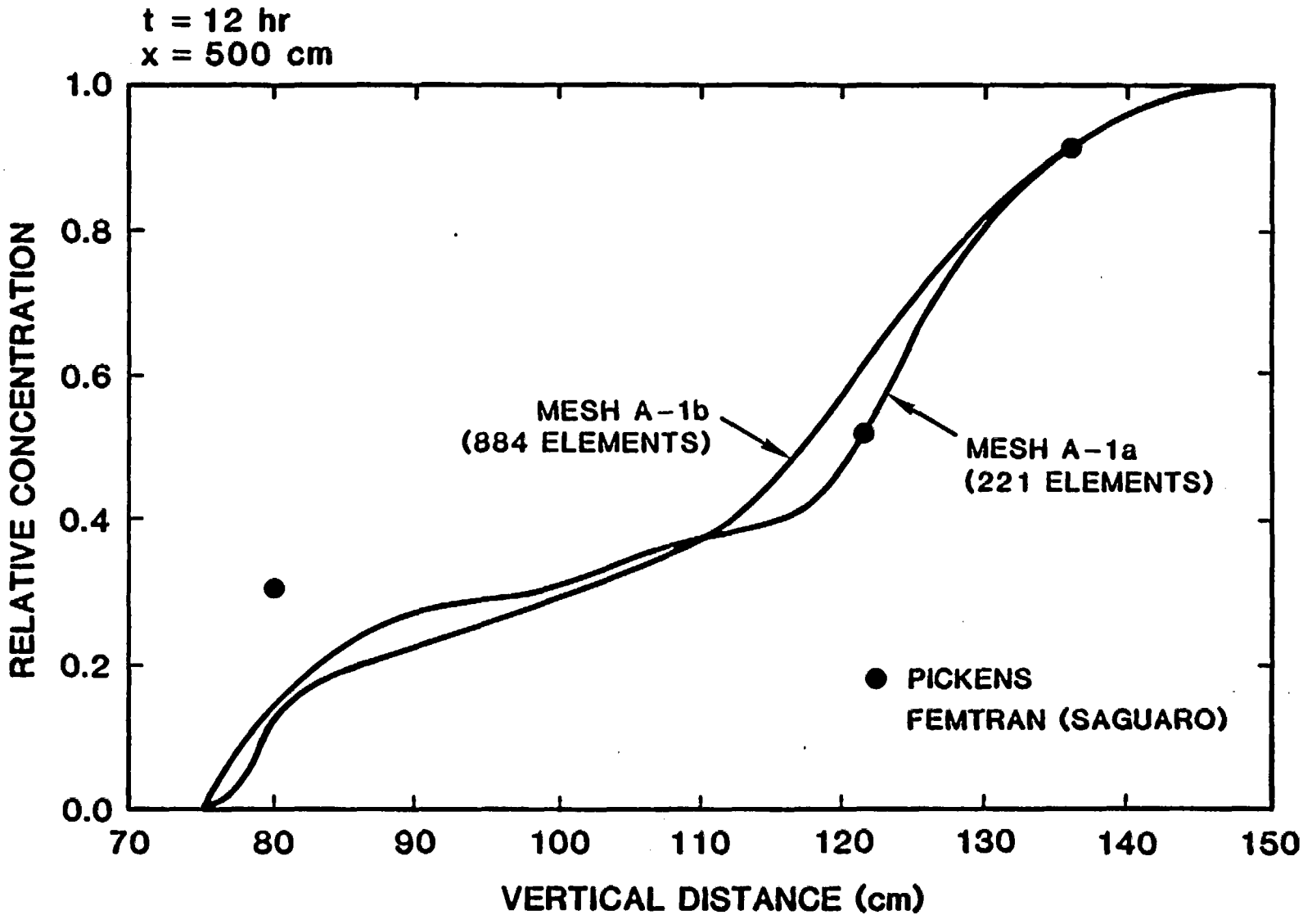

Figure 4-9. Effect of Mesh Refinement on FEMTRAN Relative Concentrations in COVE 1N

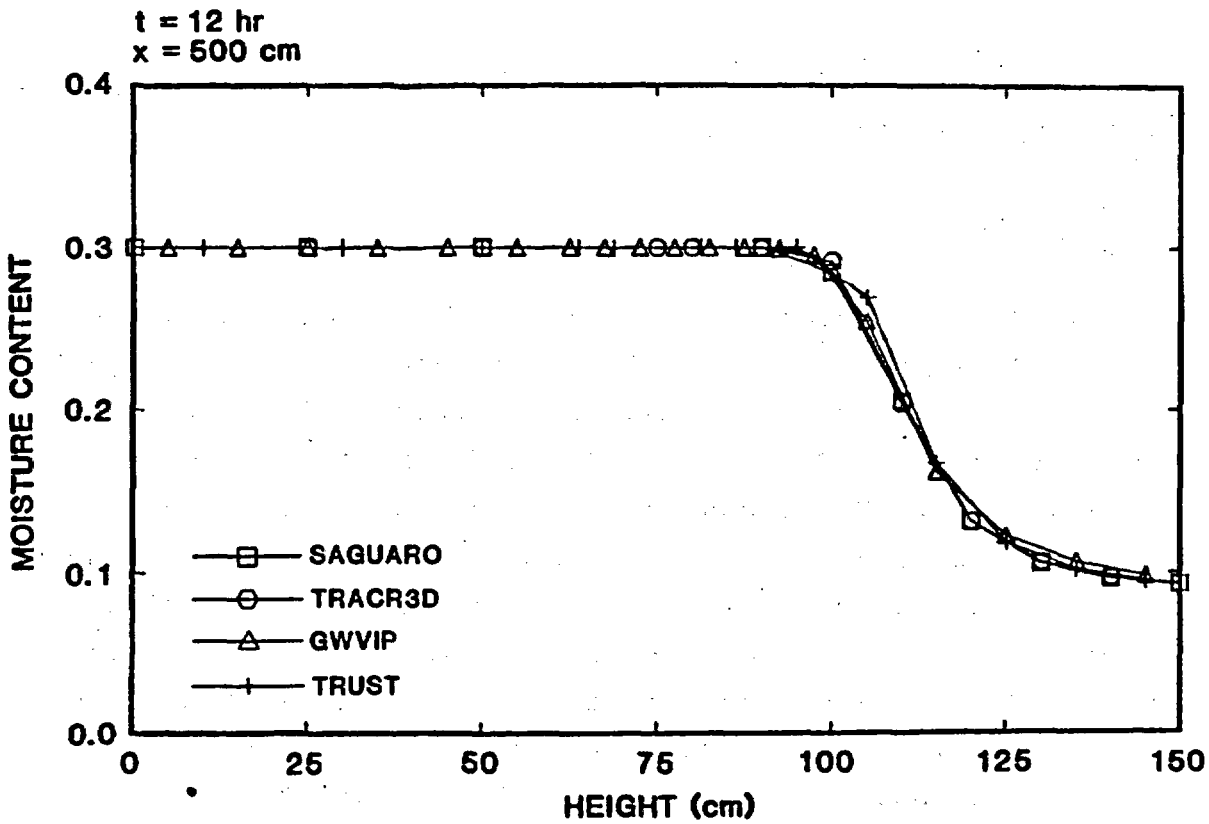

a.

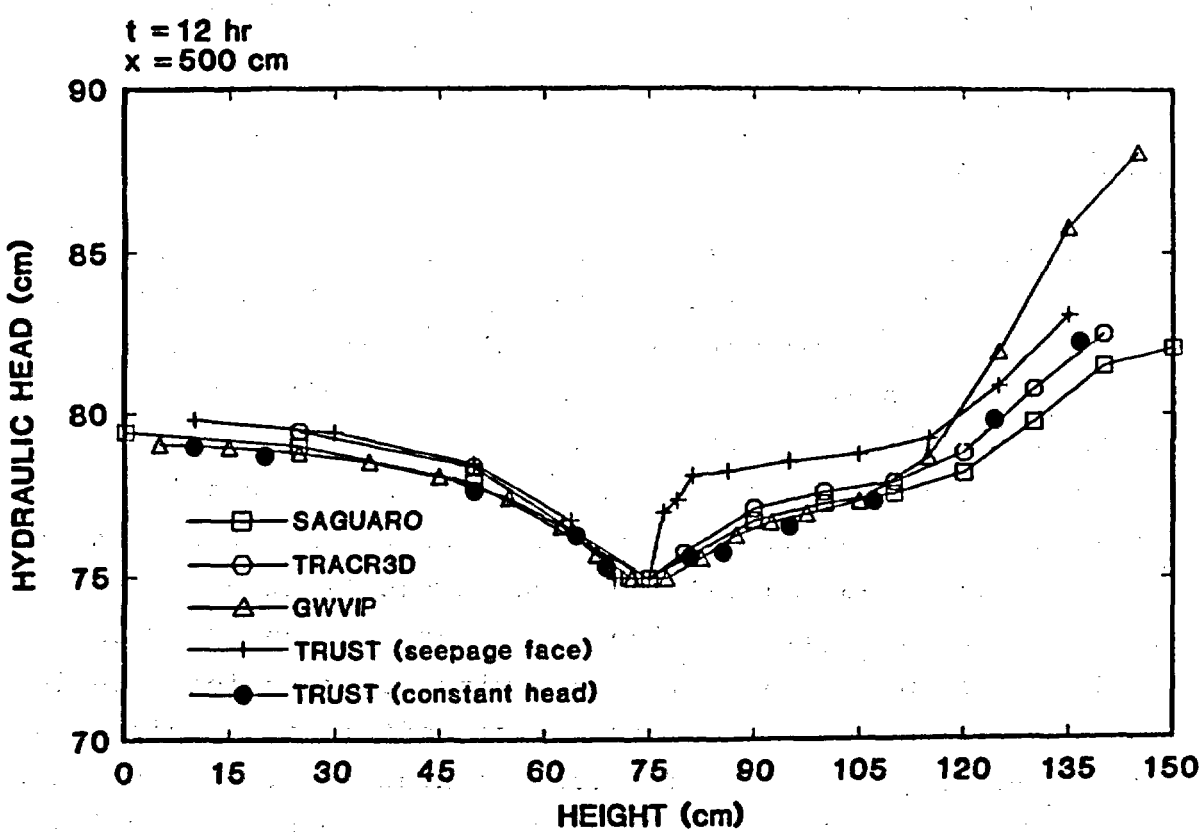

b.

Figure 4-10. Hydraulic-Head and Moisture-Content Profiles in COVE 1

little detectable difference between the moisture content profiles at the boundary (Figure 4-10b).

4.2.3 Results of COVE 1YMa

The hydrologic contours produced for COVE 1YMa using SAGUARO, TRUST, TRACR3D, and GWVIP are plotted in Figures B-1 through B-4 to allow a qualitative comparison of the results. Relative concentration contours produced by TRACR3D, TRUMP, and FEMTRAN are compared in Figures B-5 and B-6. These concentration contours are very flat, allowing a quantitative analysis of accuracy by comparing the concentration profiles to the analytic solution to the diffusion equation (Carslow and Jaeger, 1980). This comparison is made in Figure B-7 in which the results of FEMTRAN along the right boundary are plotted. Hydraulic-head and relative-concentration profiles produced by all the codes along the right boundary and at two interior points are plotted in Figures B-8 through B-10 and Figures B-11 to B-14, respectively, to compare quantitative results at different locations in the flow region.

Hydrologic Contours

Pressure-head contours at 100, 7,500, 10,000, and 20,000 yr are shown in Figures B-1 and B-2 for the four hydrologic flow codes. (In Figure B-1(c), both hydraulic-head and pressure-head contours at 1,000 yr are shown in order to compare the results more closely.) All head contours are in excellent qualitative agreement and are very close quantitatively as the pressures are usually within 5% of each other at the same location. The shapes of the moisture-content contours in Figures B-3 and B-4 are also in excellent qualitative agreement. However, the quantitative agreement between TRUST and the other codes does not appear to be as good, with dryer regions predicted by TRUST. The gradient of the moisture content in the regions where the disagreement is greatest ranges from as high as 180% change per meter (SAGUARO at t = 100 yr) to as low as 18% change per meter (SAGUARO at t = 20,000 yr). These results differ from the results of the TRUST

calculations in which gradients of moisture content range from a maximum of 46% change per meter to 5% change per meter.

Relative Concentration Contours

The moisture-content contours reflect in part the rate at which water is calculated to move through the system. This water flux, in turn, drives the transport of contaminants through the system in convection-dominated problems. The concentration contours produced by FEMTRAN, TRUMP, and TRACR3D, using the hydrologic fields calculated by SAGUARO, TRUST, and TRACR3D, respectively, are compared in Figures B-5 and B-6. The contours at 100 and 1,000 yr are essentially flat, indicating one-dimensional, diffusive transport driven by contaminant gradients as opposed to convection-dominated transport. This result is to be expected because the front has not yet reached the exit hole at 1,000 yr. By 7,500 yr, the contaminant front has reached the exit hole and diffused beyond it. The nearly flat lines in Figure B-6a for FEMTRAN and TRUMP indicate that very little contaminant is transported out of the exit hole and that diffusion continues to dominate convection; the TRACR3D results show steeper gradients near the exit. However, the region of influence of the exit on concentration gradients is nearly the same for all codes, and breaks in the contour slopes below 0.15 occur at about the same horizontal location.

The wide spread in the results for the 0.15 contour near the top of the system could be caused by increasing sensitivity to time-step sizes and cell size at low concentrations and low fluxes at long time-scales. Each code used unique time-step histories, and especially significant differences were observed between FEMTRAN and TRACR3D. TRACR3D restricted the maximum time step to 3.5×10^9, compared to 3.1×10^{10} for FEMTRAN and 3.7×10^{10} for TRUST. TRACR3D also used a combined total of 291 time steps for the hydrologic flow and contaminant-transport solution, compared to a combined total of 77 time steps used by SAGUARO and FEMTRAN (Appendix A). Because numerical dispersion is related to the square of the time step, normalized by the velocity, the indication is that the contaminant-transport

results were more sensitive to differences in time steps in COVE 1YMa than in COVE 1N, where the velocities were much greater. However, concentration profiles were in closer agreement even though the time-step histories differed by the same order of magnitude as in COVE 1YMa.

At 20,000 yr, concentration contours produced by FEMTRAN and TRACR3D appear to differ significantly; however, the gradients over the entire system are very small. The steepest vertical gradients are about 10% change per meter and 30% change per meter for FEMTRAN and TRACR3D, respectively, along the right boundary. A short distance inside the boundary, at x = 4.6 m, these gradients are reduced to 7.5% change per meter and 9.75% change per meter and become even smaller farther to the left of the system. Quantitative comparison of contours in areas of very low gradients, less than about 10%, can be misleading because the region over which the values are very gradually changing is large. Thus, the rest of the COVE 1YMa results are presented as profiles and histories at specific times and locations in Figures B-7 through B-10.

Comparison to Analytic Solution for Relative-Concentration Profiles

The concentration profiles calculated with FEMTRAN at the right boundary compare exactly to the analytic solution for diffusive transport (Carslaw and Jaeger, 1980) for 100 and 1,000 yr (Figure B-7). Even at 7,500 yr, there is no visible difference in the predicted concentration profiles, which is what would be expected considering the flat concentration contours shown for FEMTRAN (Figure B-6). These results demonstrate that, for the hydrologic field calculated by SAGUARO in COVE 1YMa and input to FEMTRAN, the accuracy of the FEMTRAN results in COVE 1YMa is exact. Thus, differences at early times between the TRACR3D and FEMTRAN results are probably attributable to differences in the hydrologic input for the transport calculation because TRACR3D predicts stronger convection than that predicted by SAGUARO. In addition, if numerical dispersion accounts for the difference in the concentration contours in Figures B-5 and B-6, this difference occurs because diffusive transport of water is enhanced

through numerical dispersion in the hydrologic calculations, not because of differences in the contaminant transport calculations. This argument is supported by the numerous calculations performed using FEMTRAN in which variations in time-step sizes were shown to have little effect on the results reported. No corresponding sensitivity study for the time-step size was performed using SAGUARO. Also, differences in the hydrologic modeling, such as application of boundary conditions and geometries used by the modelers, could be equally responsible for these quantitative differences in the concentration profiles.

Hydraulic Head and Relative Concentrations Along the Exit Boundary

There is no visible difference in the hydraulic-head profiles at the right boundary for SAGUARO, TRACR3D, or GWVIP at 100 yr (Figure B-8), except near the exit, where different formulations of the boundary condition were used. In reviewing the input of the codes, it was discovered that the TRACR3D calculations for COVE 1YMa did not use the specified boundary condition of Ψ = -8,800 cm at the exit, and TRUST used a seepage-face boundary condition. In addition, SAGUARO specified an initial hydraulic head, Φ = -1,000 cm, instead of a constant pressure head, Ψ = -1,000 cm. Even so, there is only a slight spread in the hydraulic-head profiles at 1,000 and 7,500 yr (Figures B-9 and B-10).

The corresponding concentration profiles along the right boundary were also very close, except for the different rates at which the fronts appeared to move down through the system. Because the rate of movement of the front depends on the velocities calculated from the head distributions, some difference was introduced by going from nearly exact head profiles to the concentration profiles. These results would be expected because all codes used slightly different techniques and different cell sizes in calculating the velocities.

Hydraulic Heads and Relative Concentrations at Interior Nodes

Along the interior lines located at x = 25 cm and x = 425 cm (Figures B-11 through B-13), the TRACR3D and GWVIP results for the head profiles always agree within 3%. At 100 yr, SAGUARO, TRUST, TRACR3D, and GWVIP, give essentially the same hydraulic-head profile on the right side of the system (Figure B-11). However, at 1,000 yr and 7,500 yr, the TRUST profiles are consistently lower; that is, the system is drier by 25%-50%. The SAGUARO results at 1,000 yr are slightly higher than the TRACR3D and GWVIP results along the 425-cm line but are essentially the same along the 25-cm line. The widest spread between head profiles was near 425 cm at 7,500 yr, with SAGUARO again showing higher heads than TRACR3D and GWVIP. However, near 25 cm, there was no difference between SAGUARO and TRACR3D, and GWVIP profiles were lower by less than 2%. The participants in COVE 1 concurred that the differences in hydraulic heads were the result of (1) the different exit conditions used, (2) the different treatments of the bottom boundary condition, (3) the different initial conditions used by SAGUARO, and (4) effects of numerical dispersion related to the very low fluxes in the problem.

Relative concentration histories calculated using TRUMP, FEMTRAN and TRACR3D are compared at the two interior points, x = 25 cm, z = 75 cm and x = 125 cm, z = 75 cm in Figure B-14. As in COVE 1N, TRACR3D predicted lower concentrations than did FEMTRAN, although the shapes of the curves are the same. This result suggests differences in the amount of numerical dispersion of the water in the hydrologic inputs to the transport calculations in FEMTRAN and TRACR3D. The quantitative agreement between the FEMTRAN, TRACR3D, and TRUMP solutions shown in Figure B-14 is within 50% at all times. This agreement was considered acceptable in light of the deviation from the specified boundary conditions that occurred.

4.2.4 Results of COVE 1YMb

In the third case, COVE 1YMb, the same geometry, material properties, and initial conditions used in COVE 1YMa were specified. Only the hydrologic boundary conditions were changed: a transient flux at the upper boundary was imposed, and flow through the bottom boundary was induced by specifying a fixed-pressure gradient. This problem was defined to compare the effect of the transient and flow-through boundary conditions in the codes. The hydrologic part of the problem was solved by TRACR3D, SAGUARO, and TRUST. Concentrations were calculated with TRACR3D, FEMTRAN, and TRUMP, using hydrologic results of TRACR3D, SAGUARO, and TRUST, respectively, as input. Results to 7,500 yr for hydraulic heads, relative concentrations, and moisture contents are shown in Appendix C. Only a few profiles are shown because most of the results are qualitatively similar to those in COVE 1YMa. No quantitative comparison was warranted because the results of TRACR3D were produced using a different bottom boundary condition from that used in TRUST or SAGUARO.

The relative concentrations at an interior node were compared to determine the effect of the differences in hydrology on contaminant transport. Figure C-4 shows close agreement between FEMTRAN and TRACR3D at the interior node, with maximum differences of 30%.

Hydraulic Heads and Relative Concentration Along the Exit Boundary

The hydraulic heads calculated along the right boundary using TRACR3D, SAGUARO, and TRUST, and the corresponding relative concentrations calculated using TRACR3D, FEMTRAN and TRUMP are shown in Figures C-1, C-2, and C-3 for 100, 1,000, and 7,500 yr, respectively. There is qualitative agreement in the profile shapes, but quantitative differences of almost a factor of 3 are seen in the values for concentrations. These differences are consistent with those seen in COVE 1YMa in that the relative concentrations calculated using TRACR3D are lower than those using FEMTRAN. The quantitative agreement in the hydrologic heads predicted by TRUST and SAGUARO is within 25% at most times and locations.

Hydraulic Heads and Relative Concentrations of Interior Nodes

Hydraulic-head profiles calculated using SAGUARO, TRUST, and TRACR3D are plotted at the two interior locations, x = 25 cm and x = 425 cm, at 100, 1,000, and 7,500 yr in Figures C-5 through C-7. At 100 yr, there is very good qualitative agreement, with a maximum spread of 15% in the results, which occurs in the top 25 cm of the system. This difference was attributed to variations in the initial time steps and grid spacing near the top boundary (Appendix A). At 1,000 yr, the agreement remained good, and the differences were again no more than about 15% and were spread over a larger region of the system. At 7,500 yr, however, the TRACR3D results are qualitatively, as well as quantitatively, different from those produced using SAGUARO and TRUST. TRACR3D shows hydraulic heads much higher than those in SAGUARO or TRUST. Investigations for the cause of this difference revealed that a bottom boundary condition of Ψ = +980 cm was inadvertently used in these TRACR3D calculations. The corresponding differences in saturation state caused nonlinearly greater hydraulic conductivities as the system approached saturation. As a result, a different steady state was calculated using TRACR3D even though (to 1,000 or more years) solutions at early times were in reasonable agreement.

5.0 SUMMARY

COVE has been established to begin certification of the hydrologic flow and contaminant transport codes used for performance assessment in the NWWSI Project. The primary goal of COVE is to verify the numerical accuracy and sensitivity of the codes by intercomparison of the results from equivalent codes. However, as the codes are verified, it is advisable to gain practical experience with the numerical difficulties likely to be encountered when the equations are used to solve the nonlinear, unsaturated-flow problems representative of Yucca Mountain. Thus, additional goals of the COVE 1 activity were to (1) evaluate the computer requirements of the different codes proposed for use in NNWSI performance assessment calculations and (2) to identify and resolve problems, if any, in running the codes. The COVE 1 results did give indications of the relative numerical accuracy and sensitivity of the codes; the results of subsequent COVE activities will be analyzed for more definitive verification of the numerical accuracy of the codes.

The goals of COVE 1 were accomplished by comparing the results of five water-flow and contaminant transport codes (SAGUARO, FEMTRAN, TRUST, TRUMP, and TRACR3D) currently being used for performance assessment by the NNWSI Project. In addition, GWVIP, a reservoir engineering code, was used to compare hydrologic results obtained using Richard's equation for a single fluid to results obtained using an additional equation that accounts for the presence of air as a second fluid in the system.

Three cases of a drainage problem in an isothermal, homogeneous geologic material were run in COVE 1 (Figures 2-1, 2-2, and 2-3). Material properties and boundary conditions were used in COVE 1N that

correspond to a medium-grain sand and, in COVE 1YMa and COVE 1YMb, to a nonwelded tuff (Figures 2-1, 2-4, and Table 2-1). A small system was modeled to demonstrate capabilities of the codes and to investigate sensitivities to numerical techniques in this first phase of code verification. The hydraulic heads, pressure heads, moisture contents, and velocities predicted using the hydrologic codes TRACR3D, SAGUARO, TRUST, and GWVIP were compared. Relative concentrations calculated using the contaminant transport codes TRACR3D, TRUMP, and FEMTRAN were compared. The TRUMP code used TRUST results for the water-flow field as input, and FEMTRAN used SAGUARO results.

Pressure-head, moisture-content, and relative-concentration contours and profile shapes were qualitatively compared. These comparisons showed the ability of the codes to solve a coupled, unsaturated-flow and transport problem and gave an indication of the numerical accuracy of the codes. The quantitative values for the parameters were not expected to compare exactly because the meshes, numerical techniques, and convergence and accuracy criteria used were not identical for each code.

Because of the latitude allowed in choosing numerical modeling parameters, quantitative agreement within 20% to 50% was considered reasonable in most cases for the first evaluation, as long as the qualitative behavior was the same. After an initial comparison at a workshop held in Albuquerque, New Mexico, in September 1983, several participants independently varied the mesh sizes, accuracy criteria, and time steps to investigate the sensitivities of the codes they used. A final workshop was held in April 1984 in La Jolla, California during which most of the results described in this report were presented and a consensus regarding the interpretation of the comparisons was reached by the modelers and the author of this report. Some revised results using GWVIP were transmitted to the author after the workshop in La Jolla (Pahwa, 1984).

The use of alternative boundary and initial conditions by some of the modelers made quantitative comparisons difficult to interpret.

Where alternative boundaries and initial conditions were used, it will not be possible to reach a definitive conclusion regarding the quantitative agreement between the codes until the cases have been rerun and the participants have matched the specified boundary conditions as closely as possible. In future COVE exercises, more stringent control on the numerical modeling constraints will be specified so that sensitivities to different numerical parameters can be estimated in a consistent manner for all codes and numerical acccuracy can be quantitatively evaluated. The definition of the modeling constraints must be an interative process because the appropriate mesh, time-step, and accuracy criteria cannot be determined until after several attempts have been made to a solve a problem.

In COVE 1, it was demonstrated that TRACR3D and the paired codes--SAGUARO and FEMTRAN, and TRUST and TRUMP--are capable of solving a coupled, unsaturated-flow and transport problem using nonwelded tuff properties representative of Yucca Mountain. In addition, some initial results of sensitivity studies were shown, and some questions and cautions were raised that must be addressed further to establish the numerical accuracy of predictions made with the codes.

5.1 Results for COVE 1N

Differences in moisture-content contours calculated by all codes were negligible for all three COVE 1 cases. Qualitative agreement of the calculations for the hydraulic heads in COVE 1N was good. Sensitivity to the area and shape of the exit hole was studied using TRUST and SAGUARO. The exit geometry was shown to affect the TRUST results by about 40%. The same sensitivity was seen in the studies performed using SAGUARO. In addition, the effect of using a seepage-face boundary condition instead of a constant-pressure boundary condition at the exit was investigated using TRUST.

Relative-concentration contours calculated in COVE 1N using FEMTRAN, TRACR3D, and TRUMP agreed qualitatively but varied by as much as a factor of 5 at and above the exit along the right boundary and by

a factor of 2 at interior nodes. This variation was attributed to the differences in the water velocities calculated from the pressure fields. In addition, TRACR3D ran with time steps that were much smaller than those used with the other codes, reducing numerical diffusion.

Mass balances of water and contaminant in COVE 1N were calculated by all the codes to be within 2% of the total mass remaining in the system at any one time. However, differences of up to 50% were seen in the water productions calculated by GWVIP, SAGUARO, TRACR3D, and TRUST at the exit. Using the seepage-face boundary condition at the exit, the TRUST results for all three COVE 1 problems consistently predicted drier conditions, lower hydraulic heads, and more water production. Results of TRUST, using a constant-head boundary condition, were generally more consistent with the GWVIP results.

A sensitivity study of the effect of mesh size on COVE 1N results was performed using the SAGUARO and TRACR3D codes, and the effect on the concentration fields of using different numerical techniques for calculating velocities was investigated using SAGUARO and FEMTRAN. A coarse mesh of 221 elements led to serious mass-balance errors in the contaminant transport in FEMTRAN but had little effect on the pressure fields in SAGUARO. A similar result was reported by Pickens et al. Results obtained using the 884-element mesh did not differ from results obtained using the 247-element mesh.

A study of velocity formulation was performed using SAGUARO and FEMTRAN. The study showed that the traditional discontinuous method of calculating velocities in finite-element codes gave the same results as a continuous method using the finite-element technique to derive velocities from the pressure field. Lumped-mass techniques were shown to be inferior for this problem, although the differences between velocities calculated with the lumped-mass technique and the discontinuous method decreased appreciably as the mesh was refined.

5.2 Results for COVE 1YMa

The moisture-content and pressure-head contours calculated for COVE 1YMa using SAGUARO, TRACR3D, and GWVIP agreed both qualitatively and quantitatively at both interior and boundary nodes to 20,000 yr. As in COVE 1N, the pressure-head profiles predicted with TRUST at interior nodes were lower than the profiles produced by other codes, although the shape of the profiles was similar. At 7,500 yr, qualitative as well as quantitative differences in the TRACR3D and FEMTRAN results for relative concentrations were seen near the exit. By 20,000 yr, the spread was as much as a factor of 2. This difference between TRACR3D and FEMTRAN concentrations at the exit, beginning at 7,500 yr, was attributed to numerical sensitivities to the modeling parameters (time-step size, mesh, and velocity formulation), although this inference was not proven. Other factors, such as sensitivity to the progressively larger time steps used by all codes for the late-time calculations, were not investigated. Contaminant transport appeared to be diffusion-dominated because of the very low convective fluxes in the nonwelded tuff representative of Yucca Mountain.

5.3 Results for COVE 1YMb

The COVE 1YMb comparisons of hydraulic-head and concentration profiles were similar to those of COVE 1YMa, except that the hydraulic heads predicted by TRACR3D at late times were about 40% higher than those predicted by SAGUARO or TRUST. This result was not surprising, however, because a different bottom boundary condition was inadvertently used in these TRACR3D calculations. The results produced by TRUST in COVE 1YMb were closer to the SAGUARO results than the results of TRUST in either COVE 1N or COVE 1YMa. As in COVE 1N and COVE 1YMa, the relative-concentration profiles calculated using FEMTRAN and TRACR3D agreed qualitatively, although quantitative differences of up to a factor of 2 were seen at very late times. The contaminant transport appeared to be diffusion-dominated as in COVE 1YMa.

In the course of solving these COVE 1 problems, several important code modifications were made. These modifications included (1) enhanced techniques for calculating accurate velocities for input to the transport calculations, (2) material property models in all the codes capable of accepting characteristic curves representative of Yucca Mountain tuff, and (3) interpolation routines for investigating behavior at specified locations.

6.0 CONCLUSIONS

The COVE 1 benchmarking activity demonstrated that the hydrology codes, TRACR3D, SAGUARO, TRUST, and GWVIP, and the contaminant transport codes, FEMTRAN, TRACR3D, and TRUMP have similar capabilities for modeling system behavior using material properties and conditions representative of the nonwelded tuff matrix at Yucca Mountain. In addition, these codes (which use different numerical solution techniques and incorporate slightly different mathematical models) have independently reproduced the qualitative solutions published by Pickens et al. for water flow and contaminant transport out of a plot of sand. This exercise has established the relative capabilities of the codes for solving transient, isothermal water-flow and contaminant-transport problems in homogeneous porous media, identified several numerical sensitivities, and suggested areas that warrant further investigation for establishing the uniqueness of solutions for long-time predictions using properties typical of Yucca Mountain.

The TRACR3D code and the combination of the SAGUARO and FEMTRAN codes appear to have similar two-dimensional modeling capabilities and produce qualitatively similar contaminant-transport results. The TRUMP code, using TRUST input, was shown to produce results comparable to those calculated using TRACR3D and FEMTRAN for nondispersive transport. All the hydrology codes have similar modeling capabilities with regards to the physics of the problem studied. The GWVIP study showed that using a separate equation to consider the air phase had no effect on modeling the nonwelded tuff unit. The experiences gained in coupling the SAGUARO and FEMTRAN codes and the TRUST and TRUMP codes demonstrated the ability to perform flow and transport calculations efficiently. However, it is prudent to use an equivalent mesh in the water-flow code and the contaminant-transport code because of the

sensitivity of the transport calculations to the calculated velocity fields. Using Darcy's law, the velocities are calculated to be proportional to the pressure gradient within a cell. For this reason, the velocities can be very sensitive to the cell size in regions of the mesh where pressure gradients are steep.

For the problems in which the flux is low and the permeabilities are small, the various sensitivity studies performed in COVE 1 showed the following results.

- Concentration results can be significantly affected by mesh size even though pressure fields are relatively unaffected.

- Discontinuous methods of velocity calculations in the finite-element method are adequate for problems with low fluxes and are preferable to the lumped-mass methods.

- The exit area can affect hydrologic flow and contaminant transport results, but the effect becomes small more than 10 diameters away from the exit.

- Hydrologic results are relatively insensitive to the specification of constant pressure head, as opposed to total head at an exit.

In addition, it was shown that global mass balances of water fluxes do not ensure a rigorous impermeable boundary in the finite-element codes. The lack of a rigorously impermeable boundary can result in errors in contaminant-transport calculations. Consideration of these numerical effects led to the conclusion that the accuracy and uniqueness of long-time predictions of flow at and transport long times at Yucca Mountain usually require sensitivity analyses of the numerical calculations to the mesh size, boundary condition specifications, geometries and, perhaps, velocity-calculation techniques. In addition, the COVE 1 results suggest that the effect of time-step sizes on numerical dispersion in problems representative of the physical system at Yucca Mountain should be investigated further.

In Cove 1YMA, the results from the FEMTRAN code agree well with an analytic solution for transport by diffusion alone. This agreement suggests that the transport process will be dominated by diffusion in the nonwelded units at Yucca Mountain. The same might not be true in blocks of welded tuff because the fractures present in the welded tuff matrix may enhance convective transport under high flux conditions.

Future COVE activities should address the relative accuracy of the codes, as well as the relative capabilities and sensitivities of the codes investigated in COVE 1. The sensitivity studies and inter-code comparisons performed in COVE 1 indicated that satisfaction of stability and accuracy criteria within a code does not necessarily ensure the uniqueness of solutions for hydraulic heads, moisture contents, or contaminant transport. The accuracy and uniqueness of solutions for these variables must be further demonstrated by inter-code comparison of more representative problems and by comparison of the results with laboratory and field data. In particular, the following flow and transport problems should be part of NNWSI benchmarking activities:

- a large-scale, layered, variably saturated problem (COVE 2), and
- a nonisothermal problem including vapor (COVE 3).

COVE 1 has been an important first step in the certification of the NNWSI performance assessment codes in that benchmarking to study numerical sensitivities and accuracies has been initiated. The results, which have been archived for future reference, will be available, if necessary, to demonstrate compliance with certain benchmarking requirements specified in NUREG-0856. In addition, the experiences gained in modeling COVE 1YMa and COVE 1YMb can be used in future performance assessment models of the Yucca Mountain system. Activities for COVE 2 and COVE 3 are currently being planned (1) to address some of the questions raised by COVE 1 and the issues listed above and (2) to investigate the physical validity of the models being used for the hydrologic and geochemical transport mechanisms at Yucca Mountain.

7.0 REFERENCES

Bixler, N., "NORIA-A Finite-Element Computer Program for Analyzing Water, Vapor, Air, and Energy Transport in Porous Media", SAND84-2057, Sandia National Laboratories, Albuquerque, NM, in preparation.

Carslaw, H. S., and J. C. Jaeger, "Conduction of Heat in Solids," Oxford University Press, Oxford, England, 1980.

Eaton, R. R., et al., "SAGUARO - A Finite Element Computer Program for Partially Saturated Porous Flow Problems", SAND82-2772, Sandia National Laboratories, Albuquerque, NM, June 1983.

Eaton, R. R., memo to Distribution, Sandia National Laboratories, Albuquerque, NM, September 18, 1984.

Edwards, A. L., "TRUMP: A Computer Program for Transient and Steady State Temperature Distribution in Multidimensional Systems", UCRL-14754, Revision 3, Lawrence Livermore Laboratory, Livermore, CA, 1972.

Freeze, R. A., and J. A. Cherry, Groundwater, Prentice-Hall, Inc., Englewood Cliffs, NJ, 1979.

Gartling, D. K., and C. E. Hickox, "MARIAH - A Finite Element Computer Program for Incompressible Porous Flow Problems: User's Manual," SAND79-1623, Sandia National Laboratories, Albuquerque, NM, September 1980.

Gartling, D. K., and C. E. Hickox, "MARIAH - A Finite Element Computer Program for Incompressible Porous Flow Problems: Theoretical Background," SAND79-1622, Sandia National Laboratories, Albuquerque, NM, September 1982.

Gee, G. W., letter report to R. R. Peters, Battelle Pacific Northwest Laboratories, Richland, WA, July 18, 1983.

Hadley, G. R., "PETROS - A Program For Calculating Transport of Heat, Water, Water Vapor and Air Through A Porous Material", SAND84-0878, Sandia National Laboratories, Albuquerque, NM, May 1985.

Haverkamp, R., et al., Soil Sci Soc., Am. J. 41(2): 285-294, 1977.

Hirt, "Heuristic Stability Theory for Finite Difference Equations," J. Comp. Physics, 2, pp. 339-355, 1968.

Martinez, M. J., "FEMTRAN - A Finite Element Computer Program for Simulating Radionuclide Transport Through Porous Media", SAND84-0747, Sandia National Laboratories, Albuquerque, NM, January 1985.

Metcalf, D., Intera Technologies, Inc., Houston, TX, letter to N. K. Hayden, Sandia National Laboratories, Albuquerque, NM, March 22, 1984.

Montazer, P. and W. E. Wilson, "Conceptual Hydrologic Model of Flow in the Unsaturated Zone, Yucca Mountain, NV," U.S. Geological Survey Water Resources Investigations Report 84-4345, 1984.

Mualem, Y., Water Resour. Res. 12(3): 513-522, 1976.

Narasimhan, T. N., and P. A. Witherspoon, "An Integrated Finite Difference Method for Analyzing Fluid Flow in Porous Media," Water Resource Res., Vol. 12, No. 1, pp. 57-64, 1976.

Narasimhan, T. N., and P. A. Witherspoon, "Numerical Model for Saturated-Unsaturated Flow in Deformable Porous Media 1 Theory," Water Resource Res, Vol. 13, No. 3, pp. 657-664, 1977.

Narasimhan, T. N., et al., "Numerical Model for Saturated-Unsaturated Flow in Deformable Porous Media 2, The Algorithm," Water Resource Res., Vol. 14, No. 2, pp. 255-261, 1978.

NRC (U.S. Nuclear Regulatory Commission), "Disposal of High-Level Radioactive Wastes in Geologic Repositories - Licensing Procedures," Code of Federal Regulations, Energy, Title 10, Part 60, June 1983.

Pahwa, S., Intera Technologies, Inc., Houston, TX, letter to K. Johnstone, Sandia National Laboratories, Albuquerque, NM, June 1, 1983.

Pahwa, S., Intera Technologies, Inc., Houston, TX, letter to N. K. Hayden, Sandia National Laboratories, Albuquerque, NM, April 18, 1984.

Peters, R. R., et al., "Preliminary Matrix Hydrologic Stratigraphy at Yucca Mountain," memo to R. R. Eaton, Sandia National Laboratories, Albuquerque, NM, December 3, 1982.

Peters, R. R., and J. Gauthier, personal communication, Sandia National Laboratories, Albuquerque, NM, August 12, 1983.

Pickens, J. F., et al., "Finite Element Analysis of the Transport of Water and Solutes in Tile-Drained Soils," J. Hydrolog., 40, pp. 243-264, 1979.

Pruess, K., and J. S. Y. Wang, "TOUGH - A Numerical Model for Nonisothermal Unsaturated Flow in Fractured Porous Media," Lawrence Berkeley Laboratory, University of California, Berkeley, CA, in preparation.

Silling, S. A., "Final Technical Position on Documentation of Computer Codes for High-Level Waste Management," NUREG-0856, U. S. Nuclear Regulatory Commission, Washington, DC, 1983.

Travis, B. J., "TRACR3D: A Model of Flow and Transport in Porous/Fractured Media", LA-9667-MS, Los Alamos National Laboratories, Los Alamos, NM, May 1984.

Travis, B. J., "WAFE: A Model for Two Phase, Multi-Component Mass and Heat Transport in Porous Media," Los Alamos National Laboratories, Los Alamos, NM, in preparation.

Yeh, G. T., and D. S. Ward, "FEMWASTE: A Finite Element Model of Waste Transport through Saturated-Unsaturated Porous Media," ORNL-5601, Oak Ridge National Laboratory, Oak Ridge, TN, 1981.

TABLE A-1. CATEGORY A PARAMETERS--COMPUTER-RUN STATISTICS

	PICKENS	SAGUARO	TRUST	GWVIP	TRACR3D	FEMTRAN
Time(s) (on CRAY computer unless noted otherwise)						
1N	120[a]	493	120[b]	1,700[c]	2,700	500
1YMa	--	226	68[a]	650[c,d]	1,920	37.7
1YMb	--	760[e]	67[b,f]	--	814[c,f]	26.3
INITIAL TIME STEP(S)						
1N		.06	1.5×10^{-4}	8.6	0.01	9.7
1YMa	--	2.3×10^{9}	1.5×10^{2}	8.6×10^{4}	3.1×10^{7}	3.1×10^{7}
1YMb	--	6.3×10^{8}	1.0×10^{7}	--	3.1×10^{6}	
MAXIMUM TIME STEP(S)						
1N		3.6×10^{3}	1.0×10^{3}	7.7×10^{3}	1.4×10^{3}	6.0×10^{2}
1YMa	--	6.3×10^{10}	1.0×10^{3} yr	9.64×10^{10}	3.5×10^{9}	3.1×10^{10}
1YMb	--	3.1×10^{9}	5.0×10^{2} yr	--	2.5×10^{9}	
TOTAL NUMBER OF TIME STEPS						
1N	40	81	780	45	251	92
1YMa	--	21	178	20	291	56
1YMb		84[e]	244	--	277	41
NUMBER OF ELEMENTS						
1N	1360	247	434	420	1,728	1,040
1YMa	--	247	434	420	600	247
1YMb		221	427	--	375	221

a. Calculated on an IBM 360.
b. Calculated on CDC 7600 computer.
c. Calculated on HARRIS 800 computer.
d. Calculation ran to 10,000 yr.
e. To 20,000 yr.
f. Did not include transient pulse.

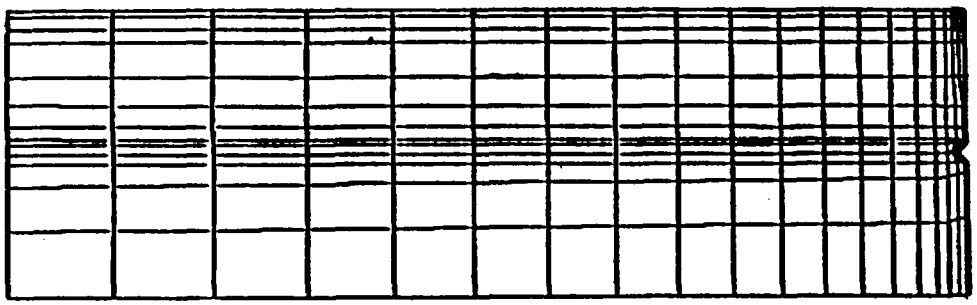

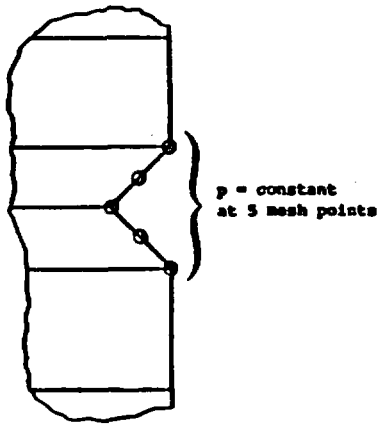

SAGUARO Finite-Element Mesh (247 Elements) Train Triangular Exit Hole

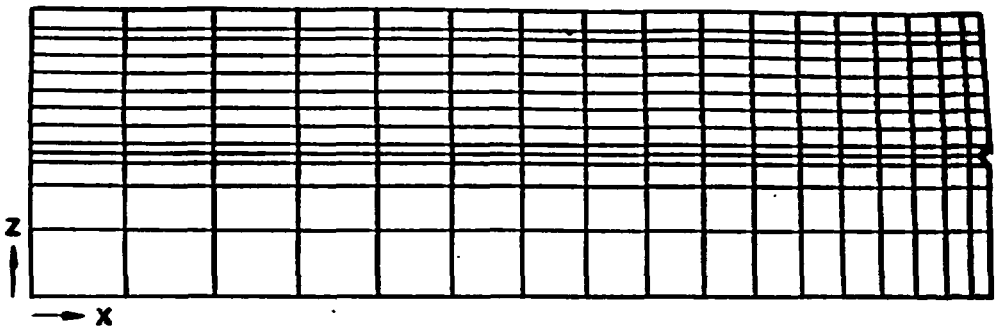

SAGUARO Finite-Element Coarse Mesh (221 Elements)

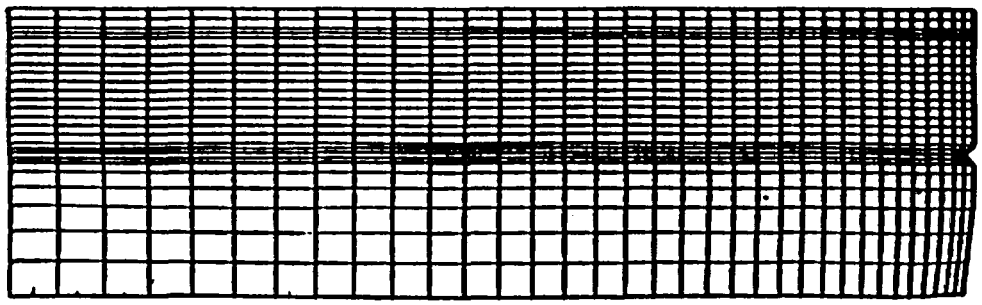

SAGUARO/FEMTRAN Finite-Element Fine Mesh (884 Elements)

Figure A-1. SAGUARO Finite-Element Mesh

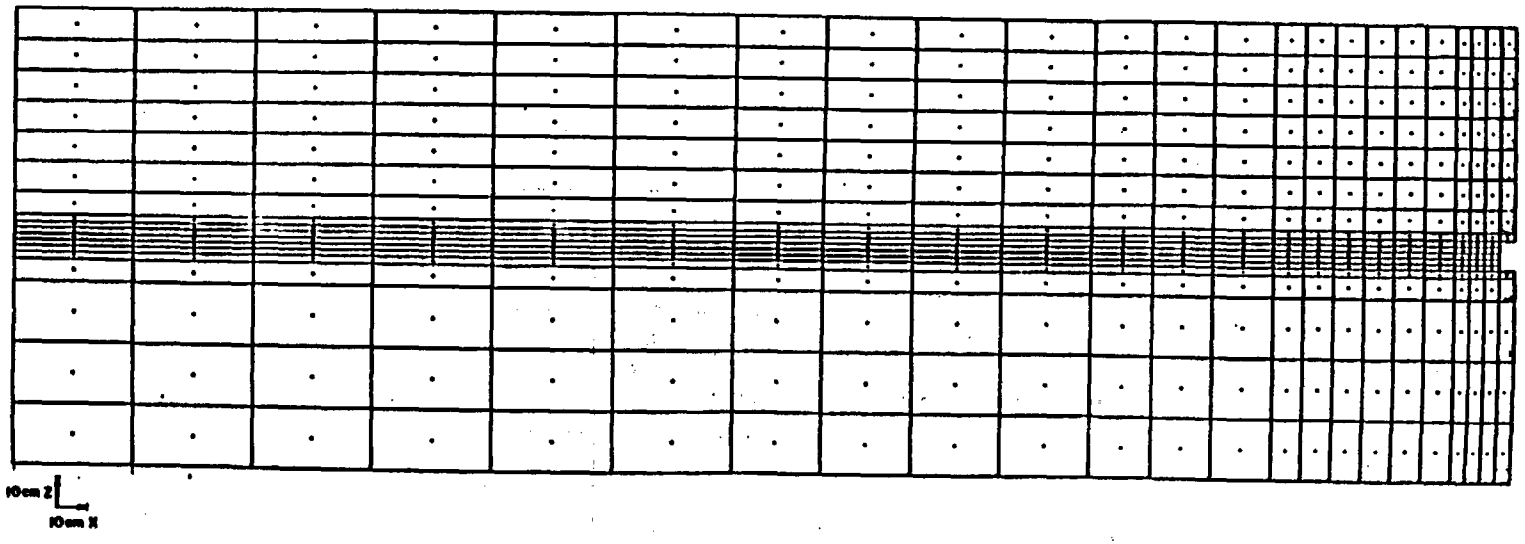

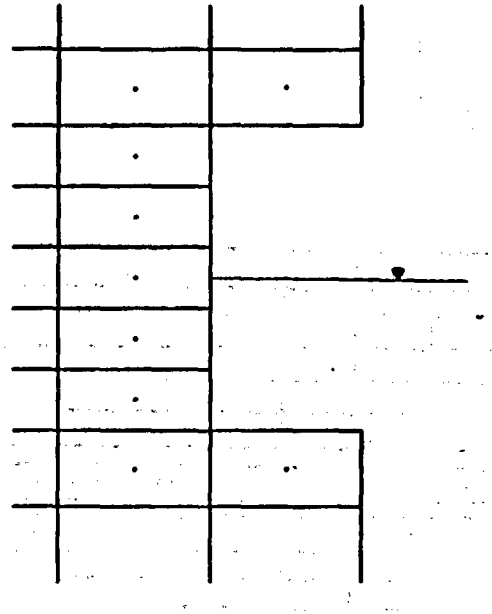

RECTANGULAR EXIT HOLE

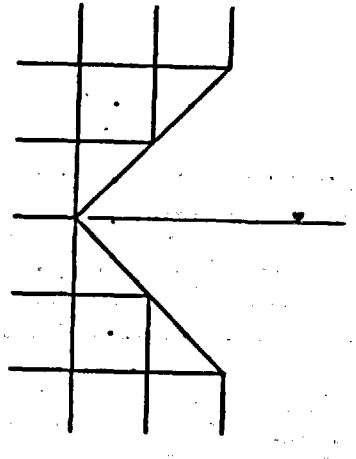

TRIANGULAR EXIT HOLE

Figure A-2. TRUST Finite-Difference Mesh

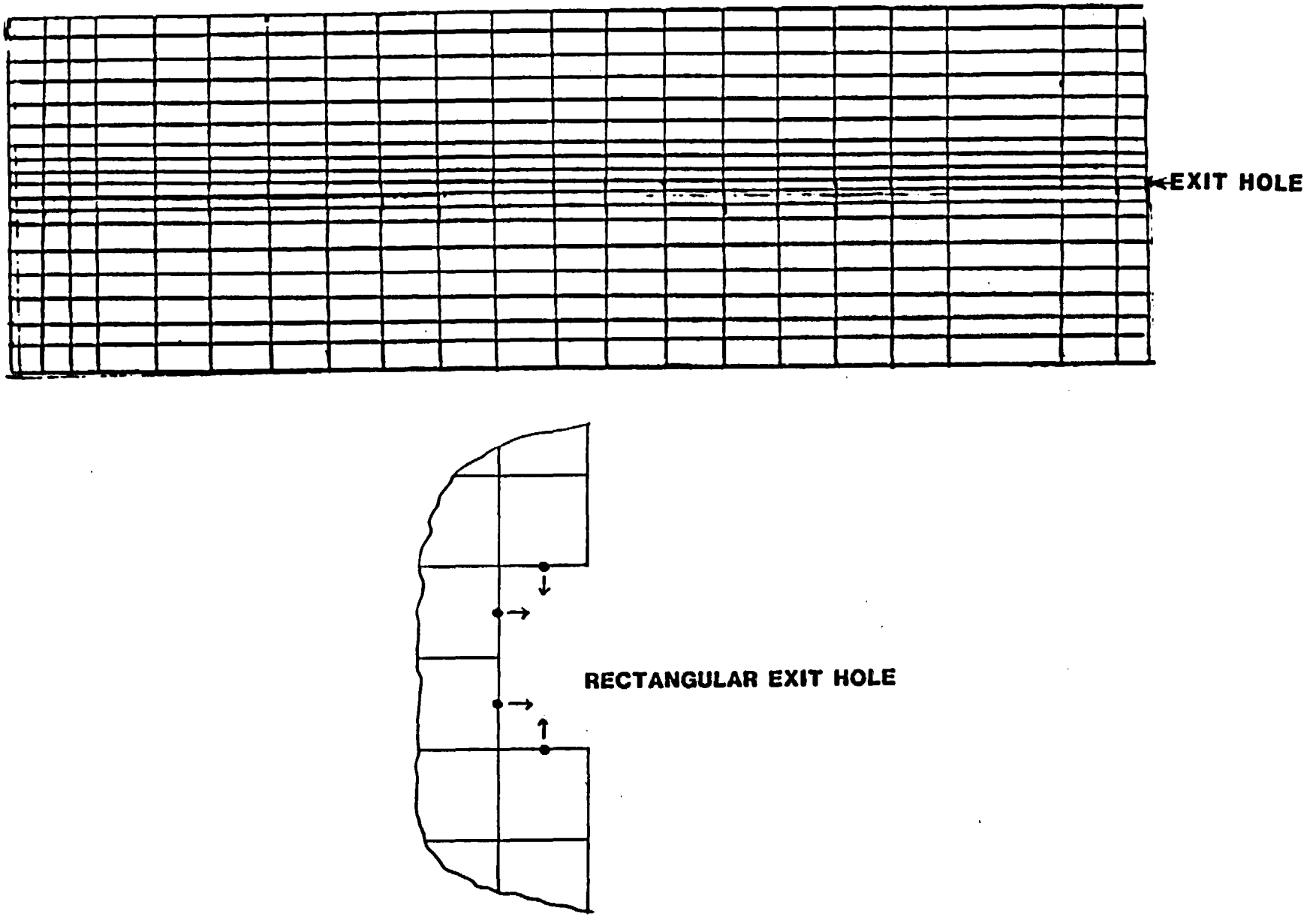

Figure A-3. GWVIP Finite-Difference Mesh

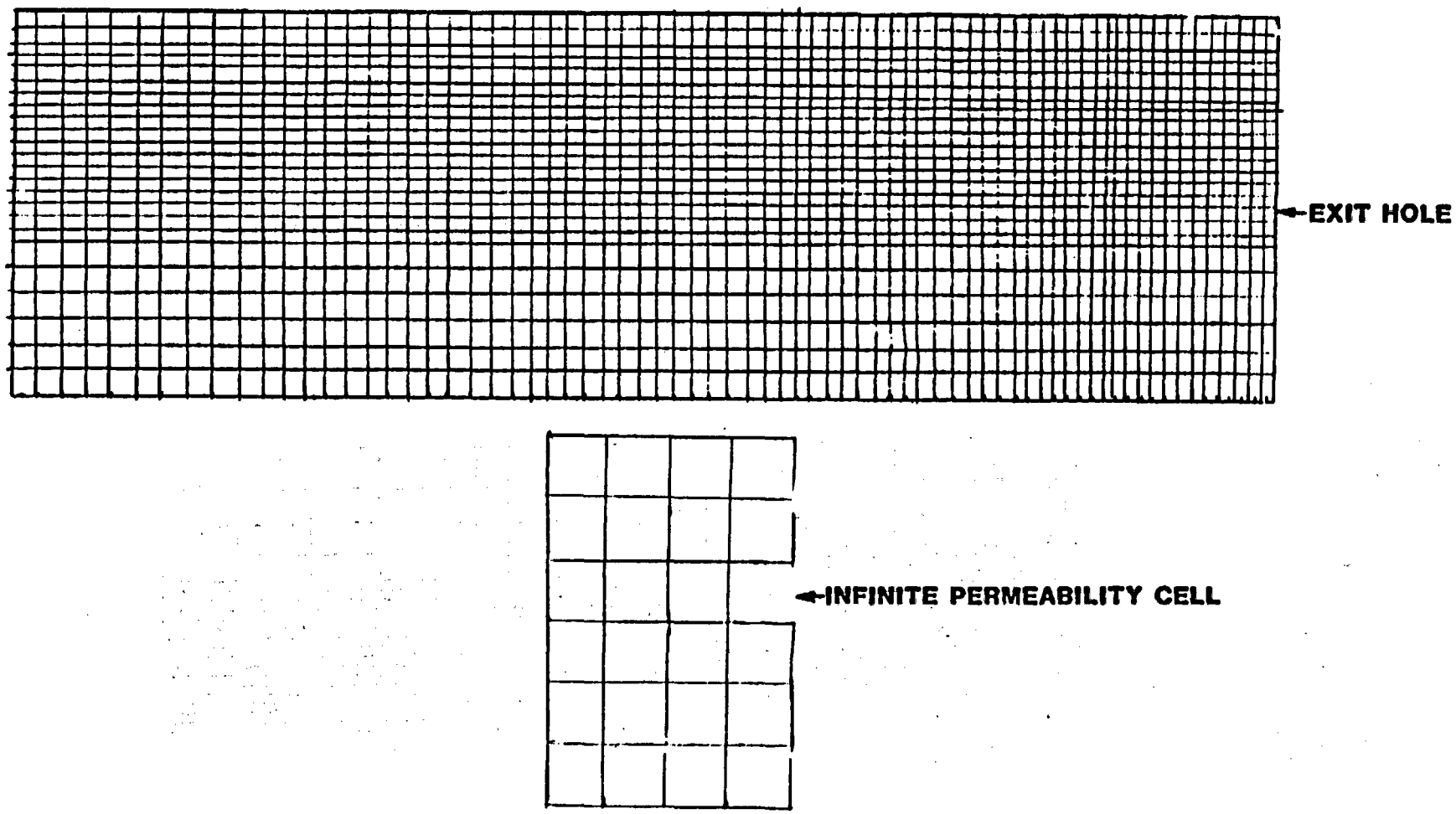

Figure A-4. TRACR3D Finite-Difference Mesh

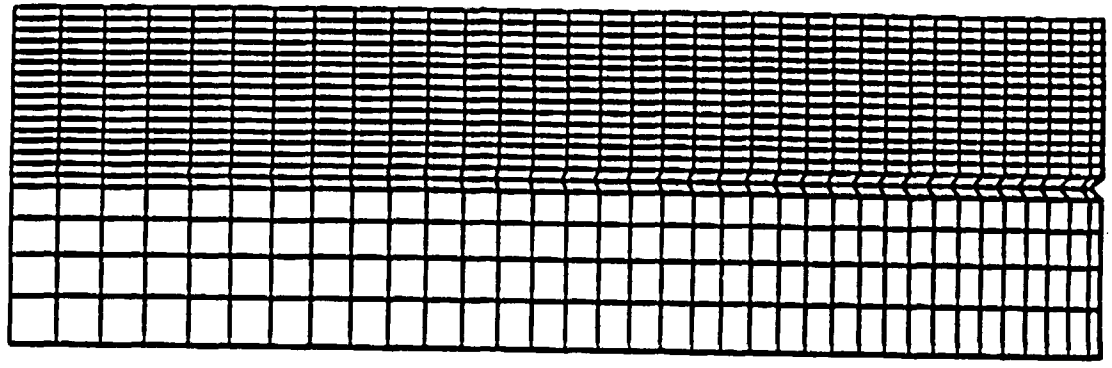

Figure A-5. FEMTRAN Finite-Element Mesh

APPENDIX B

RESULTS OF COVE 1YMa

In Figures B-8 through B-14, the following symbols are used:

○ TRACR3D

△ GWVIP

+ TRUST
TRUMP

□ SAGUARO
FEMTRAN

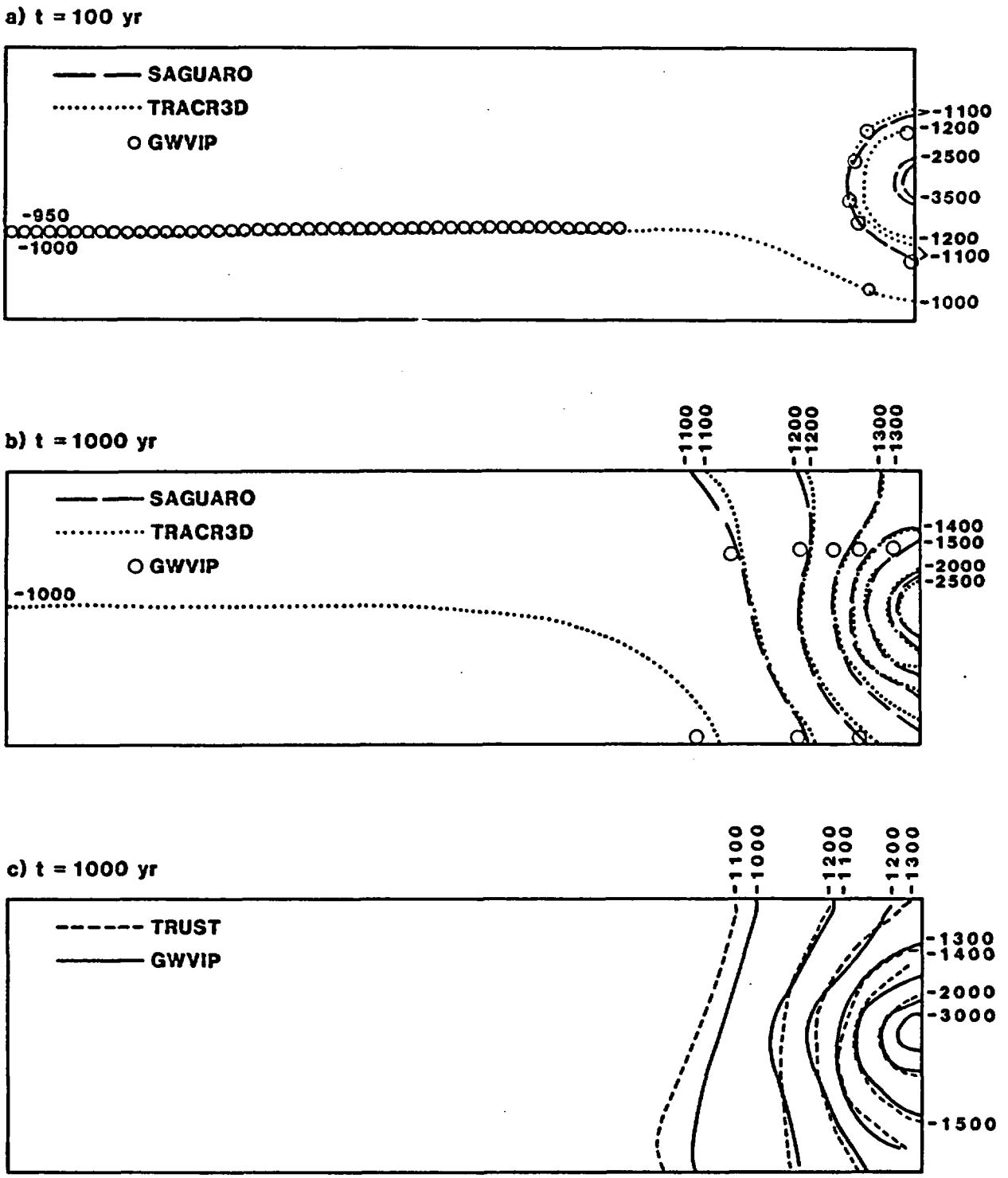

Figure B-1. Pressure-Head (a and b) and Hydraulic-Head (c) Contours for COVE 1YMa

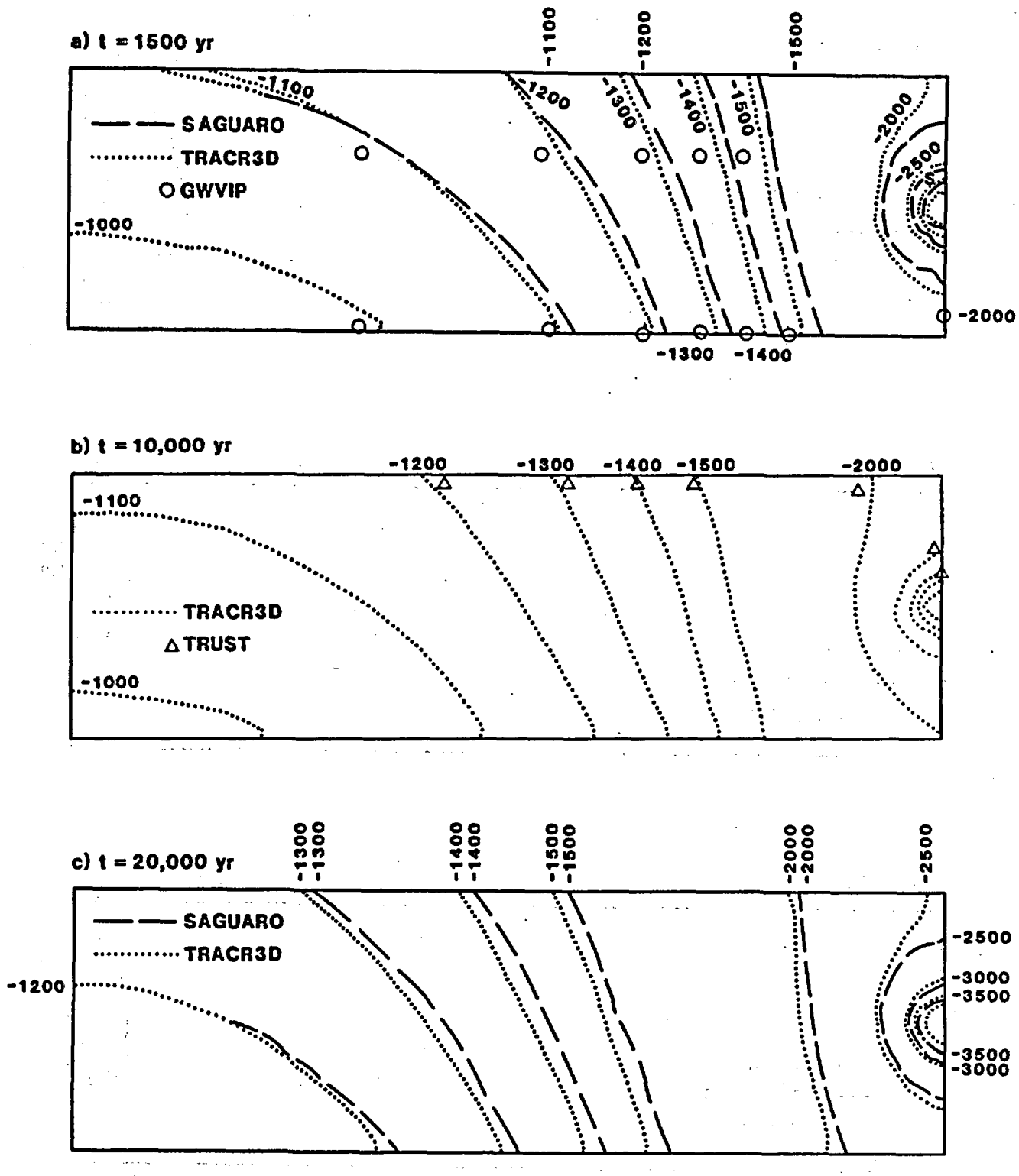

Figure B-2. Pressure-Head Contours for COVE 1YMa

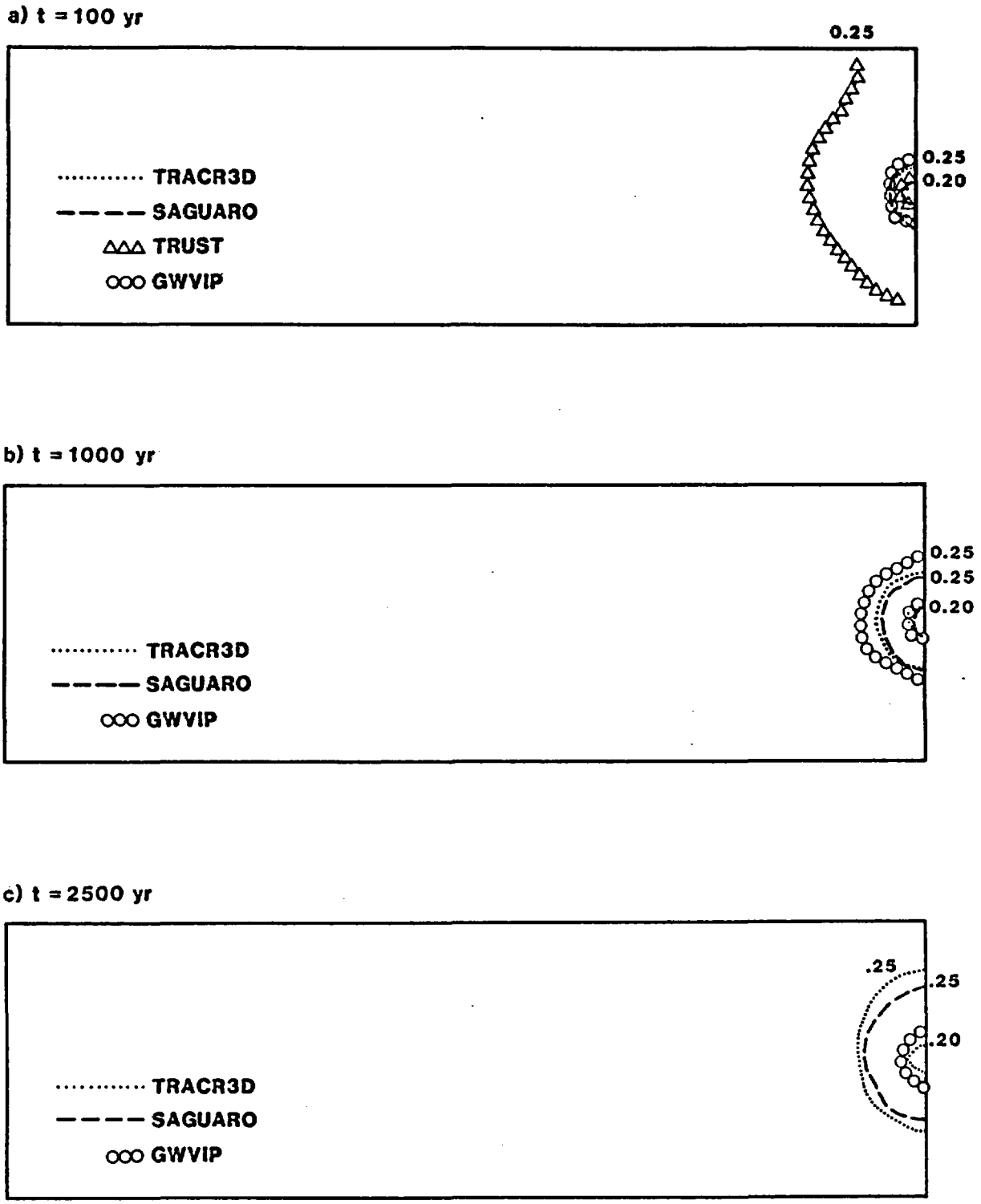

Figure B-3. Moisture Content for COVE 1YMa at t = 100, 1,000 and 2,500 yr.

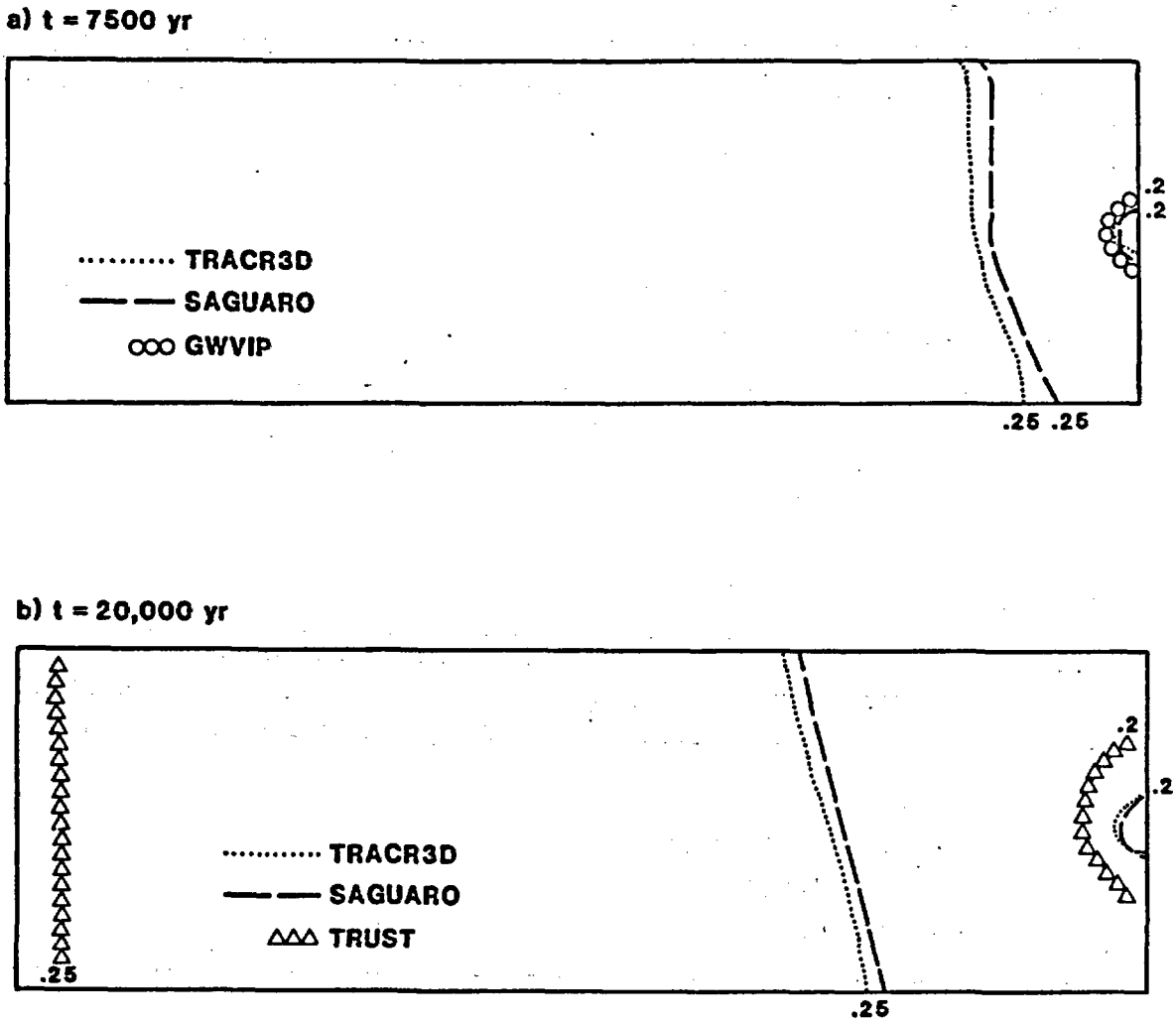

Figure B-4. Moisture Content for COVE 1YMa at t=7,500 and 25,000 yr

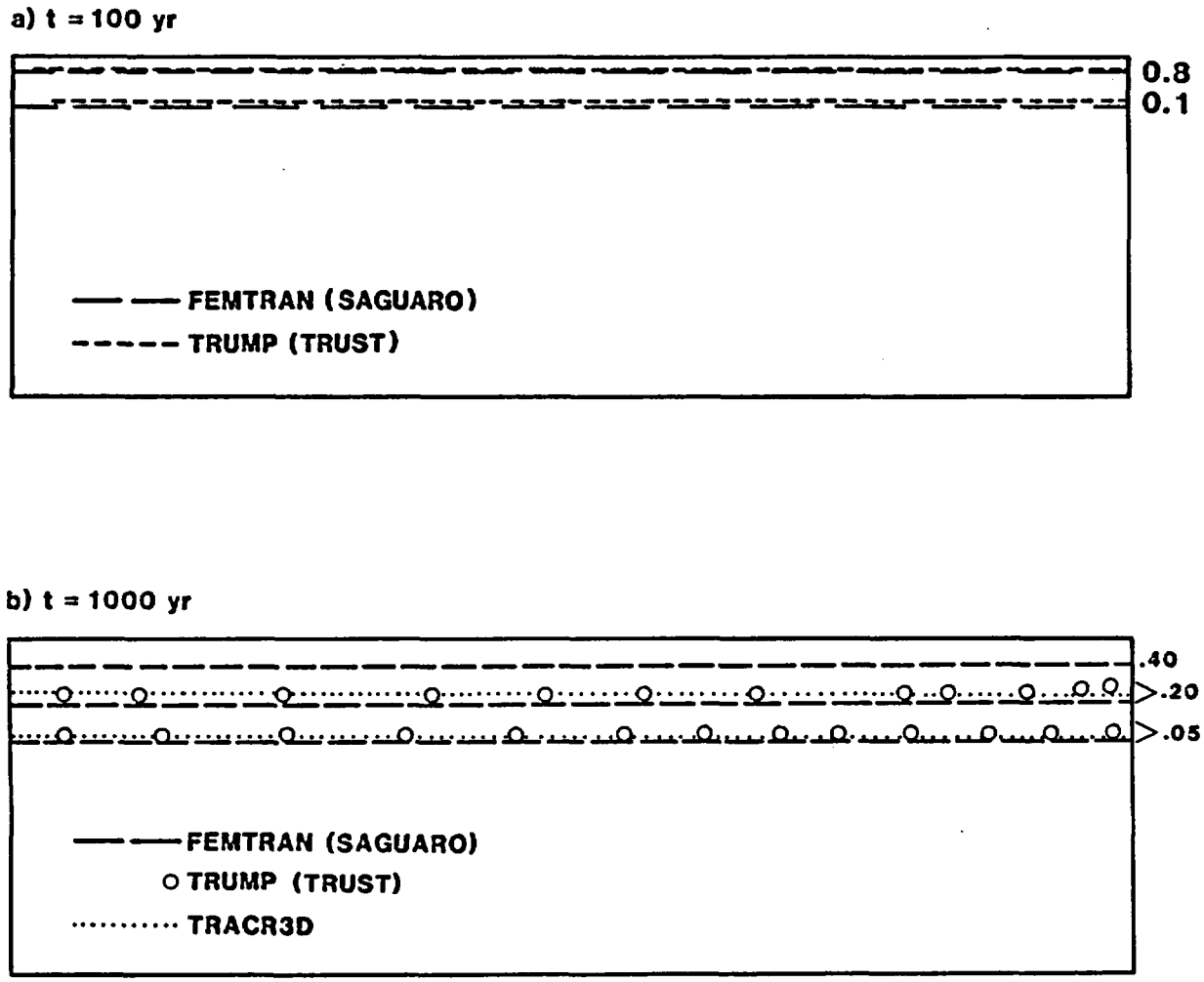

Figure B-5. Concentration Contours for COVE 1YMa at t =100 and 1,000 yr

a) t = 7500 yr

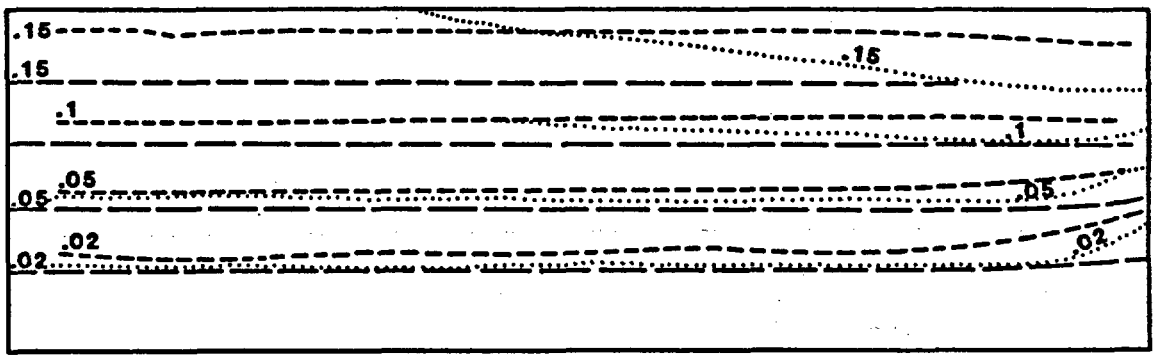

FEMTRAN (SAGUARO)
TRUMP (TRUST)
TRACR3D

b) t = 20,000 yr

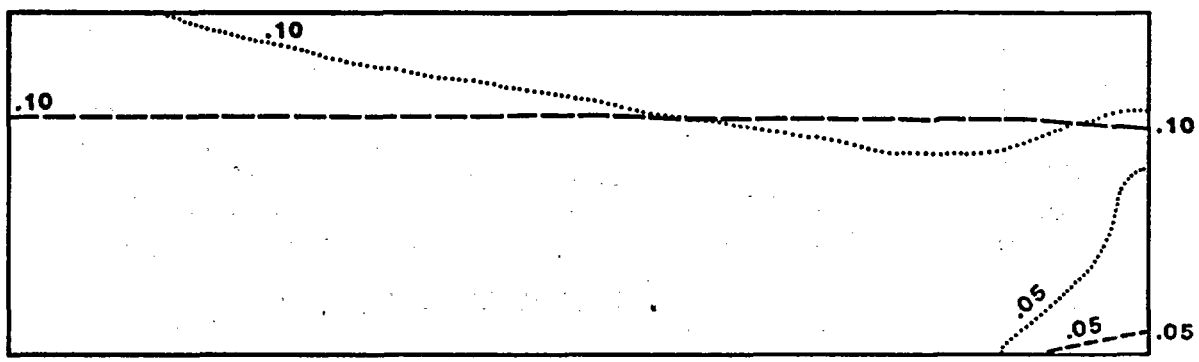

FEMTRAN (SAGUARO)
TRUMP (TRUST)
TRACR3D

Figure B-6. Concentration Contours for COVE 1YMa at t = 7,500 and 25,000 y

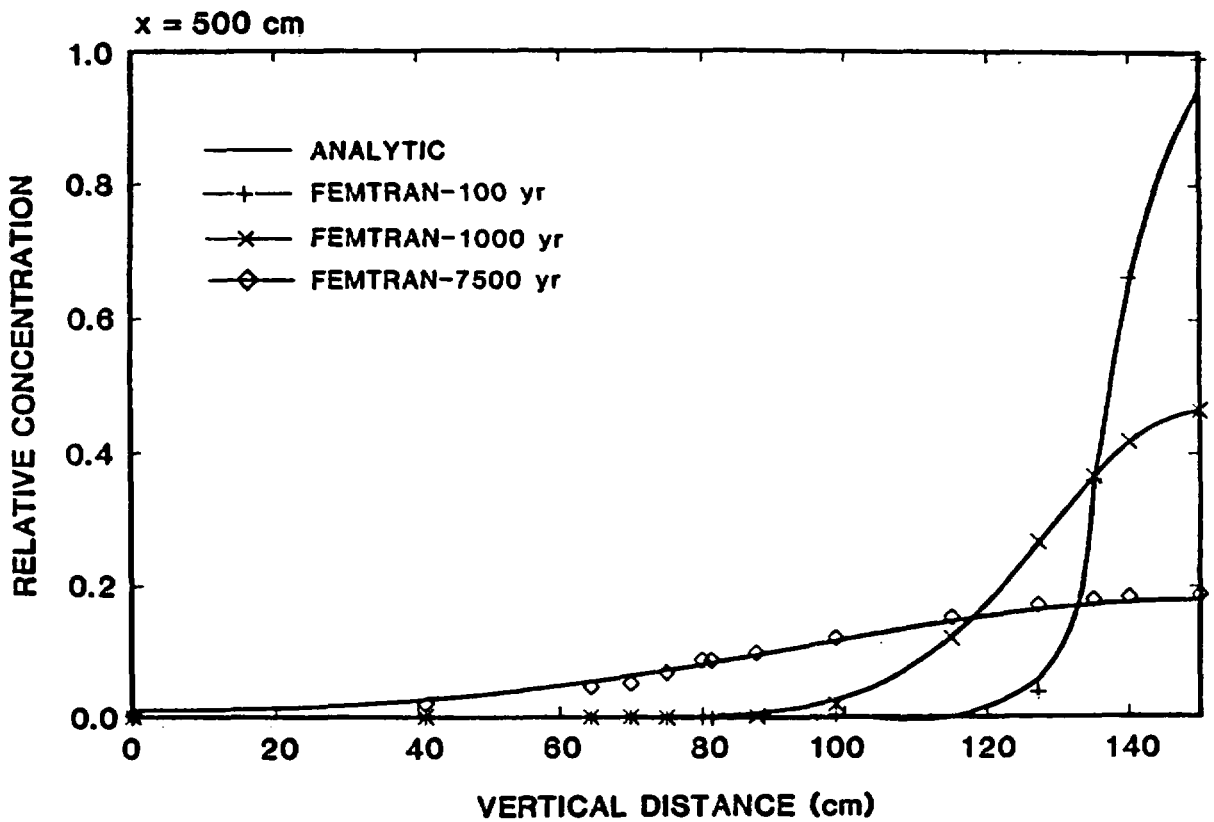

Figure B-7. Comparison of FEMTRAN to Analytic Approximation of COVE 1YMa

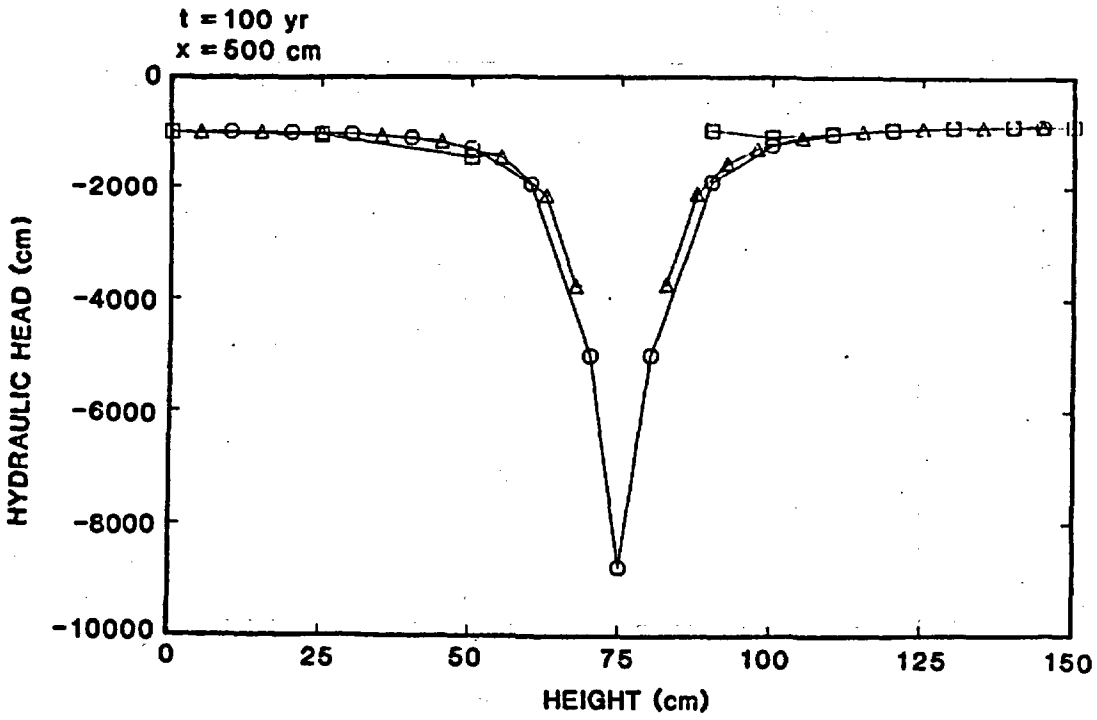

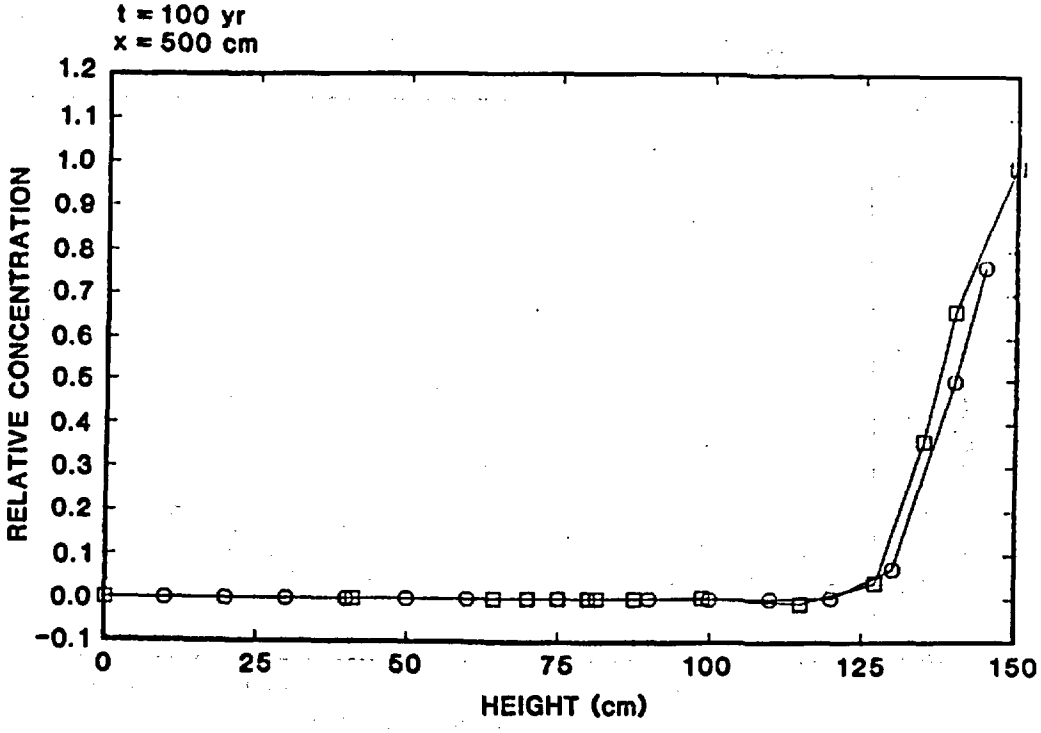

Figure B-8. Hydraulic-Head and Relative-Concentration Profiles along Right-Side Boundary for COVE 1YMa at t = 100 yr

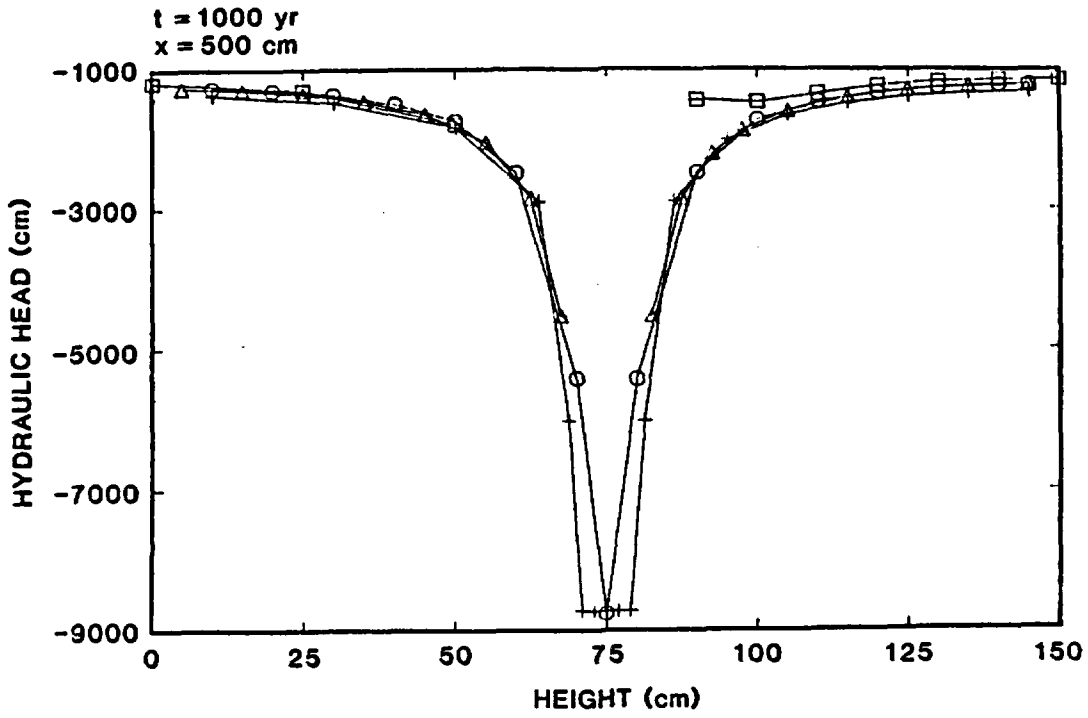

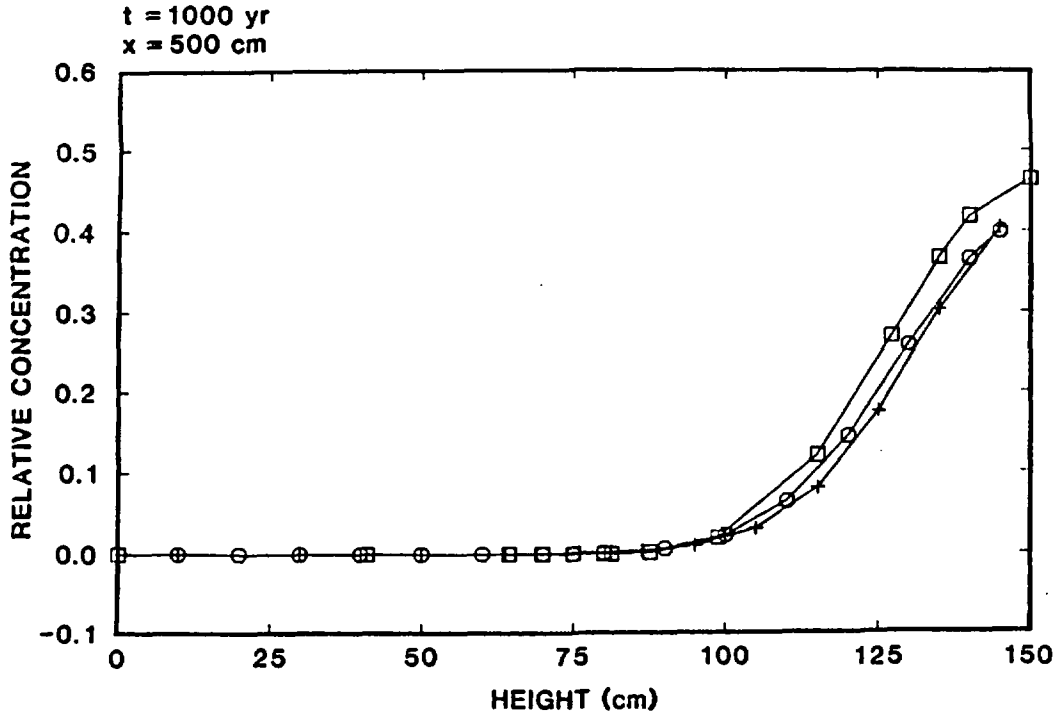

Figure B-9. Hydraulic-Head and Relative-Concentration Profiles along Right-Side Boundary for COVE 1YMa at t = 1,000 yr

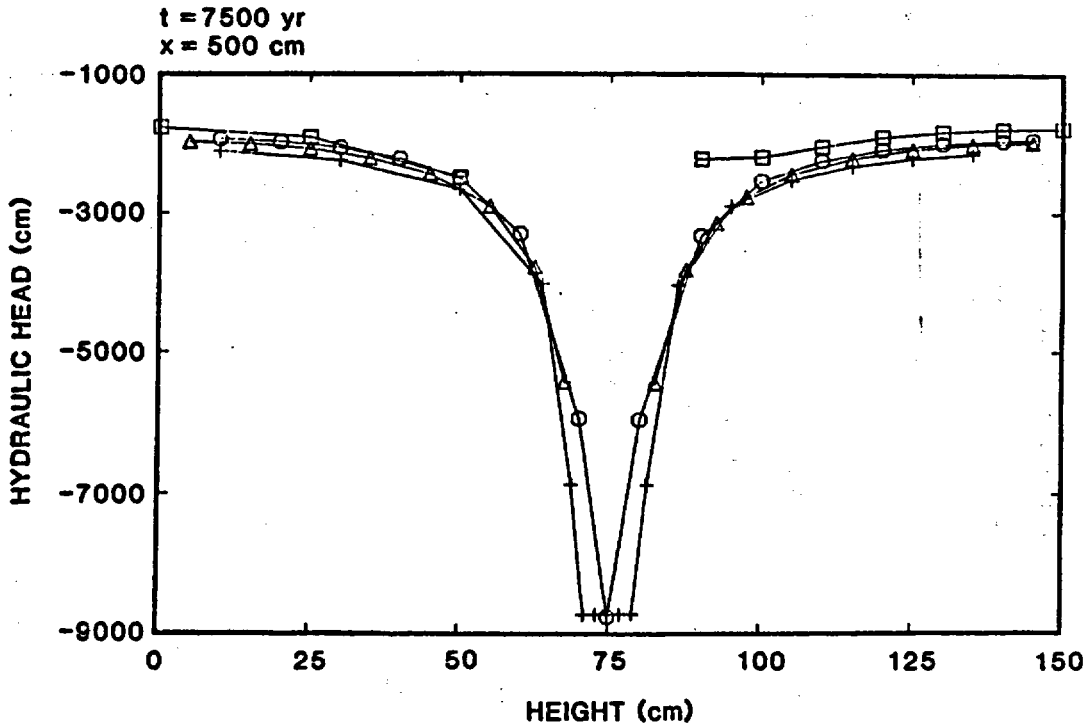

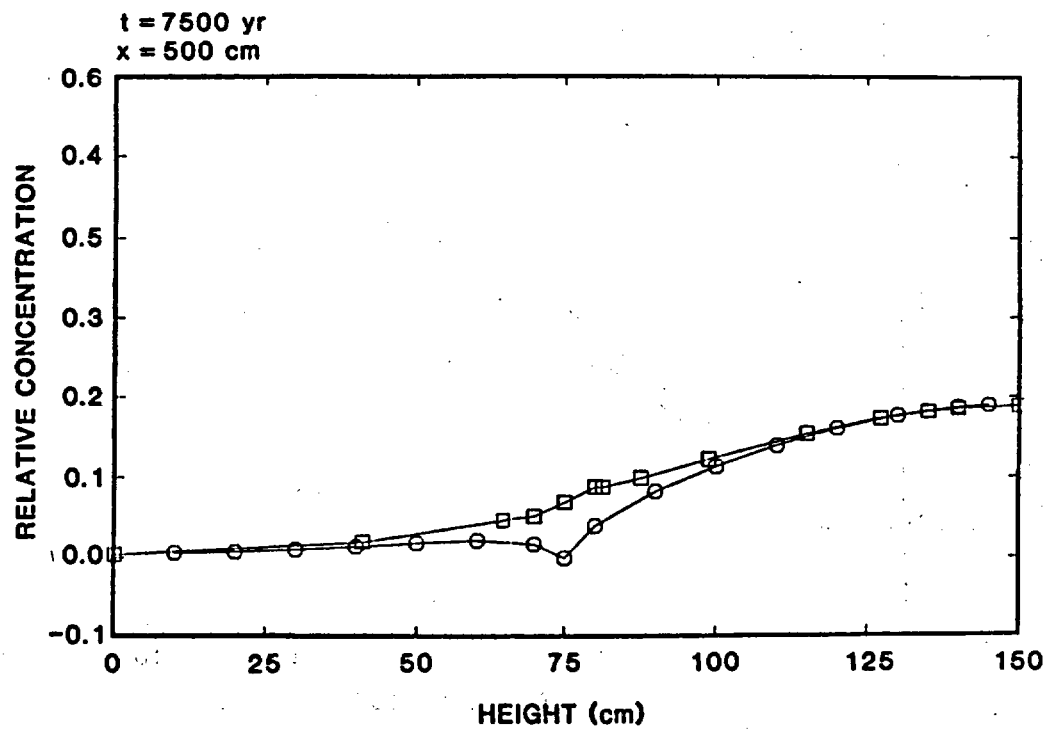

Figure B-10. Hydraulic-Head and Relative-Concentrations along Right-Side Boundary for COVE 1YMa at t = 7,500 yr

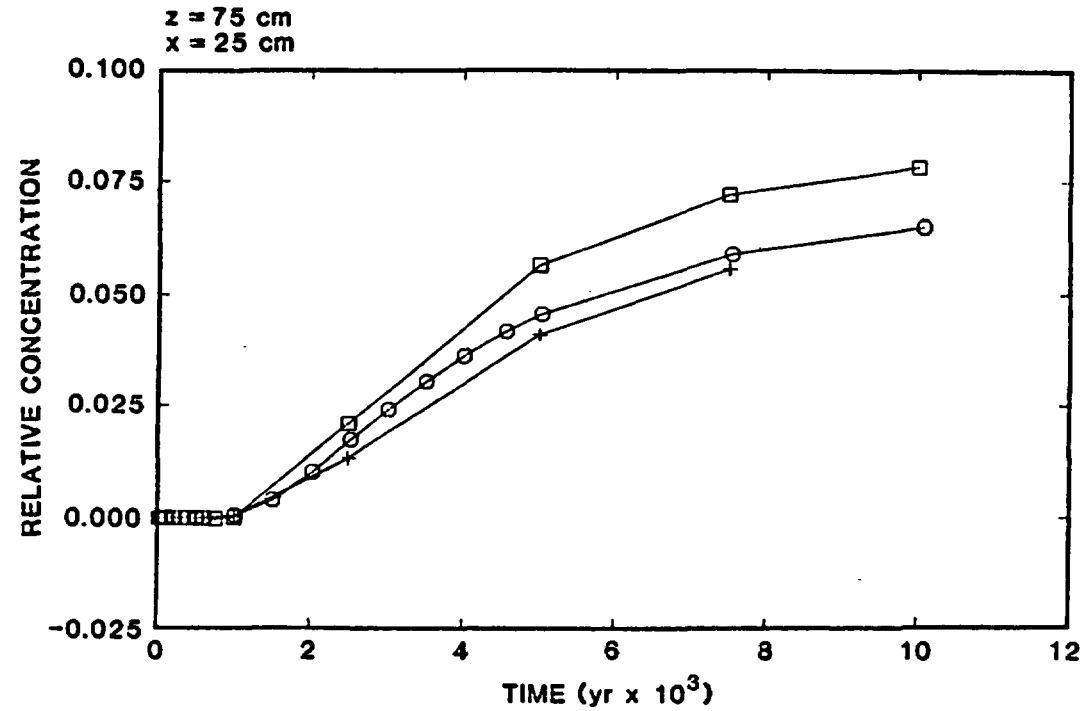

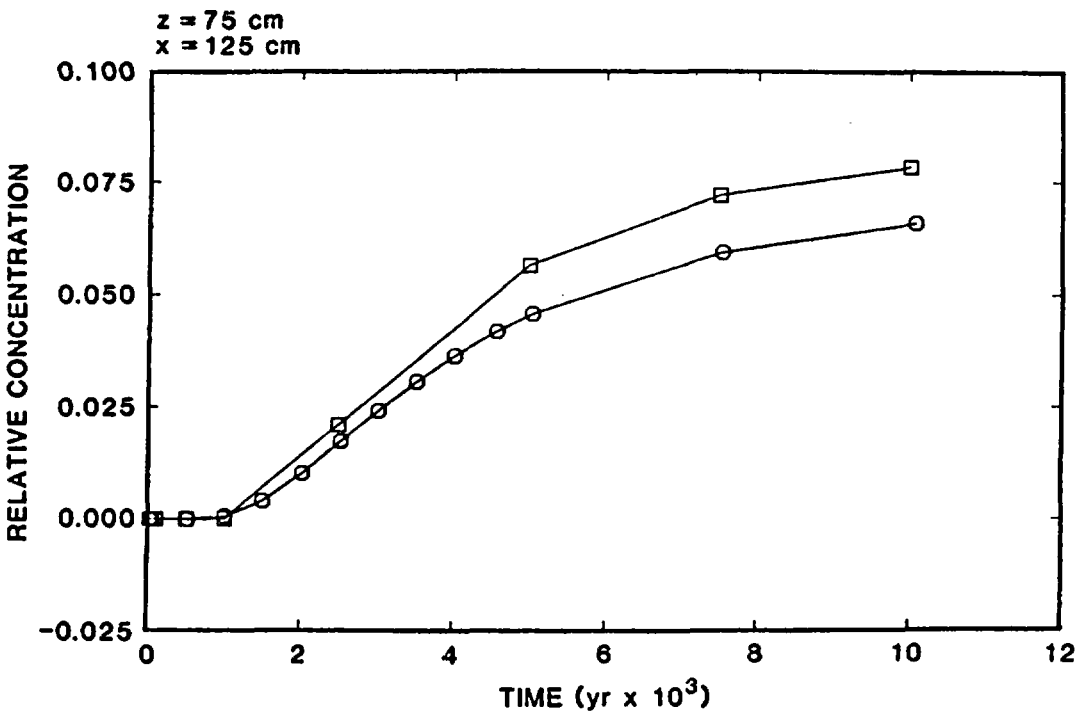

Figure B-11. Relative-Concentration Histories at Two Interior Nodes for COVE 1YMa

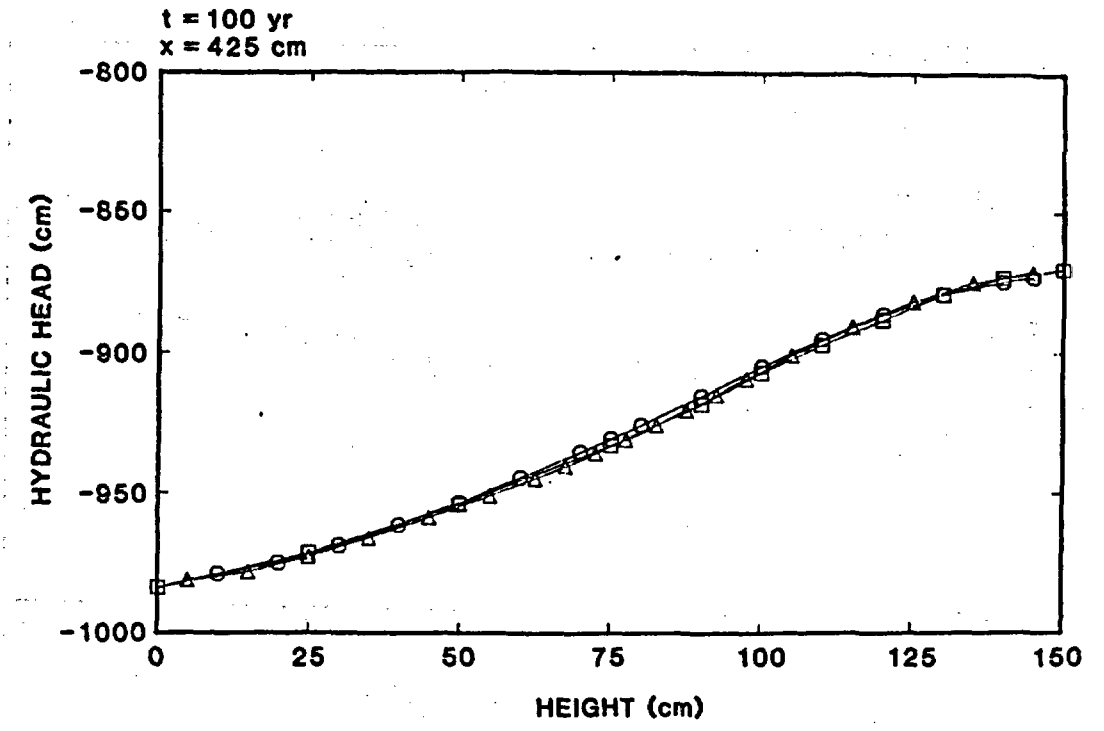

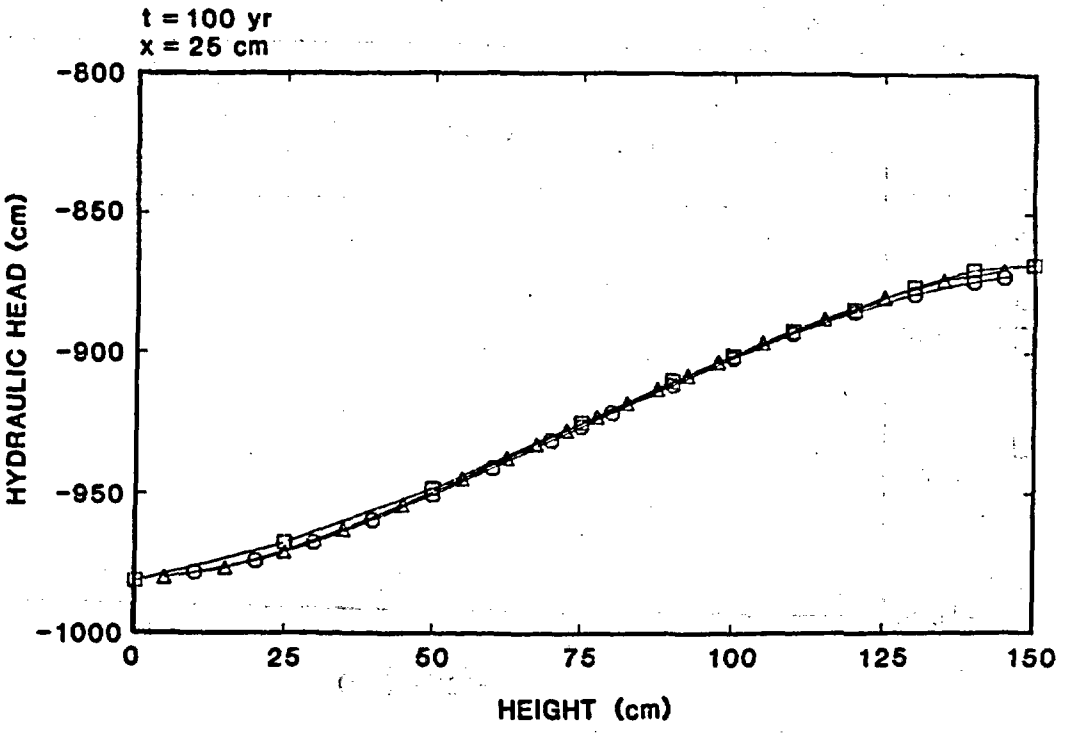

Figure B-12. Hydraulic-Head Profiles at Two Interior Nodes for COVE 1YMa at t = 100 yr

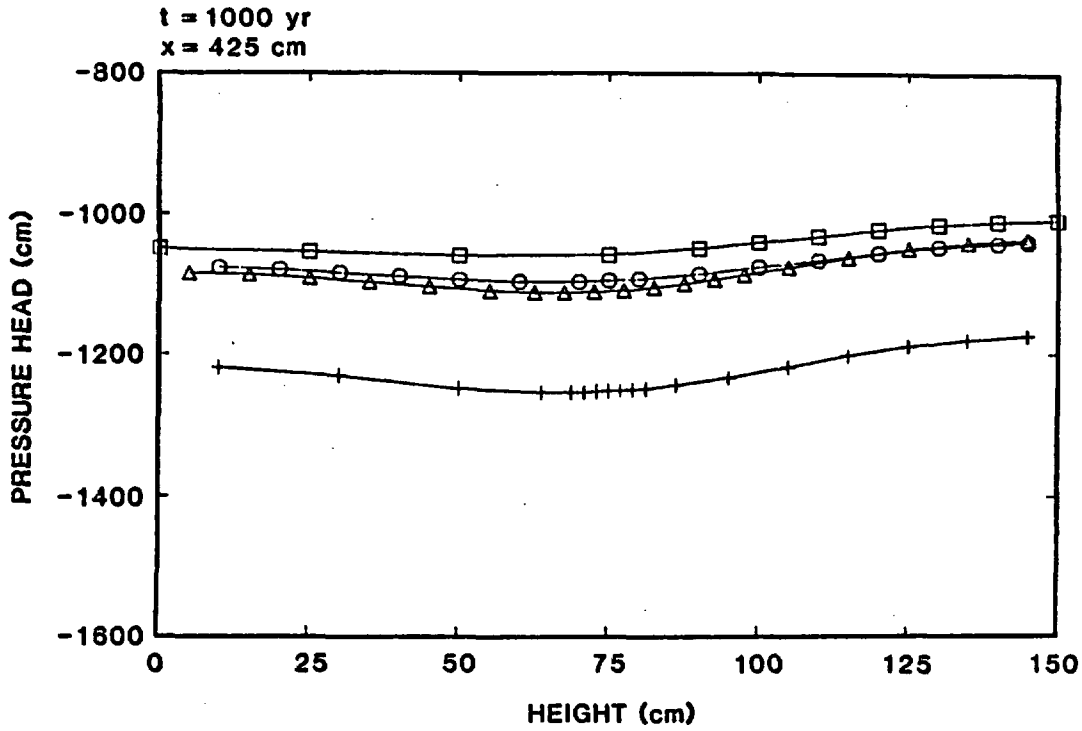

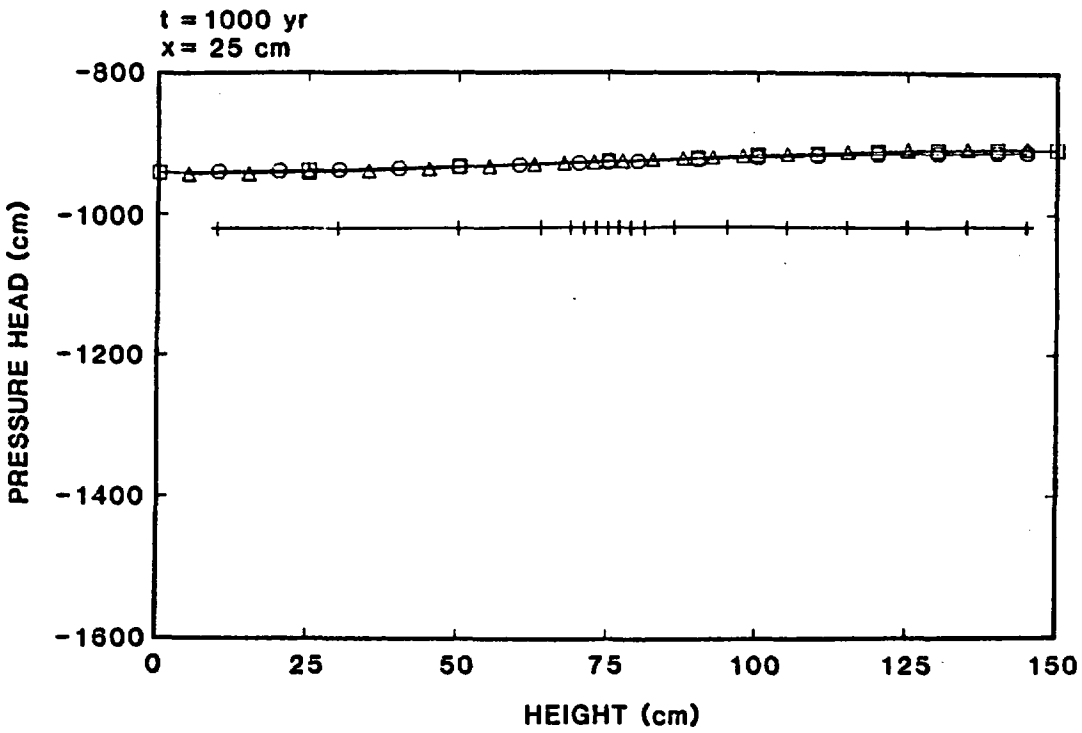

Figure B-13. Pressure-Head Profiles at Two Interior Nodes for COVE 1YMa at t = 1,000 yr

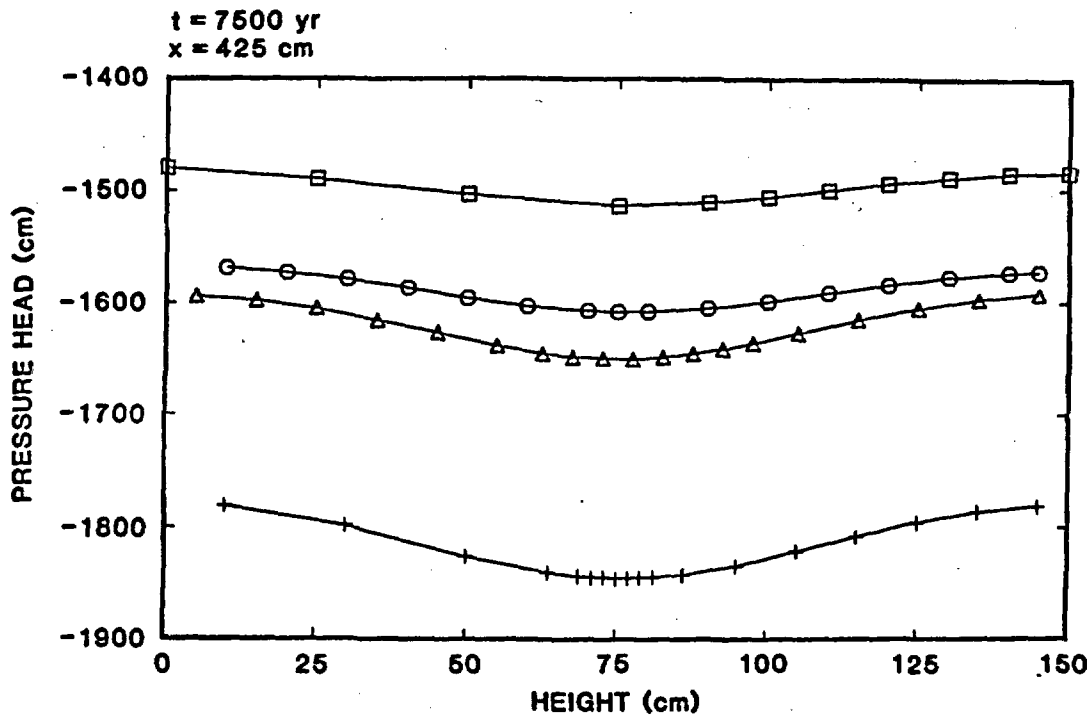

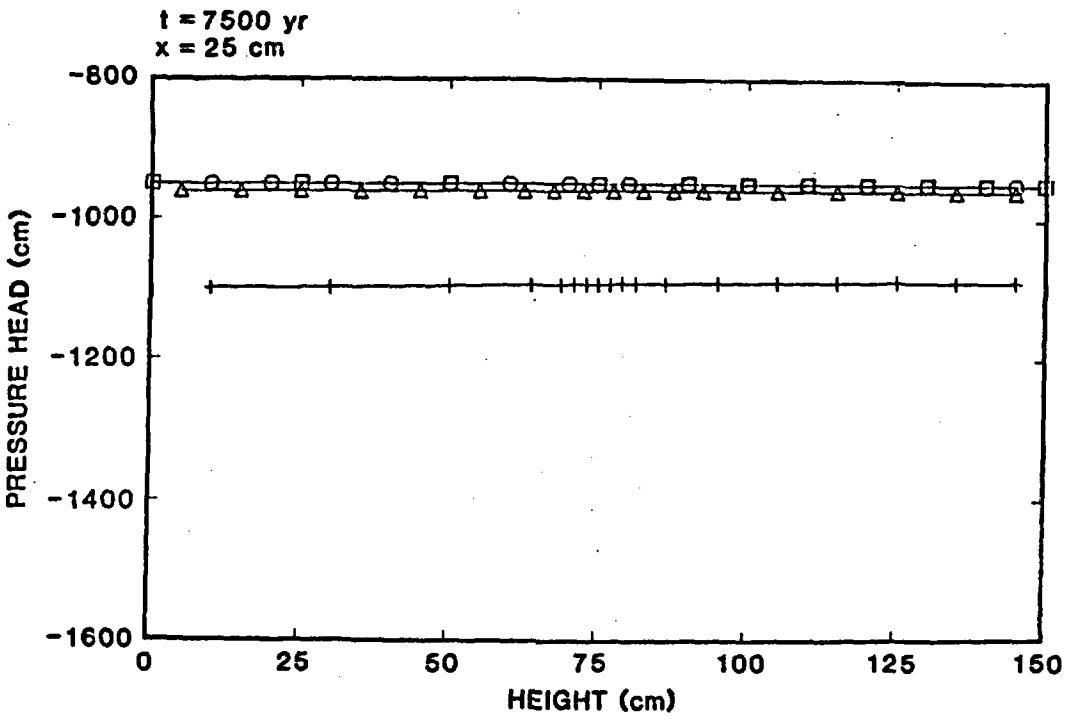

Figure B-14. Pressure-Head Profiles at Two Interior Nodes for COVE 1YMa at t = 7,500 yr

APPENDIX C

RESULTS OF COVE 1YMb

In Figures C-1 through C-7, the following symbols are used:

○ TRACR3D

△ GWVIP

+ TRUST
TRUMP

□ SAGUARO
FEMTRAN

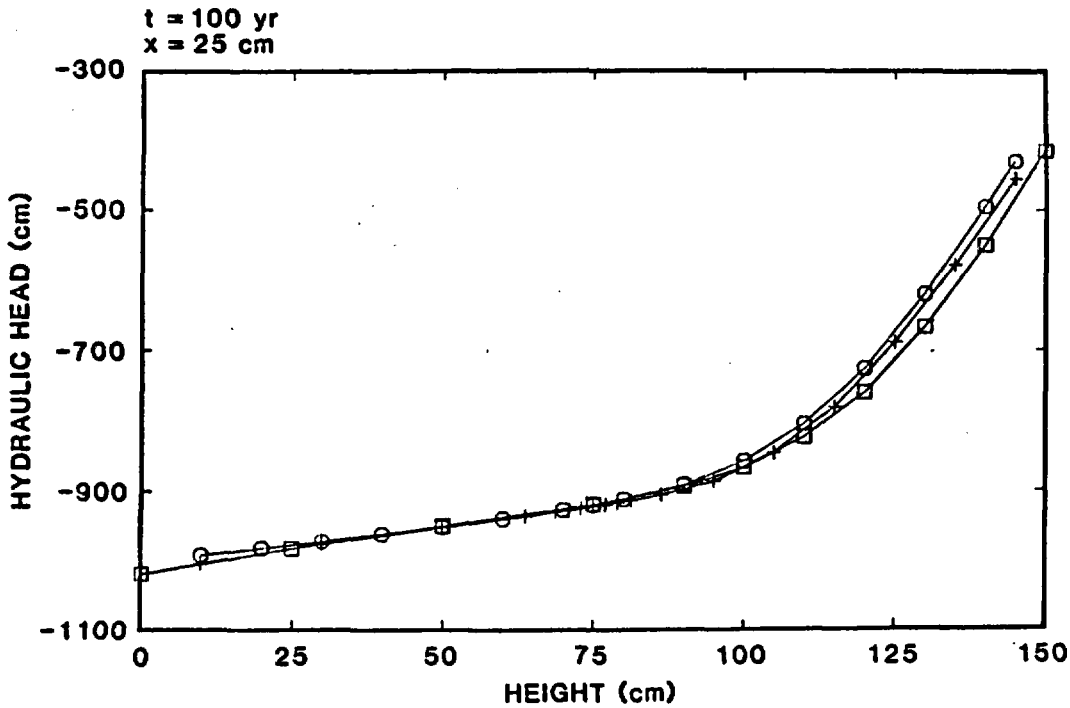

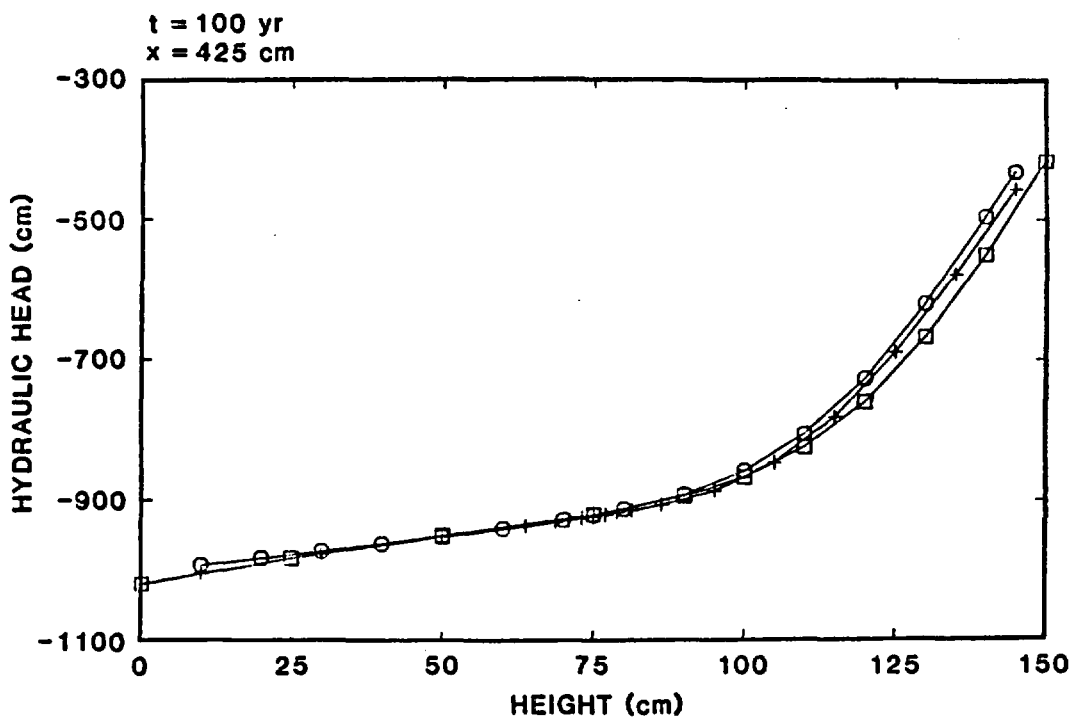

Figure C-1. Hydraulic-Head Profiles at Two Interior Nodes for COVE 1YMb at t = 100 yr

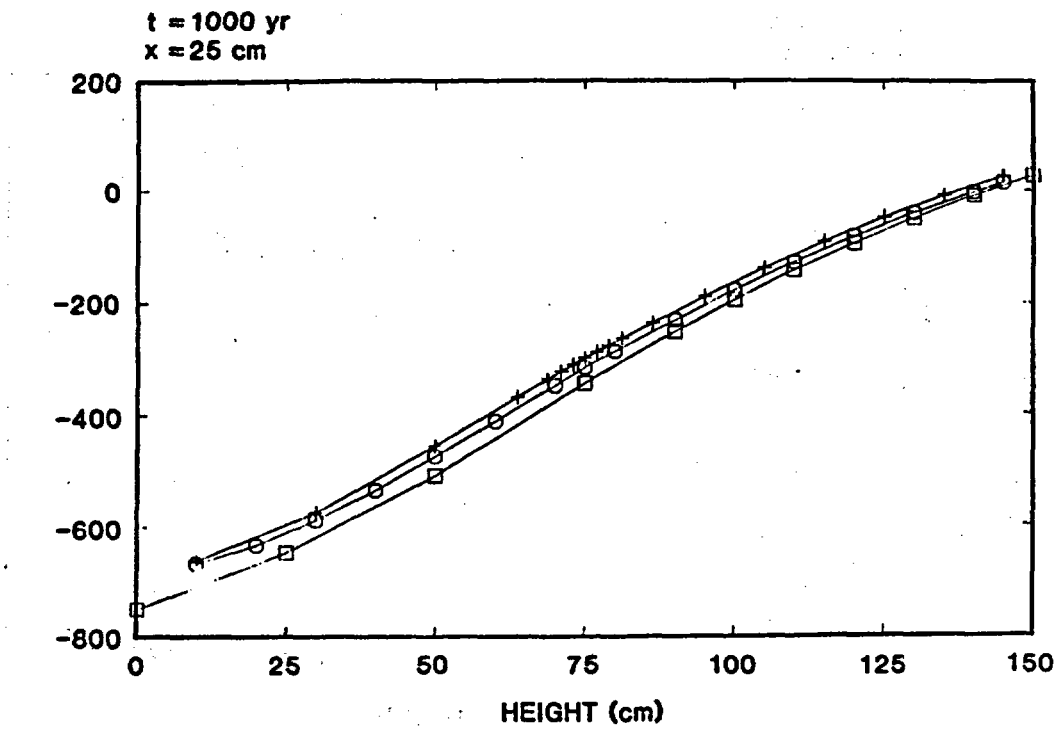

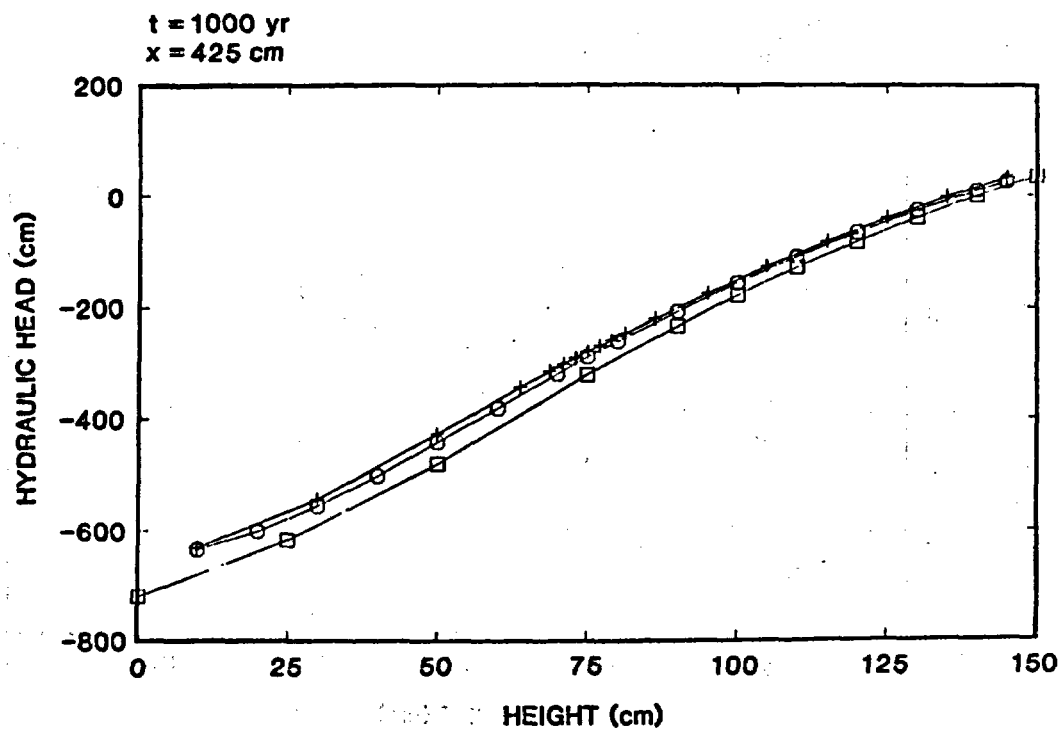

Figure C-2. Hydraulic-Head Profiles at Two Interior Nodes for COVE 1YMb at t = 1,000 yr

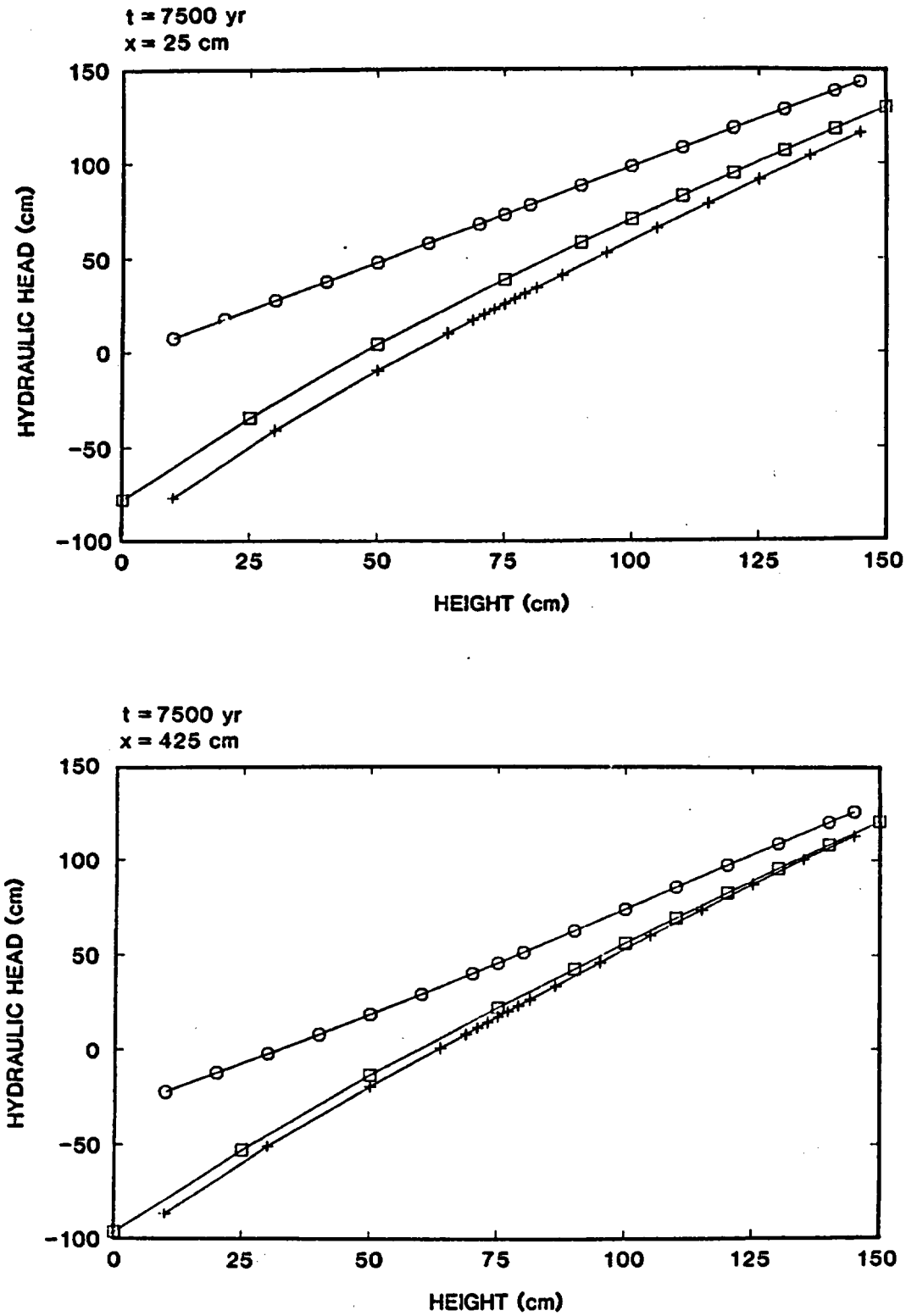

Figure C-3. Hydraulic-Head Profiles at Two Interior Nodes for COVE 1YMb at t = 7,500 yr

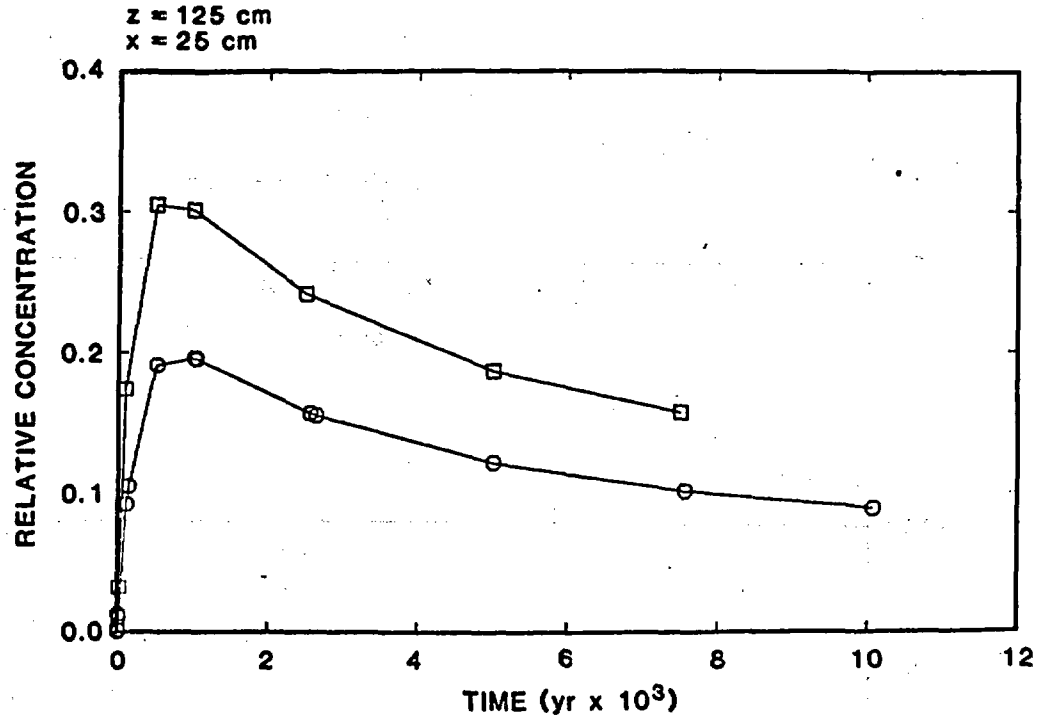

Figure C-4. Relative-Concentration History at an Interior Node for COVE 1YMb

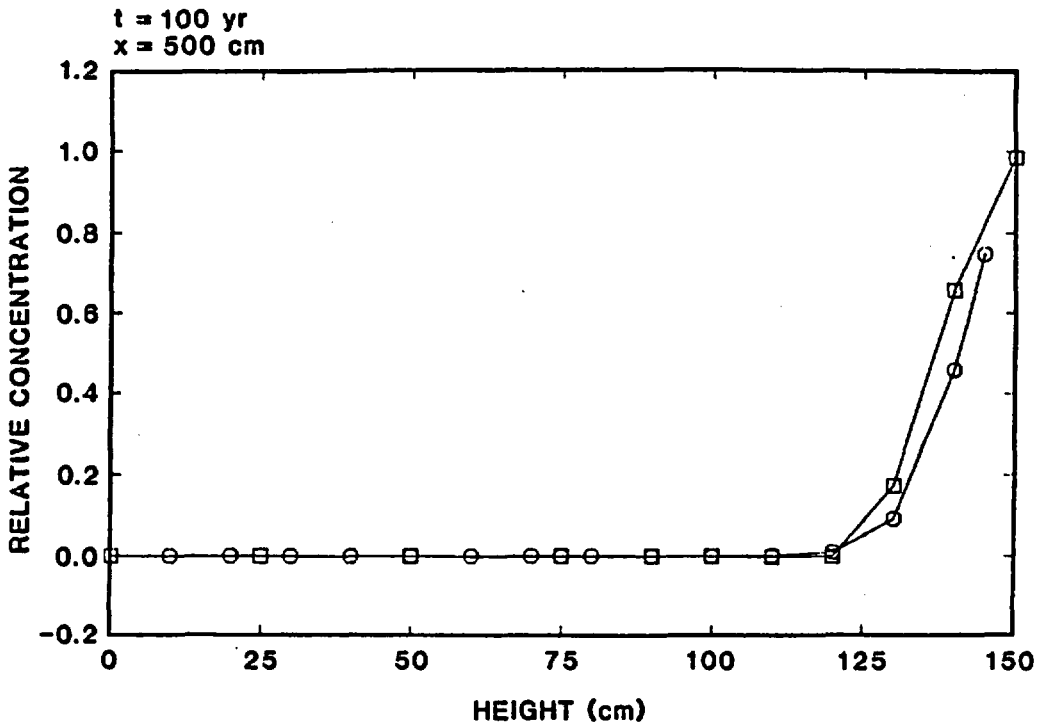

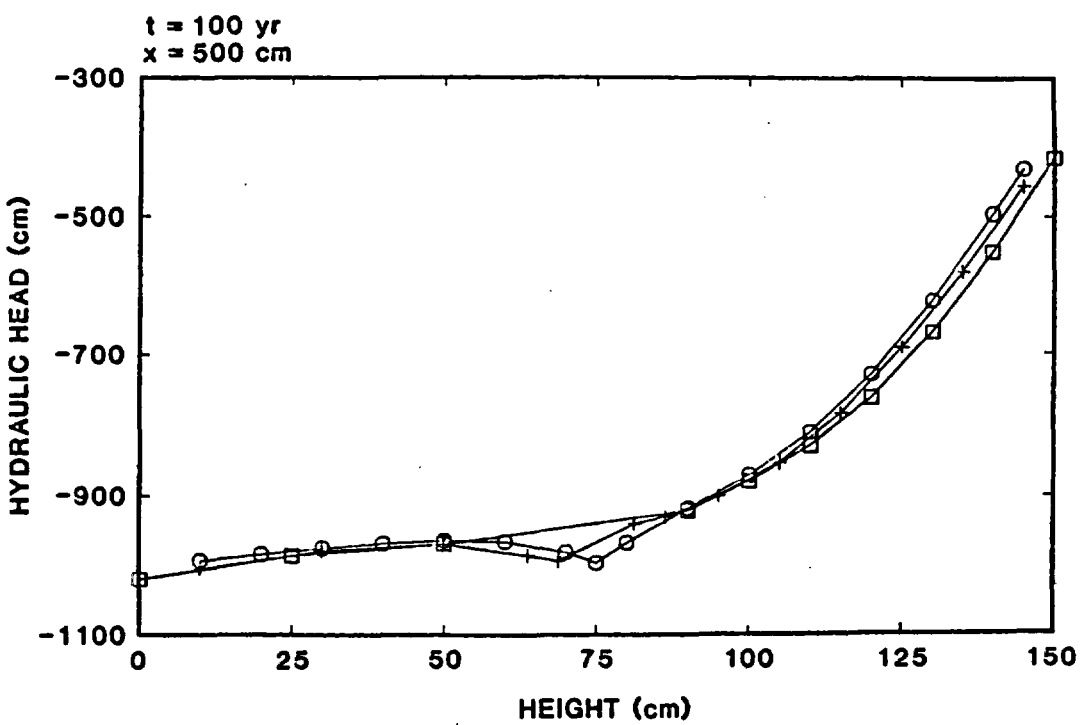

Figure C-5. Hydraulic-Head and Relative-Concentration Profiles Along Right-Side Boundary of COVE 1YMb at t = 100 yr

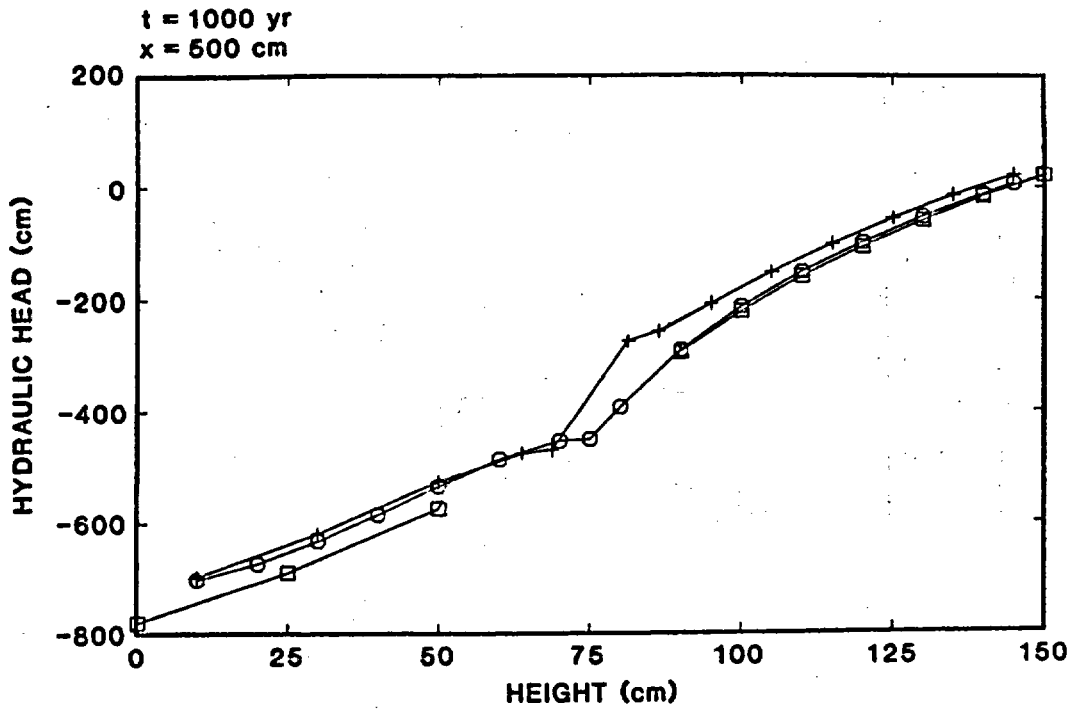

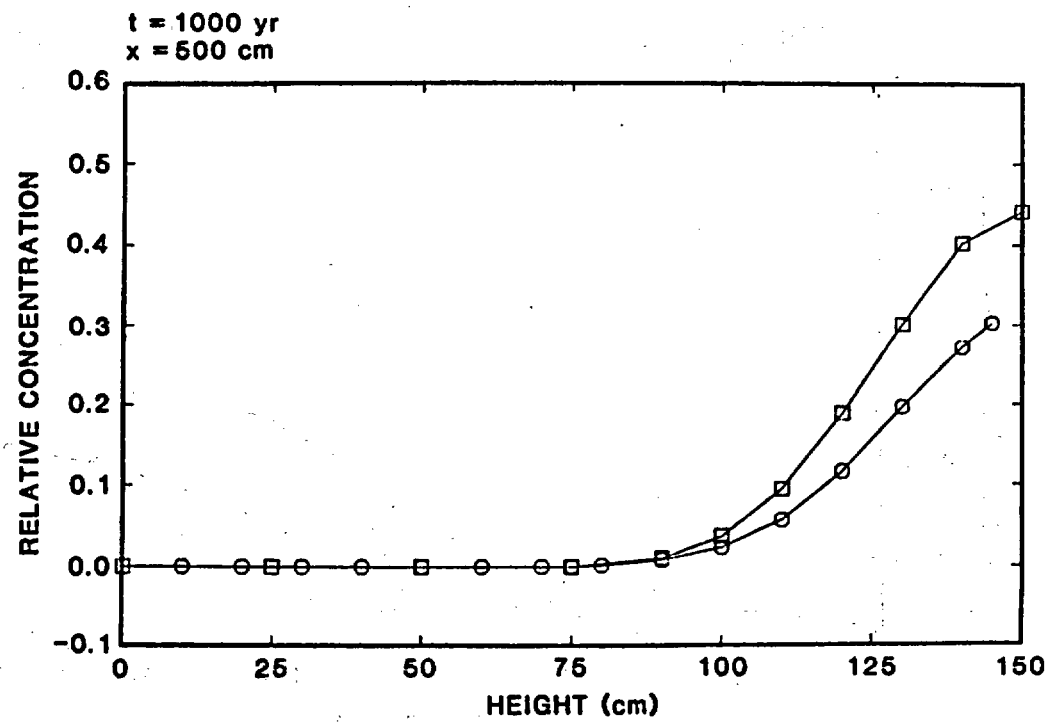

Figure C-6. Hydraulic-Head and Relative-Concentration Profiles Along Right-Side Boundary of COVE 1YMb at t = 1,000 yr

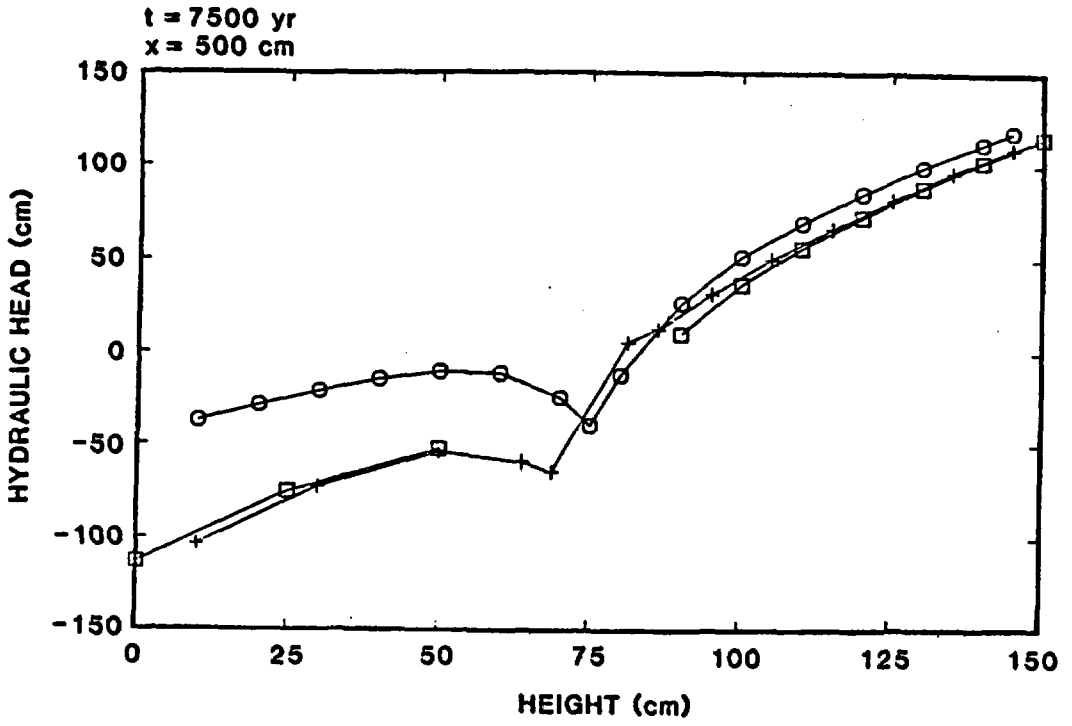

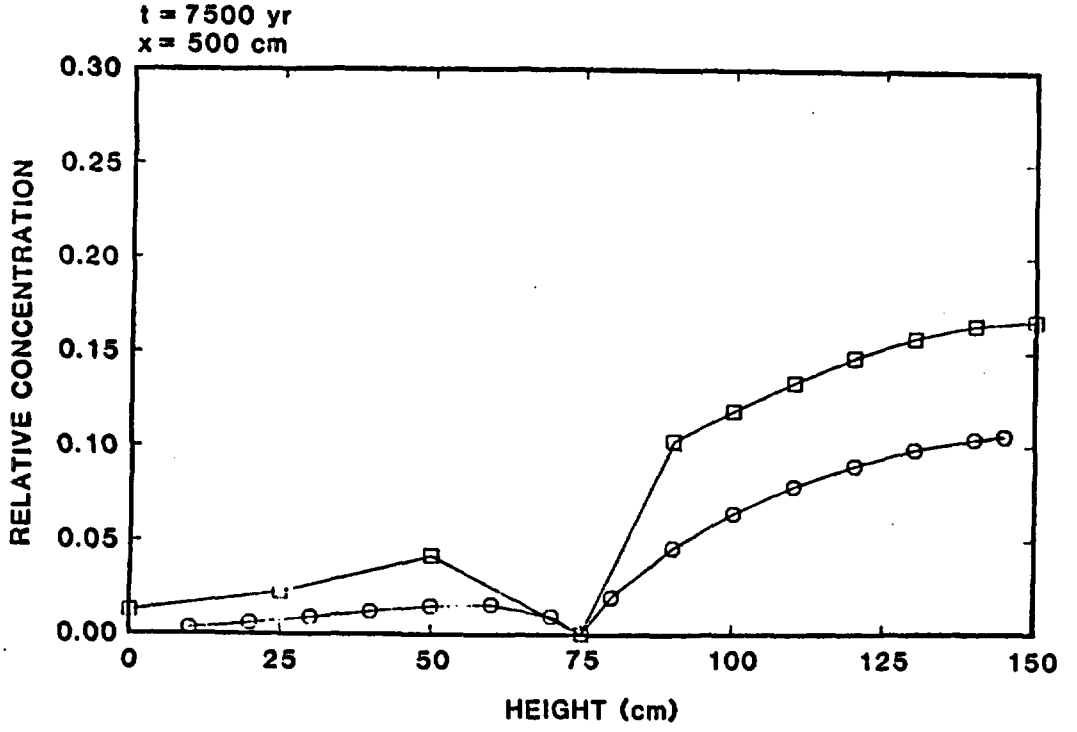

Figure C-7. Hydraulic-Head and Relative-Concentration Profiles Along Right-Side Boundary for COVE 1YMb at t = 7,500 yr

DISTRIBUTION LIST

B. C. Rusche (RW-1)
Director
Office of Civilian Radioactive
Waste Management
U.S. Department of Energy
Forrestal Building
Washington, DC 20585

J. W. Bennett (RW-22)
Office of Geologic Repositories
U.S. Department of Energy
Forrestal Building
Washington, DC 20585

Ralph Stein (RW-23)
Office of Geologic Repositories
U.S. Department of Energy
Forrestal Building
Washington, DC 20585

J. J. Fiore, (RW-22)
Program Management Division
Office of Geologic Repositories
U.S. Department of Energy
Forrestal Building
Washington, DC 20585

M. W. Frei (RW-23)
Engineering & Licensing Division
Office of Geologic Repositories
U.S. Department of Energy
Forrestal Building
Washington, DC 20585

E. S. Burton (RW-25)
Siting Division
Office of Geologic Repositories
U.S. Department of Energy
Forrestal Building
Washington, D.C. 20585

C. R. Cooley (RW-24)
Geosciences & Technology Division
Office of Geologic Repositories
U.S. Department of Energy
Forrestal Building
Washington, DC 20585

T. P. Longo (RW-25)
Program Management Division
Office of Geologic Repositories
U.S. Department of Energy
Forrestal Building
Washington, DC 20585

Cy Klingsberg (RW-24)
Geosciences and Technology Division
Office of Geologic Repositories
U. S. Department of Energy
Forrestal Building
Washington, DC 20585

B. G. Gale (RW-25)
Siting Division
Office of Geologic Repositories
U.S. Department of Energy
Forrestal Building
Washington, D.C. 20585

R. J. Blaney (RW-22)
Program Management Division
Office of Geologic Repositories
U.S. Department of Energy
Forrestal Building
Washington, DC 20585

R. W. Gale (RW-40)
Office of Policy, Integration, and
Outreach
U.S. Department of Energy
Forrestal Building
Washington, D.C. 20585

J. E. Shaheen (RW-44)
Outreach Programs
Office of Policy, Integration and
Outreach
U.S. Department of Energy
Forrestal Building
Washington, DC 20585

J. O. Neff, Manager
Salt Repository Project Office
U.S. Department of Energy
505 King Avenue
Columbus, OH 43201

D. C. Newton (RW-23)
Engineering & Licensing Division
Office of Geologic Repositories
U.S. Department of Energy
Forrestal Building
Washington, DC 20585

O. L. Olson, Manager
Basalt Waste Isolation Project Office
U.S. Department of Energy
Richland Operations Office
Post Office Box 550
Richland, WA 99352

D. L. Vieth, Director (4)
Waste Management Project Office
U.S. Department of Energy
Post Office Box 14100
Las Vegas, NV 89114

D. F. Miller, Director
Office of Public Affairs
U.S. Department of Energy
Post Office Box 14100
Las Vegas, NV 89114

D. A. Nowack (12)
Office of Public Affairs
U.S. Department of Energy
Post Office Box 14100
Las Vegas, NV 89114

B. W. Church, Director
Health Physics Division
U.S. Department of Energy
Post Office Box 14100
Las Vegas, NV 89114

Chief, Repository Projects Branch
Division of Waste Management
U.S. Nuclear Regulatory Commission
Washington, D.C. 20555

Document Control Center
Division of Waste Management
U.S. Nuclear Regulatory Commission
Washington, D.C. 20555

S. A. Mann, Manager
Crystalline Rock Project Office
U.S. Department of Energy
9800 South Cass Avenue
Argonne, IL 60439

K. Street, Jr.
Lawrence Livermore National
Laboratory
Post Office Box 808
Mail Stop L-209
Livermore, CA 94550

L. D. Ramspott (3)
Technical Project Officer for NNWSI
Lawrence Livermore National
Laboratory
P.O. Box 808
Mail Stop L-204
Livermore, CA 94550

W. J. Purcell (RW-20)
Office of Geologic Repositories
U.S. Department of Energy
Forrestal Building
Washington, DC 20585

D. T. Oakley (4)
Technical Project Officer for NNWSI
Los Alamos National Laboratory
P.O. Box 1663
Mail Stop F-671
Los Alamos, NM 87545

W. W. Dudley, Jr. (3)
Technical Project Officer for NNWSI
U.S. Geological Survey
Post Office Box 25046
418 Federal Center
Denver, CO 80225

NTS Section Leader
Repository Project Branch
Division of Waste Management
U.S. Nuclear Regulatory Commission
Washington, D.C. 20555

V. M. Glanzman
U.S. Geological Survey
Post Office Box 25046
913 Federal Center
Denver, CO 80225

P. T. Prestholt
NRC Site Representative
1050 East Flamingo Road
Suite 319
Las Vegas, NV 89109

M. E. Spaeth
Technical Project Officer for NNWSI
Science Applications
International, Corporation
2769 South Highland Drive
Las Vegas, NV 89109

SAIC-T&MSS Library (2)
Science Applications
International, Corporation
2950 South Highland Drive
Las Vegas, NV 89109

W. S. Twenhofel, Consultant
Science Applications
International, Corp.
820 Estes Street
Lakewood, CO 80215

A. E. Gurrola
General Manager
Energy Support Division
Holmes & Narver, Inc.
Post Office Box 14340
Las Vegas, NV 89114

J. A. Cross, Manager
Las Vegas Branch
Fenix & Scisson, Inc.
Post Office Box 15408
Las Vegas, NV 89114

N. E. Carter
Battelle Columbus Laboratory
Office of Nuclear Waste Isolation
505 King Avenue
Columbus, OH 43201

J. B. Wright
Technical Project Officer for NNWSI
Westinghouse Electric Corporation
Waste Technology Services Division
Nevada Operations
Post Office Box 708
Mail Stop 703
Mercury, NV 89023

ONWI Library
Battelle Columbus Laboratory
Office of Nuclear Waste Isolation
505 King Avenue
Columbus, OH 43201

W. M. Hewitt, Program Manager
Roy F. Weston, Inc.
2301 Research Blvd., 3rd Floor
Rockville, MD 20850

H. D. Cunningham
General Manager
Reynolds Electrical &
Engineering Co., Inc.
Post Office Box 14400
Mail Stop 555
Las Vegas, NV 89114

T. Hay, Executive Assistant
Office of the Governor
State of Nevada
Capitol Complex
Carson City, NV 89710

R. R. Loux, Jr., Director (3)
Nuclear Waste Project Office
State of Nevada
Capitol Complex
Carson City, NV 89710

C. H. Johnson, Technical
Program Manager
Nuclear Waste Project Office
State of Nevada
Capitol Complex
Carson City, NV 89710

John Fordham
Desert Research Institute
Water Resources Center
Post Office Box 60220
Reno, NV 89506

Department of Comprehensive Planning
Clark County
225 Bridger Avenue, 7th Floor
Las Vegas, NV 89155

Lincoln County Commission
Lincoln County
Post Office Box 90
Pioche, NV 89043

Community Planning and Development
City of North Las Vegas
Post Office Box 4086
North Las Vegas, NV 89030

City Manager
City of Henderson
Henderson, NV 89015

V. J. Cassella (RW-22)
Office of Geologic Repositories
U.S. Department of Energy
Forrestal Building
Washington, DC 20585

N. A. Norman
Project Manager
Bechtel National Inc.
P. O. Box 3965
San Francisco, CA 94119

Flo Butler
Los Alamos Technical Associates
1650 Trinity Drive
Los Alamos, New Mexico 87544

Dr. Martin Mifflin
Desert Research Institute
Water Resources Center
Suite 1
2505 Chandler Avenue
Las Vegas, NV 89120

Planning Department
Nye County
Post Office Box 153
Tonopah, NV 89049

Economic Development Department
City of Las Vegas
400 East Stewart Avenue
Las Vegas, NV 89101

Director of Community Planning
City of Boulder City
Post Office Box 367
Boulder City, NV 89005

Commission of the European Communities
200 Rue de la Loi
B-1049 Brussels
BELGIUM

Technical Information Center
Roy F. Weston, Inc.
2301 Research Boulevard, Third Floor
Rockville, MD 20850

R. Harig
Parsons Brinckerhoff Quade & Douglas, Inc.
1625 Van Ness Ave.
San Francisco, CA 94109-3678

Dr. T. N. Narasimhan (2)
Earth Sciences Division
Lawrence Berkeley Laboratory
1 Cyclotron Road
Berkeley, CA 94720

B. J. Travis
Los Alamos National Laboratory
P.O. Box 1663
Los Alamos, NM 87545

Mike Toibner
Science Application International
Corp.
2950 South Highland Drive
Las Vegas, NV 89109

Kjell Anderson
Swedish Nuclear Power Inspectorate
Box 27106
S-102 52 Stockholm
Sweden

Eckhart Butow
Institut fur Kerntechnik
der Technische
Universitat Berlin
Marchstrabe 18
D-1000 Berlin
West Germany

Bertil Grundfelt
KEMAKTA Consultants Co.
Luntmakargatan 94
S-113 51 Stockholm
Sweden

P. Hufschmied
Nationale Genossenschft fur die
Lagerung Radioacktiver Abfalle
NAGRA
Parkstrabe 23
CH-5401 Baden
Switzerland

Charles Keller
Los Alamos National Laboratory
P.O. Box 1663
Los Alamos, NM 87545

Mike Revelli
Lawrence Livermore National
Laboratory
P.O. Box 808
Mail Stop L-204
Livermore, CA 94550

Suresh Pahwa
Intera Environmental
Consultants, Inc.
11999 Katy Freeway
Suite 610
Houston, TX 77079

Tim Broyd
Atkins Research and Development
Woodcote Grove
Ashley Road
Epsom
Surrey KT18 5BW
United Kingdom

Charles Cole
Battelle Pacific Northwest
Laboratories
Battelle Blvd.
Richland, WA 99352

David Hodgkinson
AERE
Harwell
GBR-Didcot Oxon OX11 ORA
United Kingdom

Hideo Kimura
JAERI
Tokai-mura
Naka-gun
Ibaraki-ken
Japan

Thomas Nicholson
U.S. Nuclear Regulatory Commission
Earth Sciences Branch
Division of Radiation Programs
and Earth Sciences
Washington, D.C. 20555

Haruto Nakarmua
JAERI
Chief of HLW Management Research
Laboratory
Division of Environmental Safety
Research
Tokai-mura
Naka-gun
Ibaraki-ken
Japan

Seppo Vuori
Technical Research Centre of Finland
Nuclear Engineering Laboratory
P O. Box 169
SF-001 81 Helsinki
Finland

Mike Foley
Battelle Pacific Northwest
Laboratories
Battelle Blvd.
Richland, WA 99352

Steve Schneider
Battelle Pacific Northwest
Laboratories
Battelle Blvd.
Richland, WA 94720

T. R. Pigford
Department of Nuclear Engineering
University of California
Berkeley, CA 94720

Donald R. F. Harleman
Ford Professor of Engineering
Building 48
Massachusetts Institute of
Technology
Cambridge, MA 02139

J. F. Pickens
Geologic Testing Consultants, Ltd.
785 Carling Avenue, Fourth Floor
Ottawa, Ontario k1S 5H4
Canada

Emil Frind
Earth Sciences Dept.
University of Waterloo
Waterloo, Ontario
Canada

David Noy
Nicker Hill
Nottingham NG12 5GG
United Kingdom

Anthony Muller
Nuclear Energy Agency
38, Boulevard Suchet
F-75016 Paris
France

1511 G. Weigand
1511 N. Bixler
1511 R. R. Eaton
1511 P. Hopkins
1513 J. Schutt
6300 R. W. Lynch
6310 T. O. Hunter
6310 NNWSICF
6311 L. W. Scully
6311 L. Perrine (2)
6312 F. W. Bingham
6312 J. W. Braithwaite
6312 N. K. Hayden (20)
6312 B. S. Langkopf
6312 R. R. Peters
6312 R. W. Prindle
6312 M. S. Tierney
6312 J. G. Yeager
6313 T. E. Blejwas
6313 E. A. Klavetter
6314 J. R. Tillerson
6314 S. Bauer
6314 J. A. Fernandez
6314 A. J. Mansure
6315 S. Sinnock
6315 Y. T. Lin
6332 WMT Library (20)
6430 N. R. Ortiz
6431 B. Cranwell
3141 C. M. Ostrander (5)
3151 W. L. Garner (3)
8024 M. A. Pound
DOE/TIC (28)
(3154-3, C. H. Dalin)

Org.	Bldg.	Name	Rec'd by	Org.	Bldg.	Name	Rec'd by

Sandia National L